MULTISPECTRAL MULTI-TEMPORAL CROP COVER CLASSIFICATION OVER TÜRKİYE USING RANDOM FOREST ALGORITHM

A THESIS SUBMITTED TO
THE GRADUATE SCHOOL OF NATURAL AND APPLIED SCIENCES
OF
MIDDLE EAST TECHNICAL UNIVERSITY

BY

ELİF DÖNMEZ ALTINDAL

IN PARTIAL FULFILLMENT OF THE REQUIREMENTS
FOR
THE DEGREE OF MASTER OF SCIENCE
IN
CIVIL ENGINEERING

JULY 2022

Approval of the thesis:

MULTISPECTRAL MULTI-TEMPORAL CROP COVER CLASSIFICATION OVER TÜRKİYE USING RANDOM FOREST ALGORITHM

submitted by **ELİF DÖNMEZ ALTINDAL** in partial fulfillment of the requirements for the degree of **Master of Science** i**n Civil Engineering, Middle East Technical University** by,

Prof. Dr. Halil Kalıpçılar
Dean, Graduate School of **Natural and Applied Sciences** _____

Prof. Dr. Erdem Canbay
Head of the Department, **Civil Engineering** _____

Assoc. Prof. Dr. Mustafa Tuğrul Yılmaz
Supervisor, **Civil Engineering, METU** _____

Examining Committee Members:

Prof. Dr. İsmail Yücel
Civil Engineering, METU _____

Assoc. Prof. Dr. Mustafa Tuğrul Yılmaz
Civil Engineering, METU _____

Prof. Dr. Elçin Kentel Erdoğan
Civil Engineering, METU _____

Assoc. Prof. Dr. Koray Kamil Yılmaz
Geological Engineering, METU _____

Assoc. Prof. Dr. Abdulla Sakallı
Industrial Engineering, Iskenderun Technical University _____

Date: 28.07.2022

I hereby declare that all information in this document has been obtained and presented in accordance with academic rules and ethical conduct. I also declare that, as required by these rules and conduct, I have fully cited and referenced all material and results that are not original to this work.

Name Last name : Elif Dönmez Altındal

Signature :

ABSTRACT

MULTISPECTRAL MULTI-TEMPORAL CROP COVER CLASSIFICATION OVER TÜRKİYE USING RANDOM FOREST ALGORITHM

Dönmez Altındal, Elif
Master of Science, Civil Engineering
Supervisor : Assoc. Prof. Dr. Mustafa Tuğrul Yılmaz

July 2022, 86 pages

Accurate crop cover maps are beneficial for various aspects like water resources management, crop yield prediction, regulation insurance policies, and investigation of the effects of climate change. In this thesis, agricultural crop mapping is performed over Türkiye. Sentinel-2 Level-2A images with 10-meter spatial resolution acquired between March 15, 2019, and October 15, 2019, are reduced to 15-day median images. In addition to spectral bands, Normalized Difference Vegetation Index (NDVI) and Normalized Difference Water Index (NDWI) are used as classification features. Twenty years of ERA5-Land 2-meter temperature data is averaged to divide the study area into three temperature zones as Low (LTZ), Medium (MTZ), and High-Temperature Zones (HTZ). Before the classification, feature selection using random forest importance is performed to select the most successful features. After that, a random forest classifier is created for each temperature zone. LTZ reached 89% overall accuracy (OA) with a 0.88 Kappa. MTZ reached 91% OA with 0.92 Kappa, and HTZ reached 94% OA with 0.94 Kappa, giving the best accuracy among the classifiers. Finally, test sets of all temperature zones are combined, and OA of 92% with a Kappa of 0.93 is achieved with this

combined test set. To test the advantage of temperature zoning, classification is also performed without the temperature zones, and it is observed that temperature zoning increases the OA and Kappa by 1%. A land cover classification map is then created using temperature zone classifiers with 34 crop classes and six non-agricultural classes.

Keywords: Crop Cover Mapping, Remote Sensing, Machine Learning, Supervised Classification

ÖZ

RASTGELE ORMAN ALGORİTMASI KULLANILARAK TÜRKİYE ÜZERİNDE MULTİSPEKTRAL VE ÇOK ZAMANLI TARIM ÜRÜNÜ ÖRTÜSÜ SINIFLANDIRMASI

Dönmez Altındal, Elif
Yüksek Lisans, İnşaat Mühendisliği
Tez Yöneticisi: Doc. Dr. Mustafa Tuğrul Yılmaz

Temmuz 2022, 86 sayfa

Doğru tarımsal mahsul örtüsü haritaları, su kaynakları yönetimi, mahsul verimi tahmini, gıda güvenliği değerlendirmesi, sigorta poliçelerinin düzenlenmesi ve iklim değişikliğinin etkilerinin araştırılması gibi birçok farklı açıdan faydalıdır. Bu tezde Türkiye genelinde tarımsal ürün haritalaması yapılmıştır. 15 Mart 2019 ile 15 Ekim 2019 arasında elde edilen 10 metre uzamsal çözünürlüğe sahip Sentinel-2 Level-2A görüntüleri, sınıflandırma için 15 günlük medyan görüntülere indirgenmiştir. Spektral bantlara ek olarak Normalize Edilmiş Bitki İndeksi (NDVI) ve Normalize Edilmiş Su İndeksi (NDWI) sınıflandırma öznitelikleri olarak kullanılmıştır. ERA5-Land aylık ortalamalarının 1999-2019 yılları arasındaki ortalaması alınmıştır ve buna göre çalışma alanını düşük, orta ve yüksek sıcaklık bölgeleri olarak üç sıcaklık bölgesine bölünmüştür. Sınıflandırmadan önce Rastgele Orman Önem algoritması kullanılarak en başarılı sınıflandırma öznitelikleri bulunmuştur. Öznitelik seçiminden sonra her sıcaklık bölgesi için bir Rastgele Orman sınıflandırma algoritması oluşturulmuştur. Düşük sıcaklık bölgesi, 17 arazi örtüsü sınıfı için 0.88 Kappa katsayısı ile %89 Genel Doğruluğa, orta sıcaklık bölgesi ise, 35 arazi örtüsü sınıfı için 0.92 Kappa katsayısı ile %91 Genel Doğruluğa ulaşmıştır. Son olarak, yüksek sıcaklık bölgesi, sınıflandırıcılar arasında en iyi doğruluğu vererek 34 arazi

örtüsü sınıfı için 0.94 Kappa katsayısı ile %94 genel doğruluğa ulaşmıştır. Son olarak, sıcaklık bölgelerinin test setleri birleştirilmiş ve tüm test verisi için 0.93 Kappa katsayısı ile %92 Genel Doğruluk elde edilmiştir. Sıcaklık bölgelerinin avantajını test etmek için, sıcaklık bölgeleri olmadan da sınıflandırma yapılmış ve sıcaklık bölgelerinin genel doğruluğu ve Kappa katsayısını %1 oranında arttırdığı gözlemlemiştir. Daha sonra bu sınıflandırıcılar kullanılarak 34 tarımsal ürün sınıfı ve 6 tarım dışı sınıf içeren bir arazi örtüsü haritası oluşturulmuştur.

Anahtar Kelimeler: Tarımsal Arazi Haritası, Uzaktan Algılama, Makine Öğrenmesi, Denetimli Sınıflandırma

To my family and dogs…

ACKNOWLEDGEMENTS

First, I would like to express my deepest gratitude to my supervisor, Assoc. Prof. Dr. M. Tuğrul Yılmaz for his guidance, advice, criticism, encouragement, and insight throughout the research.

I would also like to thank Assist. Prof. Dr. Mehdi H. Afshar for his encouragements, suggestions, and comments.

I would like to express my warmest thanks to my beloved husband, Abdullah Altındal, for always being there for me since the first day.

I would also like to thank dearest friends Seda D. Taş, Elif Sezin Şahin, Ayşe Dilara Türkmen, Elif Anaçali, and Duygu Candemir for all the entertainment and emotional support.

Lastly, I would be remiss in not mentioning my family. I want to thank them for their belief in me and patience, which cannot be overlooked.

TABLE OF CONTENTS

ABSTRACT v

ÖZ vii

ACKNOWLEDGEMENTS x

TABLE OF CONTENTS xi

LIST OF TABLES xiii

LIST OF FIGURES xv

LIST OF ABBREVIATIONS xvii

CHAPTERS

1 INTRODUCTION 1

2 LITERATURE REVIEW 5

2.1 Remote Sensing Products 5

2.2 Machine Learning Algorithms 6

2.3 Classification Level 7

2.4 Studies Performed over Türkiye 7

2.5 Large Scale Crop Maps 8

3 METHODOLOGY 13

3.1 Study Area 18

3.2 Ground Truth Data 18

3.3 Remote Sensing and Reanalysis Data 19

3.3.1 Sentinel-2 for Classification Features 21

3.3.2 Era5-Land for Temperature Zones 22

3.4 Gap Filling 27

3.5 Spectral Indices 27
3.6 Data Partitioning 30
3.7 Machine Learning 32
3.7.1 Random Forest 33
3.7.2 Feature Selection 35
3.7.3 Hyperparameter tuning 38
3.8 Crop Mapping 39
3.9 Accuracy Assessment 39
4 RESULTS AND DISCUSSION 41
4.1 Random Forest Classifier Accuracy on the Test Set 41
4.1.1 Low-Temperature Zone 41
4.1.2 Medium-Temperature Zone 42
4.1.3 High-Temperature Zone 45
4.1.4 Combined Temperature Zones 47
4.1.5 Comparison with the Classifier without the Temperature Zones 49
4.2 Visual Inspection of the Classification Map 53
4.3 Percent Area Comparison with Province Production Data of Ministry of Agriculture and Forestry 58
5 CONCLUSION 67
REFERENCES 71

LIST OF TABLES

TABLES

Table 2.1. Large-Scale Crop Classification Studies 11
Table 3.1. Land Cover Classes Used in the Study 19
Table 3.2. Radiometric and Spatial Resolutions of Sentinel-2 Images (Earth Resources Observation and Science (EROS) Center, 2018)..... 21
Table 3.3. Training, Validation and Test pixel number of each class for Low, Medium and High Temperature Zones 32
Table 3.4. The Numbers of Each Band and Index in the Best Performing 120 Inputs for All Temperature Zone Classifiers and the Total of the Temperature Zones..... 37
Table 3.5. The Numbers of Bands and Indices in Each Month in the Best Performing 120 Inputs for Each Temperature Zone Classifiers and Total of the Zones. 37
Table 3.6. Hyperparameters for Random Forest 38
Table 3.7. A Simple Error Matrix and Formulas for User's Accuracy and Producer's Accuracy. 40
Table 4.1. Confusion Matrix, Producer's Accuracy, User's Accuracy, Overall Accuracy, Cohen's Kappa, and Pixel Number of Low-Temperature Zone 42
Table 4.2. Confusion Matrix, Producer's Accuracy, User's Accuracy, Overall Accuracy, Cohen's Kappa, and Pixel number of Medium-Temperature Zone 44
Table 4.3. Confusion Matrix, Producer's Accuracy, User's Accuracy, Overall Accuracy, Cohen's Kappa, and Pixel number of High-Temperature Zone..... 46
Table 4.4. Confusion Matrix, Producer's Accuracy, User's Accuracy, Overall Accuracy, Cohen's Kappa, and Pixel number of Combined Temperature Zones... 48
Table 4.5. Confusion Matrix, Producer's Accuracy, User's Accuracy, Overall Accuracy, Cohen's Kappa, and Pixel number of Classification on Test set without Temperature Zones 51

Table 4.6. Kappa Coefficient and Overall Accuracy for Combined Temperature Zones and Classification Without Temperature Zones with Improvement in Accuracy with Temperature Zoning 52
Table 4.7. Producer's Accuracy for Each Class for Combined Temperature Zones and Classification Without Temperature Zones with Improvement in PA with Temperature Zoning 52

LIST OF FIGURES

FIGURES

Figure 3.1. Methodology Flowchart 17
Figure 3.2. NDVI vs. Day of the Year for Two Wheat Pixels. Pixel shown in red is Located in Eastern Türkiye (37.473°E,39.182°N), While the Black One is in Western Türkiye (26.424°E,41.171°N). 23
Figure 3.4. Spectral Curves of 3 Different Land Cover Types (Water, Vegetation, Soil) Obtained Using Hyperion EO-1 Hyperspectral Image 28
Figure 3.5. True Color (Red Green Blue) b) Normalized Difference Vegetation Index, c) Normalized Difference Water Index (M), d) Normalized Difference Water Index (G) Versions of a Sentinel-2 Image located at 30.268°E, 37.749°N . 30
Figure 3.6. Illustration of a decision tree with a single feature and three possible classes. The tree first splits the feature space at the value of $x1$, either predicting the class C1, or going to the next split. At the next split, at $x2$, the decision tree either predicts C2 or C2 34
Figure 4.1. Crop Classification Map 55
Figure 4.2. Misclassification of Salt Lake .....**Hata! Yer işareti tanımlanmamış.**
Figure 4.3. Misclassification as Olive in West Türkiye.....**Hata! Yer işareti tanımlanmamış.**
Figure 4.4. Patch in the Classification Map Due to Temperature Zones ... **Hata! Yer işareti tanımlanmamış.**
Figure 4.5. Misclassification as Oat in Northeast Türkiye 58
Figure 4.6. Percent Area Comparison with Province Production Data of Ministry of Agriculture and Forestry for Sugar Beet 59
Figure 4.7. Percent Area Comparison with Province Production Data of Ministry of Agriculture and Forestry for Potato 60
Figure 4.8. Percent Area Comparison with Province Production Data of Ministry of Agriculture and Forestry for Cotton 61

Figure 4.9. Percent Area Comparison with Province Production Data of Ministry of Agriculture and Forestry for Chickpea 62
Figure 4.10. Percent Area Comparison with Province Production Data of Ministry of Agriculture and Forestry for Maize 63
Figure 4.11. Percent Area Comparison with Province Production Data of Ministry of Agriculture and Forestry for Red Lentil 63
Figure 4.12. Percent Area Comparison with Province Production Data of Ministry of Agriculture and Forestry for Barley 64
Figure 4.13. Percent Area Comparison with Province Production Data of Ministry of Agriculture and Forestry for Wheat 65
Figure 4.14. Percent Area Comparison with Province Production Data of Ministry of Agriculture and Forestry for Rice Paddy 66

LIST OF ABBREVIATIONS

ABBREVIATIONS

BUGEM	Republic of Türkiye Ministry of Agriculture and Forestry General Directorate of Plant Production
GEE	Google Earth Engine
HTZ	High-Temperature Zone
LTZ	Low-Temperature Zone
MTRY	Number of classification variables used at each split for random forest
MTZ	Medium-Temperature Zone
NDVI	Normalized Difference Vegetation Index
$NDWI_G$	Normalized Difference Water Index proposed by Gao (1996)
$NDWI_M$	Normalized Difference Water Index proposed by McFeeters (1996)
NTREE	The number of classification trees for random forest
NIR	Near-Infrared
OA	Overall accuracy
PA	Producer's accuracy
RF	Random forest
TMA	Republic Of Türkiye Ministry of Agriculture and Forestry
TÜİK	Turkish Statistical Institute
UA	User's accuracy
VI	Vegetation Index

CHAPTER 1

INTRODUCTION

Land cover is the physical material observed at the Earth's surface (Di Gregorio, 2005; Liu et al., 2020), and it is a fundamental variable that affects and connects the human and physical environment in several aspects (Southworth et al., 2004). Some of the many topics that can be implemented using land cover maps and land cover change maps are: estimation of soil erosion (e.g., Chen et al., 2019; Uddin et al., 2018), flood risk and flood damage assessment (e.g., Recanatesi & Petroselli, 2020; van der Sande et al., 2003), monitoring deforestation (e.g., Erasmi et al., 2004), forest rehabilitation planning (e.g., Apan, 1997), monitoring urban growth dynamics, (e.g., Hassan, 2017; Mandal et al., 2019) and assessing ecosystem services supply and demand dynamics (e.g., Tao et al., 2018). Along with these topics, agricultural crop cover mapping, which provides information to identify major crop types in a region and determine the area covered by these crops (Bauer et al., 1978), is also studied in this context.

Accurate information on seasonal or yearly agricultural land cover benefits many aspects like water resources management, crop yield prediction, and planning of domestic and foreign policies and actions for governments (Bauer et al., 1978). Agriculture is the biggest consumer of freshwater, with almost 75% of current human water consumption worldwide (Wallace, 2000). The increasing population of the world (UNDESA, 2017) and the increasing water use exceeding twice that of the population increase (Steduto et al., 2012) show how necessary it is to manage water resources with extreme attention. Creating accurate agricultural maps and interpreting these maps can be a step toward the well-planned use of water resources.

Remote Sensing based crop classification has been done over different regions in Türkiye (e.g., Abdikan et al., 2018; Alganci et al., 2013; M Turker & Arikan, 2005). However, country-level mapping studies remain missing. Ministry of Agriculture and Forestry has datasets showing ground conditions, but these datasets depend on farmers' declarations which may not reflect the reality, particularly during disaster years. In addition, it is not possible to obtain information about which crops are planted by the farmers who do not make a declaration, as such declarations are only made for the crops that receive an incentive from the government to compensate for the oil and the fertilizer costs of the farmers. So, there is a need for an objective methodology to obtain agricultural crop classification maps over Türkiye. There are also large-scale landcover projects like CORINE (Coordination of Information on The Environment), but these projects lack local information and features unique to the country (Özür & Ataol, 2018).

It is critical that large-scale crop maps include as many of the classes available in the area as possible to represent the land cover accurately. Otherwise, classification accuracy can be misleading when the study area is covered with various types of crop classes on a regional scale. To increase the accuracy of the crop classification map, in addition to 6 non-agricultural classes (bare soil, urban, forest, steppe, green house, water), 34 crop classes (alfalfa, apple, apricot, bare soil, barley, bean (dry), cherry, chickpea, cotton, forest, grape, green house, green tea leaves, hazelnut, lemon, maize, mandarin, melon, oat, olive, onion (dry), orange, peach, pepper, poppy, potato, rapeseed, red lentil, rice paddy, steppe, sugar beet, sunflower, tobacco, tomato, triticale, urban, vetch, water, watermelon, wheat) are selected according to the production rates of the previous year are included in the crop classification map for this study.

Although Türkiye is located in the Mediterranean geography with relatively temperate climatic conditions, significant differences in climatic conditions from one region to another occur due to the variable nature of the landscape and especially the presence of mountains extending parallel to the coast (Sensoy et al., 2008). Also, previous studies show that phenology correlates highly with temperature (Siebert &

Ewert, 2012; Zhang & Tao, 2013). To capture the phenology difference and different crop distributions across Türkiye, average temperature information is included in the classification process for this study. The study area is divided into temperature zones in which separate classifications are performed with individual classificaiton algorithms for each temperature zone. It is intended to increase the accuracy of the crop map while contributing to the literature with this method of dividing a large-scale study area which has not been done in any other large-scale crop classification study.

This study aims to perform a multi-temporal, multispectral crop classification using Sentinel-2 products and random forests classifier to obtain a country-level crop map of 2019, including 40 land cover classes with 10 m spatial resolution over Türkiye. Apart from utilizing state-of-the-art methods and tools, this study pays attention to Türkiye's crop production and climatic factors aiming to represent the land cover more accurately with the help of local information.

CHAPTER 2

LITERATURE REVIEW

2.1 Remote Sensing Products

Using remote sensing products has been an effective way of mapping land cover since it allows collecting information at large scales easier and in a shorter amount of time compared to collecting field data (Jia et al., 2014). Crop classification using remote sensing products is performed in the literature with the help of mainly two types of sources, which are optical and radar remote sensing. Spectral information provided by optical products is used for crop identification by utilizing multiple spectral bands (e.g., Saini & Ghosh, 2018), time-series data (e.g., Cai et al., 2018; Maponya et al., 2020), and spectral indices (e.g., Sonobe et al., 2018; Y. Yang et al., 2015). Also, optical products enable the calculation of various indices (e.g., Normalized Difference Vegetation Index (NDVI)) that can improve land cover classification (Joshi et al., 2016). Sonobe et al. (2018) evaluated the contribution of spectral bands and vegetation indices to the classification accuracy and concluded that vegetation indices (VI's) increases the classification accuracy. Even though these articles prove that spectral band and index information explain a lot for class identification, some crops may have similar spectral characteristics in the growing period, which can decrease the classification accuracy (Yang et al., 2020). So, along with spectral information, temporal information can be used to identify different crop classes with the help of information on the growing patterns of crops (e.g., Ji et al., 2018; Yang et al., 2020). Nitze et al. (2012) show in their study that using multi-temporal data improves classification accuracy. Based on the results of these studies, temporal and spectral satellite data, in addition to spectral indices, are used in this study for more accurate crop classification.

Cloud-free radar images with high spatial resolution are also used in crop classification studies (e.g., Skriver et al., 2011; Zakeri et al., 2017). Apart from single-source classifications, there are studies in the literature that utilize both optical and radar remote sensing products (Ajadi et al., 2021; David et al., 2021; Sonobe et al., 2017). In their study, Dimov et al. (2017) showed that fusing Synthetic Aperture Radar (SAR9 and optical products improves the classification accuracy while also showing that optical products outperform SAR products. So, only the Sentinel-2 optical products are selected as the remote sensing source for this study to perform classification with high accuracy without increasing the computational cost with multiple products.

2.2 Machine Learning Algorithms

In addition to features of remote sensing products used in crop mapping, classification algorithms are vital to obtaining high accuracy (Sonobe et al., 2018). Various machine learning algorithms are vastly used for crop classification in the literature (e.g., Nitze et al., 2012; Zheng et al., 2015). Machine Learning algorithms are suitable for crop classification using remote sensing products due to their capability of handling large amounts of data and pattern recognition. Several machine learning algorithms are used in crop classification studies, such as the support vector machines (SVM) (e.g., Mathur & Foody, 2008), artificial neural networks (ANN) (e.g., Ji et al., 2018), and extreme gradient boosting (Xgboost) ((e.g., Ustuner et al., 2019). One of these algorithms is random forest (RF) classifiers, which consist of ensemble decision trees. In this study, these methods are applied to the training set, and similar accuracies are obtained, but the random forest algorithm is found to be the most cost-effective one, so it is selected as the classification algorithm that will be used in the crop classification. The high-performance of the classifier is also shown in the studies of Maponya et al. (2012) and Rodriguez-Galiano et al. (2012a) as the classifier performs well when high-dimensional data is used for classification. Another vital feature of Random forest is being consistent

with different hyperparameter combinations, which means that even though using the optimum parameters that determine how the classifier will treat the training data will increase the accuracy, similar accuracies can be obtained with different hyperparameter combinations (Ok et al., 2012). RF classifiers are also used for feature selection, which can be used for determining the most useful features or simply for decreasing the number of features to decrease the computational cost. Sonobe et al. (2018) and Hao et al. (2015) utilized random forest importance for evaluation of feature contribution to crop classification.

2.3 Classification Level

Land cover classifications can be performed in two levels: pixel-based by classifying individual pixels or object-based by aggregating a group of adjacent pixels (Long et al., 2013). In the context of crop maps, the object of the object-based classifications is fields or parcels. Object-based crop classification is studied using different methods in the literature, such as aggregating pixels after classification using parcel boundary information (e.g., Kussul et al., 2016) or performing classification over a segmented image (e.g., Zhang et al., 2016). For this thesis, pixel-level classification is performed since image segmentation for a large study increases the computational cost, and readily available parcel data could not be obtained to be used in the study.

2.4 Studies Performed over Türkiye

There are several crop classification studies performed over different regions of Türkiye. Turker and Arıkan (2005) demonstrated sequential masking classification of multi-temporal Landsat7 ETM+ images to identify summer crops at field level and achieved an accuracy of 81.3% over Karacabey, Türkiye. Ozdarici-Ok and Akyurek (2014) also performed object-based classification over Karacabey. They used SVM with multitemporal Kompsat-2 and Envisat ASAR and obtained overall accuracy (OA) and Kappa value of approximately 92% and 0.90. Ozdarici and

Turker (2011) compared field-based agricultural classifications of the SPOT4 XS, SPOT5 XS, IKONOS XS QuickBird XS, and QuickBird PS over the south-west of the town of Karacabey. Alganci et al. (2013) used Spectral Angle Mapper (SAM) and SVM methods for pixel-based classification and Maximum Likelihood (ML) for object-based classification with SPOT5 and Landsat-5 TM data over Şanlıurfa province. Akar and Güngör (2015) classified hazelnut and tea plants in the Kumru district in Trabzon-Sürmene with the RF classifier using WorldView-2 MS images taken in summer and winter. They also utilized NDVI and multiple texture information to improve classification accuracy. Abdikan et al. (2018) performed crop classification over a test area located at the Konya Basin to evaluate the sensitivity of Sentinel-1 SAR image to crop height. Even though these papers reach high accuracies, there is still an absence of a crop map that covers the whole Türkiye, and the motivation of this study is to fill this gap in the literature.

2.5 Large Scale Crop Maps

Crop mapping is practiced over large areas in several studies. Studies have similar approaches in terms of the study area, classifier, remote sensing source, and accuracy assessment are given in Table 2.1. Jiang et al. (2020) built three remote sensing-based models using multiple indicators and monitored the distribution of the major crop types in the main grain-producing area of China with Sentinel-2. They estimated images agreed well with field survey data (average OA = 94%) and the national agricultural census data (R^2 = 0.78), which proves the applicability of the Sentinel-2 data for large-scale, high-resolution crop mapping in China.

Yılmaz et al. (2020) presented preliminary results of an analysis aimed at classifying 18 different agricultural products in the Gediz Basin with different climatic areas with optical and multi-temporal satellite images using random forest and 3D-CNN methods. They observed that 3D-CNN classified crops in the Basin at pixel-level and parcel level with overall accuracies of 72.7% and 67.6%, respectively, and random forest approach, OA of 70% was achieved in the same region at parcel level.

Yang et al. (2019) proposed a new method based on grids to address the inconsistent availability of high-medium resolution images for large-scale crop classification. They first proposed a method to block the remote sensing data into grids to solve the problem of temporal inconsistency. Then they introduced a parallel computing technique to improve the efficiency on the grid scale. Random Forest and Support Vector Machines algorithms are tested for their performance, and Random Forest gave better accuracies. They obtained classification accuracies reaching 88%, 82%, and 85% in 2015, 2016, and 2017, respectively.

d'Andrimont et al. (2021) presented the first continental crop map with 19 crop types at 10-m spatial resolution for the EU based on Sentinel 1A and Sentinel 1B SAR observations for 2018 using random forest. They obtained an overall accuracy of 80.3% when grouping main crop classes and 76% when considering 19 crop type classes separately.

Woźniak et al. (2022) proposed a set of multi-temporal indices derived from time-series Sentinel-1 images to characterize crop phenology. The authors developed an object-oriented classification technique and tested it on 16 crop types for the whole of Poland. Their analysis found that OAs varied on a regional level from 86.36% to 89.13% in 2019 and from 85.95% to 89.81% in 2020. The authors also indicate that they performed classification with other machine learning algorithms, K-nearest neighbour (KNN) (Cover & Hart, 1967), Naive Bayes (NB) (Duda & Hart, 1973), Linear Support Vector Machine (SVM) (Vapnik et al, 1995), Radial Basis Function Support Vector Machine (RBF SVM) (Scholkopf et al., 1996), Neural Networks (NN) (Kohonen, 1988), Quadratic Discriminant Analysis (QDA) (Frank and Friedman, 1989), Decision Tree (DT) (Safavian & Landgrebe 1991), AdaBoost (AB) (Freund & Schapire, 1996) in addition to Random Forest and Random Forest gave the best accuracies.

Studies of Jiang et al. (2020), Yılmaz et al. (2020), Yang et al. (2019), and Woźniak et al. (2022) shows that Sentinel-2 products are suitable for large-scale crop classification. So, it is another motivation for the selection of these products as the

remote sensing sources for this study, in addition to their suitable temporal and spectral resolution.

Random forest classifier is used in the studies of Yılmaz et al. (2020), Yang et al. (2019), d'Andrimont et al. (2021), and Woźniak et al. (2022), which shows that the Random Forest classifier is preferred between all other classifiers. In addition to that, Woźniak et al. (2022) and Yang et al. (2019) show in their study that Random Forest outperforms other popular classification algorithms. Thus, the Random Forest algorithm is selected as the classifier for this study, considering its performance is proven by other studies in addition to its other benefits that are mentioned in the '2.2. Machine Learning Algorithms' subchapter of the Literature Review chapter.

The studies given in Table 2.1 have a maximum of 21 classes for classificaiton while for this study, 34 crop and six non-agricultural classes are selected for the crop map. For large-scale maps, it is important to represent the study area as accurately as possible. If the crop fields used in classification are not masked from other land covers, as the number of classes increases, the crop map's accuracy and representativeness are expected to increase. So, in this study, it is intended to use more classes than the studies in the literature for a more accurate crop cover map.

Table 2.1. Large-Scale Crop Classification Studies

Publication	Remote Sensing Source	Study Area	Number of Classes	Classifier	Accuracy
Jiang et al. (2020)	Sentinel-2	3 crop producing plains of China	5	DT	94% OA
Yılmaz et al. (2020)	Sentinel-2	Gediz Basin	18	RF 3D-CNN	70% OA & 0.65 Kappa 73% OA & 0.68 Kappa
Yang et al. (2019)	GF-1 WFV & Sentinel-2	China	4	RF SVM	86% OA & 0.76 Kappa 84% OA & 0.74 Kappa
d'Andrimont et al. (2021)	Sentinel-1	European Union	21	RF	76% OA
Woźniak et al. (2022)	Sentinel-2	Poland	16	RF	89% OA & 0.88 Kappa

CHAPTER 3

METHODOLOGY

In this chapter of the thesis, the methodology of crop classification is given. Firstly, a flowchart with numbered steps in Figure 3.1 is explained briefly for the methodology to be followed more easily. The box number for each step is given in parentheses while it is described in the text. After that, each method and the dataset are explained in detail in the related subchapters of the Methodology chapter.

Supervised classification is a machine learning method used to assign one of the predetermined classes to each data point with the help of a classification algorithm trained using predictor variables. In this study, predictor variables are spectral bands of Sentinel 2 and some spectral indices that will be explained in detail in subchapter '3.5. Spectral Indices' classification algorithm is Random Forest, the study area is Türkiye, and the predetermined classes are 40 agricultural and non-agricultural classes.

To prepare the predictors, also called classification features, Sentinel-2 Level-2 images from March 15 to October 15, 2019, are collected into 14 image collections, each covering 15-days of data (Box 1). Sentinel 2 products have a 5-day revisit time (temporal resolution), which means that these products have the image of the same area taken every five days. So, each image collection has three images for every part of the study area. Since optical satellites like Sentinel-2 Level-2 have pixels contaminated with cloud and cloud shadows, these pixels are removed from the images with the help of a cloud mask and a cloud shadow mask (Box 2). After that, image collections cleared from cloud and cloud shadow pixels are reduced to the 15-median images using the median reducer tool in Google Earth Engine (GEE) platform by taking the median of the reflectance values of each image for each pixel

(Box 3). This way, each pixel of the study area has one value for each 15-day period (Box 4).

Spectral bands (reflectance values for each wavelength range of the products) of satellite images can be utilized to calculate spectral indices. For this study, NDVI, NDWI proposed by Gao (1996), and NDWI proposed by McFeeters (1996) are calculated for each 15-day period and added to the classification features (Box 5). In addition to these indices, "spring rate" and "summer rate" represent NDVI increase in spring (from the first half of May to the second half of June) and summer (from the first half of July to the second half of August) are calculated to be used as classification features (Box 5).

The ground truth data for this study is obtained from the firm Tarla.io as coordinates of fields for crop classes (Box 6). To obtain homogeneous training and test data, this data is visualized on GEE, and rectangular polygons are selected manually from this dataset for the crop classes (Box 7). And for the non-agricultural classes, pixels are selected manually by visualizing selected scenes at the high-resolution satellite view of GEE (Box 7). After that, classification features are extracted from the Sentinel-2 and spectral index data for each selected pixel. (Box 8)

To be able to capture the phenology difference occurring due to temperature differences between regions, the study area is divided into temperature zones. For the mask, the 2-meter temperature band of the ERA5-Land monthly averaged dataset is averaged for the last 20 years (Box 9). The average temperature map is visualized in the GEE, and temperature thresholds that determine the temperature regions are selected so that the major crop plains are not divided. As a result, the study area is divided into three temperature zones as Low-Temperature Zone (Box 11), Medium-Temperature Zone (Box 12), and High-Temperature Zone (Box 13). After this step of the methodology, each step is repeated for each temperature zone separately, as it is shown with a looping arrow.

For supervised classification, three data subsets can be used to be able to create a classifier that is adjusted to give the best results on different datasets with the same

predictors. These subsets are the training set (Box 16), which is used to train the classifiers, the validation set (Box 17), which is used to test the accuracy while finding the best parameters that determine the structure of the classifier, and lastly, test (Box 15) set for final accuracy assessment of the classifier that will be used for mapping.

This study aims to create a crop map covering the whole of Türkiye with a 10-meter spatial resolution, which means classifying billions of pixels. To decrease the computational cost of this process, some classification features that are not contributing to the accuracy should be eliminated. For this purpose, feature selection by random forest importance is performed on the training data, and classes with the least contribution to classifier accuracy are removed from the dataset (Box 18). The detail of this process is also further explained in the related subchapter. At the end of this step, final classification features are obtained to be used for classification (Box 19)

A random forest classifier has two parameters that determine the classifier's structure, called hyperparameters. To find the combination of these hyperparameters that gives the highest accuracy on the validation set, hyperparameter tuning using grid search is performed (Box 20). Grid search refers to performing classification for each combination of selected options for both hyperparameters and calculating the accuracy on the validation set for these combinations. After completing this step, final hyperparameters are obtained (Box 21).

Using the final hyperparameters and classification features, a random forest classifier is created for each temperature zone (Box 22). Then, selected accuracy measures, overall accuracy, user's accuracy, producer's accuracy, and Cohen's Kappa (Cohen, 1960) are calculated to test the performance of the classifier on independent test data (Box 23). The details of the accuracy measures are given in the related subchapter. Finally, the classification features for the whole Türkiye are extracted from the 15-day median images (Box 24). Using the random forest classifiers created for each temperature zone, each pixel of Türkiye is classified according to the temperature

zone each pixel is located in. After this final step of methodology, a crop cover map of Türkiye for the year 2019 is obtained (Box 25).

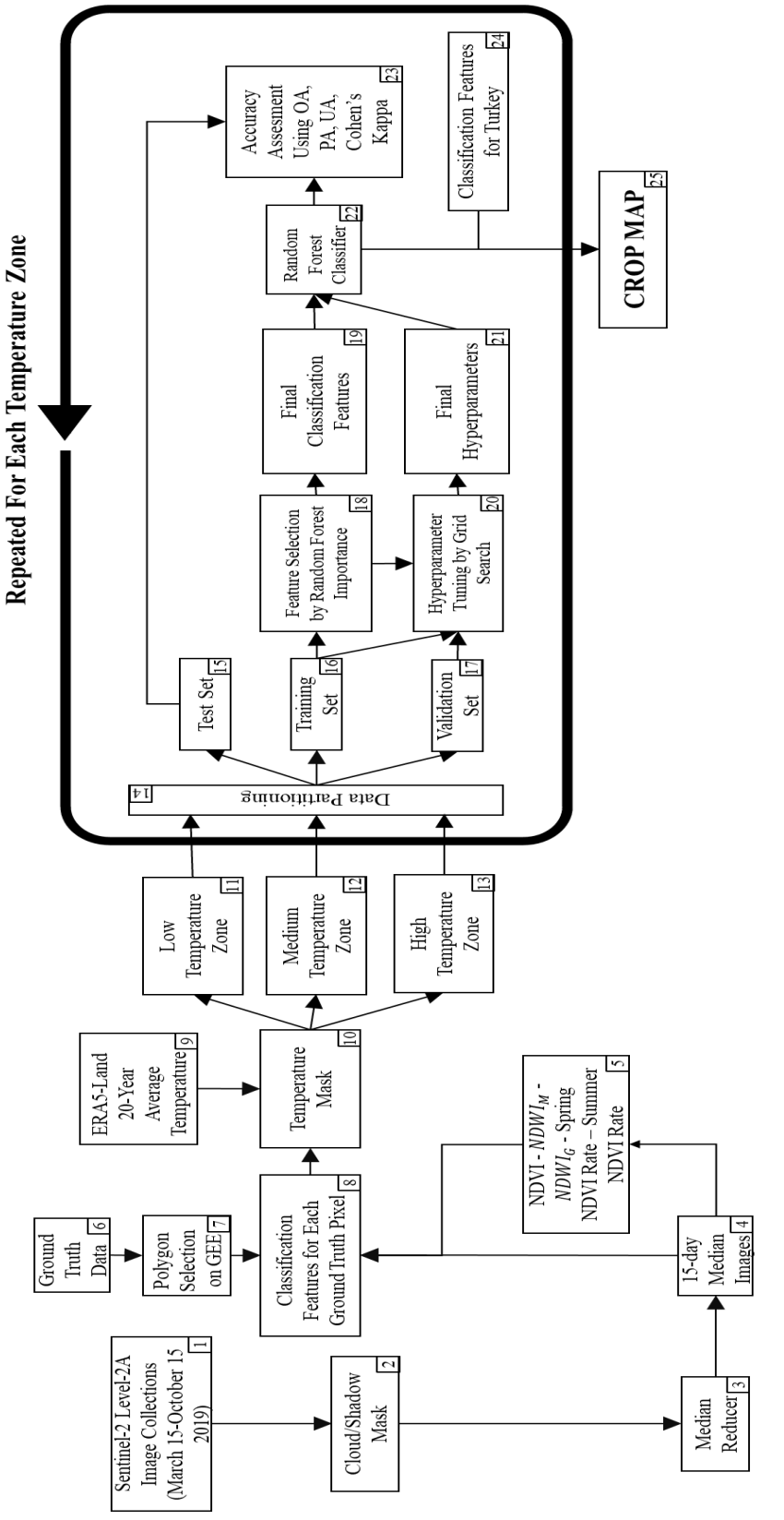

Figure 3.1. Methodology Flowchart

3.1 Study Area

Türkiye is located in Anatolia in Western Asia, with a portion in Southeast Europe, between latitudes from 35.9 to 42.0 Northern and longitudes from 25.9 to 44.6 Eastern. Although Türkiye is located in the Mediterranean geography with relatively temperate climatic conditions, significant differences in climatic conditions from one region to another occur due to the variable nature of the landscape and especially the presence of mountains extending parallel to the coast (Sensoy et al., 2008). Due to its favorable geography, fertile soil structure, and suitable climatic conditions, various products such as vegetables, grains, and cotton are grown in almost every part of the country (Cakirli Akyüz & Theuvsen, 2021). According to Plant Production Data provided by the Turkish Statistical Institute (2020), 29.5% of Türkiye's Land was used for agricultural production in 2019.

3.2 Ground Truth Data

Ground truth data is received from the observations obtained from the fields of the firm named Tarla.io. This company, which provides agricultural risk management services, does business with many farmer customers by obtaining information from the field where they plant crops. For this reason, the information they provide is considered to be reliable. No other data source is used for ground truth data for crop classes. In its raw form, data consist of parcel coordinate information of 105 types of crop fields all over Türkiye. To perform supervised classification, for which the classes should be determined prior to the classification, crop classes are selected with the help of agricultural production data for 2018 showing ton production of crops provided online by the Turkish Statistical Institute (2018). Crops are sorted according to the total ton of production, and the top 34 crops with an adequate number of data are selected as classes for the crop map. These selected crops take up

to 86% percent of the total ton of production, and the remaining crops are not included in the study since they do not cover as much area as selected crops. In addition to the crop classes, six non-crop classes: green house, bare soil, water, urban, steppe, and forest, are chosen to represent the study area more accurately. Final class names are shown in Table 3.1. To obtain homogeneous training and test data, provided ground truth data is visualized on GEE, and rectangular polygons are selected manually from this dataset. Geometry size and the pixel number in the polygons change according to the original field size. Data for non-agricultural classes are selected manually by visualizing selected scenes at the high-resolution satellite view of GEE. After the data selection, ground truth data is exported from GEE in shapefile format for classification.

Table 3.1. Land Cover Classes Used in the Study

Alfalfa	Cow vetches	Red Lentil	Peaches	Sunflower
Apples	Dry beans	Maize	Pepper	Tobacco
Apricots	Forest	Mandarin	Poppy	Tomatoes
Bare soil	Grapes	Melon	Potatoes	Triticale
Barley	Green House	Oats	Rapeseed	Urban
Cherries	Green Tea Leaves	Olive	Rice Paddy	Water
Chickpea	Hazelnuts	Onion (Dry)	Steppe	Watermelon
Cotton	Lemons	Oranges	Sugar beets	Wheat

3.3 Remote Sensing and Reanalysis Data

Remote Sensing is defined as the accusation of physical information about the Earth's surface using sensing devices positioned away from the target (Colwell & Katibah, 1976). Remote sensing sensors are basically divided into two types: passive and active sensors (Weng, 2013). While active sensors send stimulus to the Earth and acquire the response of the target to that stimulus, passive sensors receive information from reflected solar radiation (Colwell & Katibah, 1976; Viskovic et al.,

2019). Airborne light detection and ranging (LiDAR) and Synthetic-Aperture Radar (SAR) are commonly used examples of active remote sensing sensors. Radar sensors collect the backscatter, which is dependent on the structure and geometry of the target (Joshi et al., 2016). The difference in this backscatter information has been used for land cover identification in various studies (e.g., Pierce et al., 1998.; Skriver et al., 2011; Zakeri et al., 2017). For passive remote sensing, cameras and optical satellites can be given as commonly used examples. Some optical remote sensing products like Sentinel 2, Landsat Thematic Map, Satellite Pour l'Observation de la Terre (SPOT), and the Moderate Resolution Imaging Spectroradiometer (MODIS) dominate land cover studies as these products have offered consistent and easily available products for decades (Colwell & Katibah, 1976). Satellites provide information in multiple spectral bands defined by their reflectance wavelength and bandwidth (Viskovic et al., 2019). While these bands from a single image can be used to identify land cover types, various spectral indices can be calculated using multiple spectral bands, or a time series of images can be used to further understand land covers' pattern of change through the year or growing season. Using time-series information utilizes both spectral and temporal information, which can result in improved classification performance since crops have different growing patterns (Ji et al., 2018).

Another type of data used in the study is climate reanalysis data. To create climate reanalysis datasets, available climate observations are reanalyzed using advanced data assimilation methods to obtain an initial state for the following short-term forecast, creating a continuous three-dimensional field of meteorological variables (Bengtsson et al., 2004). Several climate reanalysis datasets are produced for climate and weather forecast studies, such as European Centre for Medium-Range Weather Forecasts (ECMWF) 15-year reanalysis (ERA15) (Gibson et al., 1997) and NASA Goddard Earth Observing System 1 (GEOS1) reanalysis (Schubert et al., 1993).

3.3.1 Sentinel-2 for Classification Features

The European Space Agency's Multispectral Instrument on the Sentinel-2 satellite (Earth Resources Observation and Science (EROS) Center, 2018) has been providing multispectral images every ten days since 2015 on a global extent. The Sentinel-2 mission includes two satellites developed to monitor vegetation, land cover, and the environment. The Sentinel-2A and Sentinel-2B satellites operate in a sun-synchronous orbit with a 10-day temporal resolution, and they cover Earth's surface in 5-day intervals. Spectral bands of Sentinel-2 are given in Table 3.2. A Sentinel-2 tile consists of pixels covering a 100 km*100 km area with a UTM/WGS84 (Universal Transverse Mercator/World Geodetic System 1984) projection and datum.

Table 3.2. Radiometric and Spatial Resolutions of Sentinel-2 Images (Earth Resources Observation and Science (EROS) Center, 2018)

Band Number	Central Wavelength (nm)	Bandwidth (nm)	Spatial Resolution (m)
1	443	20	60
2	490	65	10
3	560	35	10
4	665	30	10
5	705	15	20
6	740	15	20
7	783	20	20
8	842	115	10
8a	865	20	20
9	945	20	60
10	1375	30	60
11	1610	90	20
12	2190	180	20

Predictor variables are usually called features in classification and pattern recognition literature (Hastie et al., 2009) (e.g. spectral bands of setallites for remote sensing based crop classification). To obtain the classification features for this study, starting from March 15, 2019, to October 15, 2019, for each 15-day interval, tiles of

Sentinel-2 Level-2A are collected to create 15-day image collections over the whole study area. After that, images in each image collection are cleared from cloud cover using the S2 cloud probability dataset (s2cloudless) on GEE with a maximum cloud probability of 20%. Cloud shadow pixels are also masked from the images by considering cloud projection intersection with low-reflectance NIR pixels, as demonstrated by Braaten (n.d.). After the cloud masking process, cloud and cloud shadow pixels in the original satellite images have NA values. Since the Sentinel-2 Level-2 products have an image every five days, each part of the study area has an image acquired every five days. In this study, using images with 5-day intervals would increase the computational cost. So, after obtaining image collections that are cleared from cloud and cloud shadow pixels median of the images that cover the same area is taken for each 15-day interval using the median reducer tool in the Google Earth Engine platform. This way, the computational cost is decreased by decreasing the number of images used in the study, and spectral changes are captured twice a month. As a result, 14 images are obtained for classification as one image for every 15-day interval between March 15 - October 15, 2019. All bands of obtained images are exported separately for each image from GEE except for Band 10 (short wave infrared – cirrus), which is used only for cloud probability calculation before image reduction. So, 12 bands of each 14 images (168 spectral bands in total) are obtained to be used as classification inputs (classification features).

3.3.2 Era5-Land for Temperature Zones

This study utilizes crop phenology for the identification of different crops using multi-temporal satellite imagery. Previous studies show that phenology correlates highly with temperature (Siebert & Ewert, 2012; Zhang & Tao, 2013). Also, when vector data is inspected, major crop types like wheat, barley, and potatoes had different growing patterns in different regions. In Figure 3.2, this phenology difference is demonstrated with the NDVI time-series data of two wheat pixels. One pixel is located in eastern Türkiye, while the other pixel is located in western

Türkiye, where the average temperatures are much higher than in the east part of Türkiye. There is a visible difference between the growing periods of two pixels located in different climates. To capture the phenology difference occurring due to temperature differences between regions, ERA5-Land is utilized for a temperature mask.

ERA5-Land is produced by replaying the land component of the ECMWF ERA5 climate reanalysis (Muñoz-Sabater et al., 2021). It contains regular latitude-longitude gridded record with a temporal resolution of 1 hour since 1950. Horizontal coverage of the ERA5-Land product is 0.1° x 0.1°; (Native resolution is 9 km), and its vertical coverage is from 2 m above the surface level to a soil depth of 289 cm. It provides information globally with an update frequency of monthly with a delay of 2-3 months from the actual date. Some of the main variables of ERA5-Land are 2m temperature, 2m dewpoint temperature, total precipitation, and total evaporation. The data used in the study is downloaded as post-processed by monthly averaging the full ERA5-Land dataset.

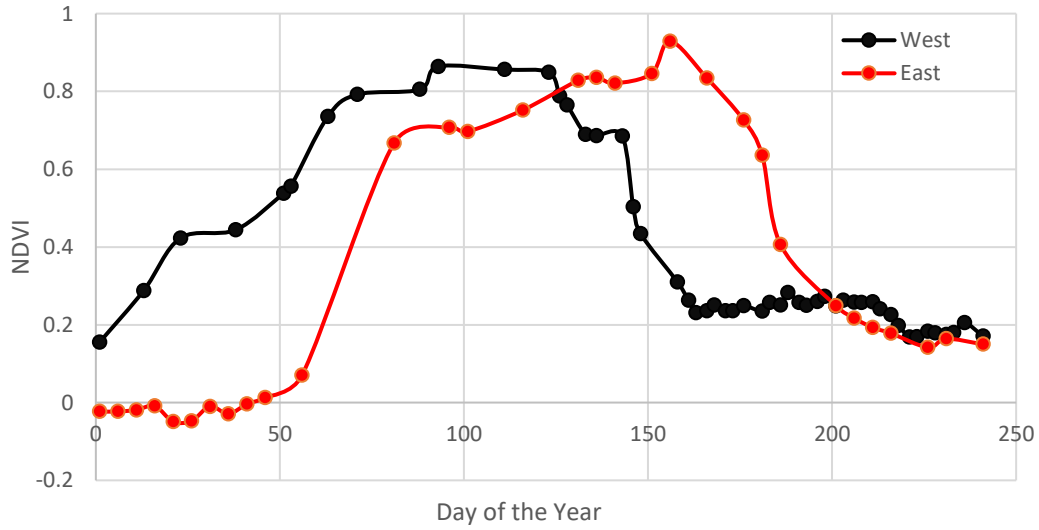

Figure 3.2. NDVI vs. Day of the Year for Two Wheat Pixels. Pixel shown in red is Located in Eastern Türkiye (37.473°E,39.182°N), While the Black One is in Western Türkiye (26.424°E,41.171°N).

For the temperature mask, the 'temperature_2 m' band of ERA5-Land monthly averaged dataset is averaged for 20 years (1999-2019). The average temperature map is visualized in the GEE, and temperature thresholds that determine the temperature regions are selected so that the major crop plains are not divided. Different thresholds were also tested, but they resulted in a greater number of crop plains that are divided to fall into two temperature zones. As a result, the Low-Temperature Zone (LTZ) is set to have a maximum temperature of 9 degrees Celsius; the Medium-Temperature Zone (MTZ) is set to have a minimum temperature of 9 degrees Celsius and a maximum temperature of 14 degrees Celsius. Finally, the High-Temperature Zone (HTZ) is set to have a minimum temperature of 14 degrees Celsius. The temperature mask raster is later exported from GEE and resized to match spatial resolutions with Sentinel-2 data on QGIS software. Due to a lack of temperature information on coastal regions resulting from spatial resolution differences between two products, the temperature mask is extended using the R programming language (R Core Team, 2020) so that each empty pixel is filled with the value of the nearest pixel with a non-NA value. After these preprocessing steps, Sentinel-2 images and the temperature mask are resized and reprojected to have the same Coordinate Reference Systems (CRS), spatial resolution, and boundaries. A total of 169 rasters (12 spectral bands for each 14 date intervals and one temperature mask) is cropped with the extent of vector coordinate data on R, and a resultant data frame is formed to have 168 spectral reflectance values, one temperature mask value, the land cover class number for each pixel. The data frame is later divided into three separate data frames based on the temperature zone information. The reason for averaging multiple years instead of selecting the year of the map is to capture the crop planting tendencies of farmers for a more realistic crop distribution over the study area. The resultant temperature map is shown in Figure 3.3. along with the distribution of agricultural and nonagricultural class pixels used in the study. Another reason for not using only 2019 data is to be able to apply these classifiers on other years when Sentinel-2 data is available. Using only 2019 temperatures would not give generalizable results thus could not to be

used in different years. But for a single year classification, temperatures of that years can also be used for temperature masking.

In addition to separate data frames for each temperature zone, one classifier is created without separating the dataset into temperature zones. The reason for this is to test whether or not the division of the study area into temperature zones increases the classification accuracy. The details for this dataset are given in the '3.6 Data Partitioning' subtitle of the Methodology chapter.

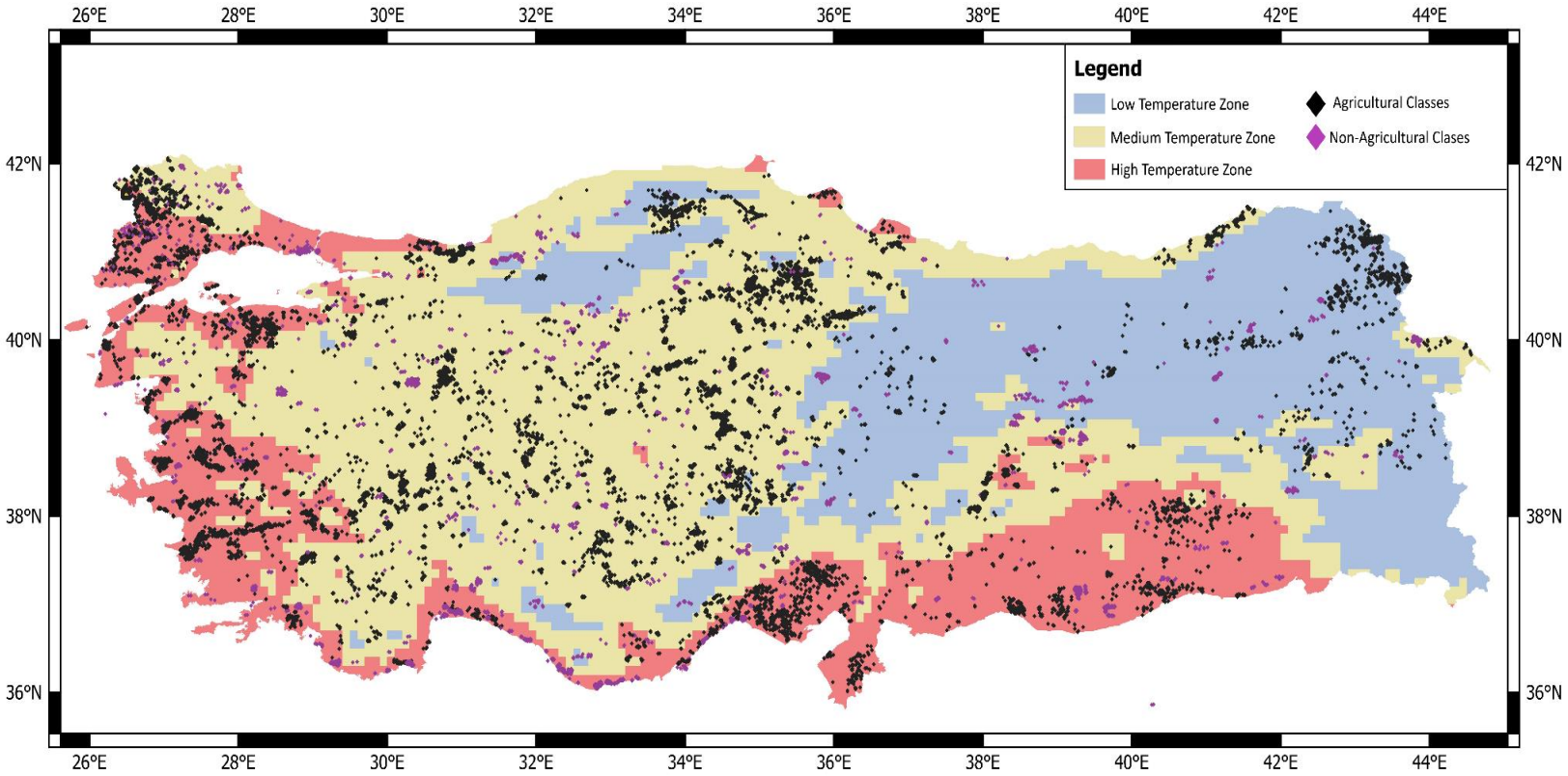

Figure 3.4. Distribution of Agricultural and Nonagricultural Class Pixels on the Resultant Temperature Map

3.4 Gap Filling

Since there are unavoidable cloud-masked gaps in the data after making cloud and cloud shadow pixels have NA values with cloud mask, some crop pixels have NA values instead of spectral reflectance values. So, these pixels become unusable since each pixel should have the same number of classification features for the classifier to work. To use as many pixels as possible, a computationally efficient gap-filling procedure based on linear interpolation is followed on a temporal scale similar to the method used by Griffiths et al. (2019). Bands with empty (NA) values are filled with the average of the next and previous months' same band. For example, if the red band of the first 15-days of the May image is NA, it is filled with the average of the red band of the second 15-days of the April image and the red band of the second 15-days of the May image. Later, cloud gaps could not be filled with this method in the first 15-day image of April due to consecutive cloud pixels, and these gaps are filled with the values of the second 15-day of March. After the gap-filling process, remaining NA pixels that could not be filled due to consecutive missing data are removed from the dataset.

3.5 Spectral Indices

Different land cover types have different spectral curves, which means that they reflect different portions of the incoming energy in each wavelength, as shown in Figure 3.4. This figure shows the spectral curves of 3 different land cover types, water (33.587°E, 39.148°N), vegetation (33.598°E, 39.152°N), and soil (33.590°E, 39.148°N), obtained using a Hyperion EO-1 Hyperspectral image of June 2016.

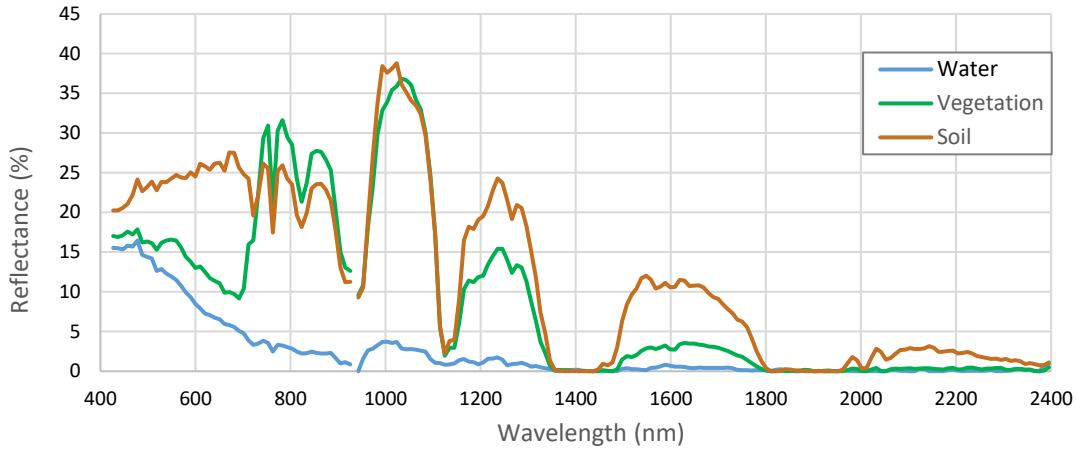

Figure 3.5. Spectral Curves of 3 Different Land Cover Types (Water, Vegetation, Soil) Obtained Using Hyperion EO-1 Hyperspectral Image

Spectral indices are calculated using combinations of spectral bands that enhance specific spectral properties (Palacios-Orueta et al., 2006). Normalized Difference Vegetation Index (NDVI) is a commonly used spectral index that can be used to benefit from the spectral reflectance difference between near-infrared (NIR) and red wavelengths (Bremer et al., 2011). Maximum chlorophyll absorption of a green leaf occurs at about 690 nm, which corresponds to red wavelength, while at the NIR wavelength interval (650-850 nm), absorption shows a significant decrease (Myneni et al., 1995). This spectral difference is suitable for differentiation between vegetation and other classes. Also, the magnitude or time interval of maximum NDVI can be used for differentiation between vegetation classes in land cover classification. The NDVI is calculated using Equation (1).

$$NDVI = (NIR - RED)/(NIR + RED) \quad (1)$$

The Normalized Difference Water Index (NDWI), proposed by McFeeters (1996) ($NDWI_M$) is a spectral index that increases the visibility of open water features in remote sensing products. $NDWI_M$ enhances the reflectance of water bodies utilizing green wavelengths and exploits the low NIR reflectance of water bodies compared to vegetation and soil. This way, water bodies that have high positive $NDWI_M$ can

be identified very easily (McFeeters, 1996). The $NDWI_M$ is calculated using Equation (2).

$$NDWI_M = (GREEN - NIR)/(GREEN + NIR) \quad (2)$$

Normalized Difference Water Index proposed by Gao (1996) ($NDWI_G$), aims to assess vegetation water content from remotely sensed data using the combination of NIR and short wave infrared (SWIR) channels (Zhang et al., 2017). Since dry soil, dry vegetation, and green vegetation has a different range of NDWI values (Gao, 1996), $NDWI_G$ can be used to differentiate these land cover classes. The $NDWI_G$ is calculated using Equation (3).

$$NDWI_G = (NIR - SWIR)/(NIR + SWIR) \quad (3)$$

The indices used in the study are demonstrated in Figure 3.5. Normalized Difference Vegetation Index, Normalized Difference Water Index proposed by Gao (1996), and Normalized Difference Water Index proposed by McFeeters (1996) are calculated for each 15-day period and added to the classification features. In addition to VIs, two features, "spring rate" and "summer rate", represent NDVI increase in spring (from the first half of May to the second half of June) and summer (from the first half of July to the second half of August) are calculated and added to classification features. With this addition, the classification algorithm has 212 input features (168 bands + 3 indices for 14 date intervals + 2 NDVI rates).

Some classification algorithms like SVM and ANN require scaled classification features to give accurate classification results. But since RF is a tree-based method that can incorporate different features in the classification process (Hastie et al., 2009), no scaling is performed even though spectral reflectance and spectral indices have very different maximum and minimum values.

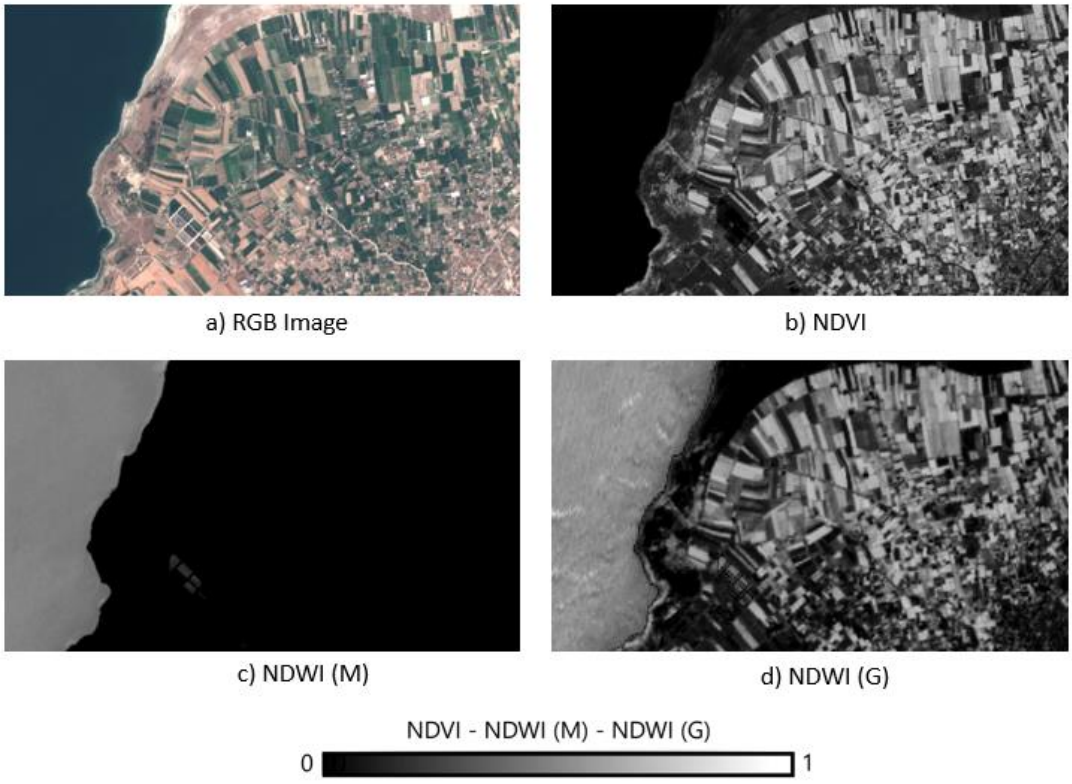

Figure 3.6. True Color (Red Green Blue) b) Normalized Difference Vegetation Index, c) Normalized Difference Water Index (M), d) Normalized Difference Water Index (G) Versions of a Sentinel-2 Image located at 30.268°E, 37.749°N

3.6 Data Partitioning

To perform an unbiased classification, the dataset is divided into three subsets as the training set (~70%), validation set (~15%), and test set (~15%). Since ground truth polygons contain more than one pixel, dividing a polygon into more than two subsets may result in overfitting, which occurs when the classification algorithm fits the training data too well and fails to predict when classification is performed on another set of data. To avoid that, polygons are distributed to subsets so that no polygon has pixels in more than one subset. After data is separated into three independent sets, the training set is used to train the classification algorithm, the validation set is used for hyperparameter tuning, and the test set is used for the final classification accuracy assessment. If a crop class does not have enough ground truth data in a temperature

zone to satisfy the needs for data partitioning, that crop is removed from the dataset for that temperature zone.

A dataset without temperature zones is created to test whether dividing the study area into temperature zones improves classification accuracy. For this dataset, the validation and test subsets, as well as the training subset of each temperature zone, are combined. Therefore, the classifier created with this data set has the number of training pixels equal to the sum of the training sets of each temperature zone. The training, validation, and test pixel number of each class for low, medium, and high-temperature zones and the dataset with no temperature zone separation are given in Table 3.3.

Table 3.3. Training, Validation and Test pixel number of each class for Low, Medium and High Temperature Zones

	LOW TEMPERATURE ZONE			MEDIUM TEMPERATURE ZONE			HIGH TEMPERATURE ZONE			WITHOUT TEMPERATURE ZONES		
	Training	Validation	Test	Training	Validation	Test	Training	Validation	Test	Training	Validation	Test
Alfalfa	1174	237	241	2413	419	471	1285	221	322	4872	877	1034
Apple				5074	1086	1089	232	34	48	5306	1120	1137
Apricot				6159	1297	1311	1794	365	402	7953	1662	1713
Bare Soil	9053	1882	1980	35679	3830	5455	12386	212	263	57118	5924	7698
Barley	7682	1624	1636	19060	4057	4075	1770	366	382	28512	6047	6093
Bean (Dry)	216	17	71	3503	711	782				3719	728	853
Cherry	231	47	52	2398	297	307	246	22	39	2875	366	398
Chickpea	426	83	99	23197	4922	4959	1061	135	165	24684	5140	5223
Cotton							31440	6666	6713	31440	6666	6713
Forest	6860	1453	1462	11920	2524	2525	4857	1020	1033	23637	4997	5020
Grape				705	138	162	9740	2069	2075	10445	2207	2237
Green House							2583	530	546	2583	530	546
Green Tea Leaves				284	57	60				284	57	60
Hazelnut				2971	597	657	673	140	145	3644	737	802
Lemon							5001	957	1066	5001	957	1066
Maize	284	16	102	27515	5676	5951	14991	3181	3200	42790	8873	9253
Mandarin							5731	1199	1198	5731	1199	1198
Melon				1430	113	454	233	46	54	1663	159	508
Oat	3020	645	649	2317	455	474				5337	1100	1123
Olive				284	13	82	5173	1092	1099	5457	1105	1181
Onion (Dry)				2807	592	608				2807	592	608
Orange							4379	870	911	4379	870	911
Peach				695	136	162	247	32	60	942	168	222
Pepper				520	58	164	876	143	208	1396	201	372
Poppy				7134	1423	1523				7134	1423	1523
Potato	1117	211	212	7711	1625	1648	125	19	26	8953	1855	1886
Rapeseed				3981	821	832	2251	157	617	6232	978	1449
Red Lentil				827	35	178	4203	665	706	5030	700	884
Rice Paddy	799	171	171	3125	644	674	14456	3023	3104	18380	3838	3949
Steppe	3403	706	722	4903	991	1027	7521	1267	1949	15827	2964	3698
Sugar Beet	622	106	143	2602	537	565				3224	643	708
Sunflower				13089	2784	2787	12530	2644	2679	25619	5428	5466
Tobacco				313	56	66	171	19	44	484	75	110
Tomato				816	149	177	3188	671	673	4004	820	850
Triticale				1361	286	288				1361	286	288
Urban	11	2	3	4932	1000	1108	5044	615	1451	9987	1617	2562
Vetch	2729	573	597	1054	217	217				3783	790	814
Water	272	32	40	1860	337	364	2055	435	438	4187	804	842
Watermelon				574	47	185	547	100	110	1121	147	295
Wheat	1234	251	255	14503	3051	3057	39419	8408	8440	55156	11710	11752

3.7 Machine Learning

Machine learning is a type of artificial intelligence in which the computer is programmed to mimic human learning to develop methods to solve problems such as classification and regression. In machine learning, the software is not explicitly programmed to have details of the processes and steps needed for the solution of a problem. Instead, they are programmed to learn from sample data and increase the accuracy of the desired results progressively.

Machine learning can be classified into two main types which are supervised learning and unsupervised learning. Supervised learning algorithms require labeled training data to be able to perform the given task, which can be finding patterns and constructing mathematical models (Nasteski, 2017). Supervised learning can be used for both classification and regression problems. In classification, prediction takes nominal values, while regression aims to obtain continuous results from the algorithm (Harrington, 2012).

Unlike supervised learning, unsupervised learning algorithms do not require training data with labels. The main objective of these algorithms is to search for similarities in the given data and categorize the data according to these similarities (Nasteski, 2017). Unsupervised classification is also called clustering, and categorized groups are called clusters. These clusters can be labeled by an experienced user in the postprocessing if class information is needed. Since the scope of this study is to obtain crop maps with crop labels for each pixel, supervised learning using ground truth data is performed for classification. Various supervised classification methods have been developed in the last decades, such as random forest (Breiman, 2001), support vector machines (Vapnik & Chervonenkis, 1964), artificial neural networks (McCulloch & Pitts, 1943), and k-nearest neighbor (Fix & Hodges Jr, 1952). In this study, the random forest algorithm is used for classification and feature selection. The computational times of algorithm training with other classifiers mentioned in the '2.2. Machine Learning Algorithms' subchapter (ANN, SVM, Xgboost) are tested and it is observed that each of them took more computational time than RF, which would make the hyperparameter tuning process very computationally costly with other methods. So, RF is preferred for the crop classification since it gives high accuracy with less computational cost among all tested classifiers.

3.7.1 Random Forest

Random forests (Breiman, 2001) are machine learning algorithms that work by growing an ensemble of decision trees and producing predictions by averaging the

results of many trees. For categorical variables, random forests choose the most popular prediction among all the trees (Breiman, 2001). Usually, a single decision tree is programmed to split the feature space at points that create the maximum separation in terms of output classes. In Figure 3.6, a decision tree is illustrated for a simple classification problem with a single feature X, and three possible classes.

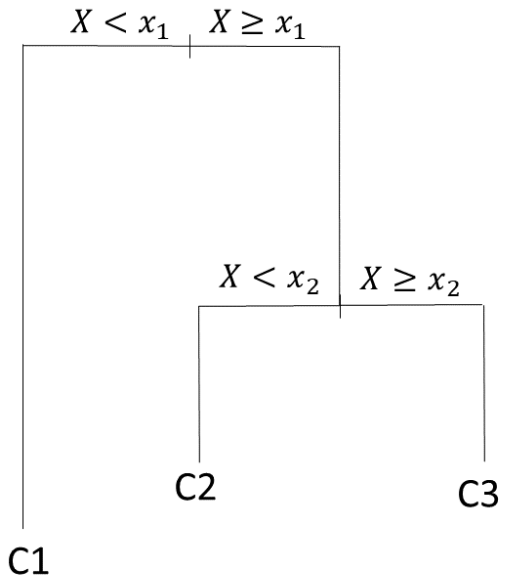

Figure 3.7. Illustration of a decision tree with a single feature and three possible classes. The tree first splits the feature space at the value of x_1, either predicting the class C1, or going to the next split. At the next split, at x_2, the decision tree either predicts C2 or C2

There are several tree-based methods that create many decision trees and provide a prediction based on the average result of the tree ensemble, such as bagging and boosting. Random forests differ from other tree-based methods by enforcing uncorrelated trees by randomly selecting candidate features for splitting, and only considering those features in the splitting process (James et al., 2013). This enforces trees to consider different sets of features for splits, resulting in uncorrelated trees with reduced variance (Hastie et al., 2009). The randomness in the algorithm also makes the classifier robust to overfitting (Breiman, 2001). Random forest classifiers

are also robust to outliers and noise (Rodriguez-Galiano et al., 2012b). Lastly, these algorithms are user-friendly as they have fewer parameters than other machine-learning algorithms (e.g., ANN or SVM) (Zhou et al., 2016). The disadvantage of the random forest algorithm is that it is a black-box algorithm that will prevent us from understanding the classification process. However, this disadvantage is also encountered in other machine learning methods that are frequently used (e.g., SVM, ANN).

Hyperparameters are user-selected parameters that determine the structure of a classifier. Two primary hyperparameters of an RF classifier are the number of classification trees (NTREE) and the number of classification variables used at each split (MTRY) (Ming et al., 2016; Rodriguez-Galiano et al., 2012b). These hyperparameters determine the structure of each classification tree. The number of classification trees reduces the chance of overfitting as it is increased and limits the value of generalization error (Breiman, 2001). The hyperparameter MTRY is the number of features randomly selected at each node, and it must be set with an integer in the interval [1, M], where M is the number of classification features (Bernard et al., 2009). MTRY determines the level of randomization in the feature selection process in such a way that a smaller MTRY means stronger randomization (Bernard et al., 2009).

3.7.2 Feature Selection

When classification feature space is too large for efficient computation, feature selection using random forest importance can be performed. To obtain the importance of each feature, the Out Of Bag (OOB) sample, which is a set of data points that are not included in the tree-building process, is selected by the algorithm (Genuer et al., 2010). For each tree, the prediction error for the OOB sample is calculated, and then it is repeated after each feature is permuted (Han et al., 2016). The difference between the errors is calculated and averaged for all trees (Han et al.,

2016). Mean decrease in accuracy for all features can be used to select features that contribute more to the classifier's accuracy.

The available input feature number has increased to 212 with the addition of vegetation indices (VIs). Considering that the aim of this thesis is to create a high-resolution crop map covering Türkiye, the computational cost of the classification is decreased through feature selection. After the dataset is processed to its final form, five different random forest algorithms are run using the randomForest package in R (Liaw & Wiener, 2002). Since different classifiers add randomness to the results, it is possible to have a more generalizable opinion with different classifier results. The average of these five random forest classifiers 'Mean Decrease Accuracy' output is taken for each feature and sorted from highest to lowest. Even though classifiers give different importance values for each feature, the order of the best performing features so not change significantly. Because of this, only the first 120 features with the highest decrease in accuracy are inspected as it is observed that after that point, feature importance decreases to have less contribution to accuracy. Table 3.3 shows the numbers of each band and index in the best performing 120 inputs for all three temperature zone classifiers. Table 3.4 shows the numbers of bands and indices in each month in the best performing 120 inputs for the temperature zone classifiers. As highlighted in the tables, Band 7 (Vegetation red edge), Band 8 (Near-infrared), and Band 8A (Narrow Near-infrared) do not contribute much to increasing accuracy. Also, median composites of March, September, and October have less contribution to accuracy when compared to other moths. These features are removed from the dataset before hyperparameter tuning to decrease the computational cost. After the elimination of these features, classification is performed using the remaining 152 features.

Table 3.4. The Numbers of Each Band and Index in the Best Performing 120 Inputs for All Temperature Zone Classifiers and the Total of the Temperature Zones.

Band	Low	Medium	High	Total
B1	13	9	9	31
B2	9	5	5	19
B3	11	7	3	21
B4	14	10	11	35
B5	11	9	10	30
B6	3	7	4	14
B7*	3	4	2	9
B8*	1	1	0	2
B8A*	2	1	2	5
B9	4	4	7	15
B11	4	7	13	24
B12	8	12	11	31
NDVI	12	14	14	40
$NDWI_M$	12	14	13	39
$NDWI_G$	11	14	14	39

* Features removed from the dataset

Table 3.5. The Numbers of Bands and Indices in Each Month in the Best Performing 120 Inputs for Each Temperature Zone Classifiers and Total of the Zones.

Month	Low	Medium	High	Total
March*	11	5	5	21
April	13	15	19	47
May	19	20	24	63
June	18	17	12	47
July	16	27	18	61
August	25	19	24	68
September*	11	10	10	31
October*	6	5	6	17

* Features removed from the dataset

3.7.3 Hyperparameter tuning

Before the crop mapping step, a random forest classifier that gives the best results on the validation set should be found. To find the best performing classifier, hyperparameter tuning using grid search is performed. Grid search is the process where each combination of hyperparameters is used for classification one by one, and the accuracy for these combinations is calculated to find the combination that gives the best accuracy. The number of classification trees (NTREE) options are selected to increase to 500 trees but no further because computational cost increases as NTREE increases. In the case of the number of classification variables used at each split (MTRY), apart from some generic numbers, $\sqrt{M}$ suggested by Bernard et al. (2009), which is also default in the randomForest package, and $(\log_2 M + 1)$ suggested by Breiman (2001) are selected for hyperparameter tuning where M is the number of classification features. Even though a decrease in MTRY weakens individual trees, an increase in MTRY reduces the randomness and creates classifiers that are more likely to overfit the training data, which results in lower accuracies (Bernard et al., 2009; Rodriguez-Galiano et al., 2012b). So, its maximum value is limited to 20 to avoid overfitting. Table 3.5 shows the hyperparameters used in the grid search. To decide on the best classifier, the overall accuracy of each combination of MTRY and NTREE is calculated for the validation set. After tuning, NTREE = 500 and MTRY = $\sqrt{M}$ is selected as final hyperparameters.

Table 3.6. Hyperparameters for Random Forest

NTREE	1, 5, 10, 50, 100, 200, 300, 500
MTRY	1, 2, 3, 4,5 ,6, 7, 8, 9, 10, 11, 12, 15, 20 $\sqrt{M}$ (Bernard et al. 2009), $(\log_2 M + 1)$(Breiman, 1996)

3.8 Crop Mapping

After determining the optimal hyperparameters, a classifier for each temperature zone is created. Each raster file is divided into tiles to make the classification possible with limited computer memory. Later, all bands for each tile are read on R and preprocessed to have the same bands and same form with the training, test, and validation sets. Resultant data frames are classified using one of three classifiers according to the temperature zone every pixel is located. After separate classification of temperature zones, all classification results are combined in one data frame for each tile. Since the used predict() function of R gives only a pixel number and the class assigned to that pixel, the resultant data frames are later converted into raster format.

3.9 Accuracy Assessment

Accuracy assessment is necessary for land cover classifications to evaluate the success of the resultant map (Stehman, 1996). The Kappa coefficient, overall accuracy (OA), user's accuracy (UA), and producer's accuracy (PA) are calculated for this study. First of all, an error matrix is formed that compares the ground truth data used for validation and test data (shown in the rows of the confusion matrices in this study) and classified data (shown in the columns of the confusion matrices in this study) (Story & Congalton, 1986). After using the information provided by the error matrix, OA, UA, PA, and Kappa coefficient (Cohen, 1960) are calculated. A simple error matrix and formulas for the user's and producer's accuracy are given in Table 3.6, where each class's correctly classified pixel number is given in bold letters (A, D). Columns show the number of classified pixels for each class, while rows show the number of ground truth pixels for each class. To calculate user's accuracy, which refers to how many of the classified pixels of a class actually belong to that class in the ground truth data, the number of correctly classified pixels for a class is divided by the column sum. To calculate the producer's accuracy, which refers to

how many ground truth pixels are classified correctly for each class, the number of correctly classified pixels for a class is divided by the row sum. Overall accuracy is the ratio of the total number of correctly classified pixels for all classes to the total number of ground truth pixels. Lastly, the Kappa coefficient is a proportion of accuracy that takes into account the possibility of correctness taking place by chance (Sun, 2011), and its formulation is given in Equations 5a, 5b, 5c, 5d, and 5e where P_e is agreement between classification and ground truth happening by chance, P_0 is the overall accuracy, $P_{Class\ 1}$ is the probability that all pixels classified as Class 1 randomly, and $P_{Class\ 2}$ is the probability that all pixels classified as Class 2 randomly.

Table 3.7. A Simple Error Matrix and Formulas for User's Accuracy and Producer's Accuracy.

		CLASSIFIED			
		Class 1	Class 2	Row Sum	Producer's accuracy
GROUND TRUTH	Class 1	**A**	B	A+B	A/(A+B)
	Class 2	C	**D**	C+D	D/(C+D)
	Column Sum	A+C	B+D		
	User's accuracy	A/(A+C)	D/(B+D)		

$$Overall\ Accuracy\ = \frac{A+D}{A+B+C+D} \tag{4}$$

$$P_{Class\ 1}\ = \left(\frac{A+B}{A+B+C+D}\right) \times \left(\frac{A+C}{A+B+C+D}\right) \tag{5a}$$

$$P_{Class\ 2}\ = \left(\frac{C+D}{A+B+C+D}\right) \times \left(\frac{B+D}{A+B+C+D}\right) \tag{5b}$$

$$P_0 = Overall\ Accuracy\ = \frac{A+D}{A+B+C+D} \tag{5c}$$

$$P_e\ =\ P_{Class\ 1} + P_{Class\ 2} \tag{5d}$$

$$Kappa\ = \frac{Po - Pe}{1 - Pe} \tag{5e}$$

CHAPTER 4

RESULTS AND DISCUSSION

4.1 Random Forest Classifier Accuracy on the Test Set

As it is mentioned in the methodology, ground truth data is divided into three subsets, training, test, and validation. The validation set is used for hyperparameter tuning, while the test set is left out until all tuning is done and final classifiers are obtained. In this chapter, classifier accuracies of three temperature zones, evaluated using measures mentioned in the accuracy assessment part of the thesis, are given.

4.1.1 Low-Temperature Zone

The confusion matrix obtained from Low-Temperature Zone (LTZ) classifier using the test set is given in Table 4.1. The number of classes in the LTZ is fewer than in the other zones since agricultural activities in this zone are sparser than in the others. Due to this sparse crop production, the training sample size is smaller than in other zones, and this can potentially be the reason for the lower classification accuracy obtained from the LTZ with OA of 89% and Kappa coefficient of 0.88. When land cover classes are inspected individually, barley, bare soil, rice paddy, forest, cherry, chickpea, water, and alfalfa classes reach PA's higher than 90%, showing the classifier's success on these classes. On the other hand, wheat, maize, potato, and urban classes reach unsatisfying PA's. When the confusion matrix is inspected, it can be seen that 94 of 255 wheat pixels are classified as barley. This misclassification can be explained by the similar phenological features of barley and wheat (Zheng et al., 2015). Another confusion occurred between maize and rice paddy as 76 of 102 maize pixels are classified as rice paddy. Since a significant similarity between phenological features of these two crops is not observed in this study, the reason

behind this confusion should be further examined. Urban pixels are misclassified as bare soil due to a lack of training data for the classifier to identify urban pixels and similar reflectance curves of bare soil and urban pixels (Piyoosh & Ghosh, 2018; Zhang et al., 2015). Despite the classes with low performance, the overall performance of the Low-Temperature Zone is decided to be used for crop mapping.

Table 4.1. Confusion Matrix, Producer's Accuracy, User's Accuracy, Overall Accuracy, Cohen's Kappa, and Pixel Number of Low-Temperature Zone

	Alfalfa	Bare Soil	Barley	Beans (dry)	Cherry	Chickpea	Cow Vetches	Forest	Maize	Oat	Potato	Rice Paddy	Steppe	Suger Beet	Urban	Water	Wheat	Row Sum	PA
Alfalfa	231	0	4	0	0	0	0	0	0	4	2	0	0	0	0	0	0	241	0.96
Bare Soil	0	1942	3	0	0	0	0	0	0	0	1	0	34	0	0	0	0	1980	0.98
Barley	16	0	1529	0	0	0	26	0	0	25	0	0	3	0	0	0	37	1636	0.93
Beans (dry)	0	0	0	57	0	0	0	0	0	0	11	0	0	3	0	0	0	71	0.80
Cherry	0	0	0	0	48	0	0	4	0	0	0	0	0	0	0	0	0	52	0.92
Chickpea	0	0	0	0	0	98	0	0	0	0	0	0	1	0	0	0	0	99	0.99
Cow Vetches	5	0	28	0	0	0	502	0	0	58	1	0	3	0	0	0	0	597	0.84
Forest	0	0	0	0	1	0	0	1460	0	1	0	0	0	0	0	0	0	1462	1.00
Maize	0	0	0	0	0	0	0	0	23	0	0	76	0	3	0	0	0	102	0.23
Oat	26	1	65	0	0	0	72	0	0	472	0	0	13	0	0	0	0	649	0.73
Potato	22	1	1	0	0	0	32	1	0	21	128	0	6	0	0	0	0	212	0.60
Rice Paddy	7	0	0	0	0	0	0	0	0	0	0	164	0	0	0	0	0	171	0.96
Steppe	57	0	40	0	0	0	0	0	0	0	0	0	625	0	0	0	0	722	0.87
Suger Beet	0	0	0	0	0	0	0	0	0	0	17	0	0	126	0	0	0	143	0.88
Urban	0	3	0	0	0	0	0	0	0	0	0	0	0	0	0	0	0	3	0.00
Water	0	0	0	0	0	0	0	0	0	0	0	0	0	0	0	40	0	40	1.00
Wheat	12	4	94	0	0	0	10	0	0	4	11	0	13	14	0	0	93	255	0.36
Column Sum	376	1951	1764	57	49	98	642	1465	23	585	171	240	698	146	0	40	130	**OA=0.89**	
UA	0.61	1.00	0.87	1.00	0.98	1.00	0.78	1.00	1.00	0.81	0.75	0.68	0.90	0.86	-	1.00	0.72	**Kappa = 0.88**	

4.1.2 Medium-Temperature Zone

Medium-Temperature Zone contains more data for classification than the other temperature zones, and it also contains a greater number of crop types due to high agricultural activity in middle Anatolia. Table 4.2 shows that the classifier gives 91% OA with Kappa of 0.92. When land cover classes are inspected individually, it is seen that 16 of 35 land cover classes (bare soil, barley, chickpea, forest, green tea leaves, hazelnut, maize, poppy, potato, rapeseed, rice paddy, steppe, sunflower, tomato, urban, water) gives PA's higher than 90% and 6 of 35 land cover classes

(wheat, apple, apricot, dry onion, alfalfa, olive) gives accuracies between 80% and 90%. There are also classes that are classified with almost complete correctness (bare soil, rice paddy, hazelnut, forest, urban, and water). On the other hand, some classes give lower user's and producer's accuracies like tobacco, pepper, and red lentils, which can be due to inadequate training data. Confusion between wheat and barley can also be observed in MTZ as it is in LTZ. Another confusion occurs between melon and tomato, as almost half of the melon pixels are classified as tomato pixels. Triticale pixels are also highly misclassified as barley and wheat, potentially due to the fact that triticale is hybrid of wheat and barley (Rußwurm & Körner, 2017). Tomato and sugar beet have much lower UA's than their PA's, unlike other classes since most melon pixels are classified as tomato, and more than one-third of the pixels classified as sugar beet belongs to the maize class. The reasons behind these misclassifications should be further investigated.

Table 4.2. Confusion Matrix, Producer's Accuracy, User's Accuracy, Overall Accuracy, Cohen's Kappa, and Pixel number of Medium-Temperature Zone

	Alfalfa	Apple	Apricot	Bare Soil	Barley	Bean (Dry)	Cherry	Chickpea	Forest	Grape	Green Tea Leaves	Hazelnut	Maize	Melon	Oat	Olive	Onion (Dry)	Peach	Pepper	Poppy	Potato	Rapeseed	Red Lentil	Rice Paddy	Steppe	Sugar Beet	Sunflower	Tobacco	Tomato	Triticale	Urban	Vetch	Water	Watermelon	Wheat	Row Sum	PA
Alfalfa	412	5	9	0	21	0	1	11	0	0	0	0	0	0	0	0	0	0	0	4	8	0	0	0	0	0	0	0	0	0	0	0	0	0	471	0.87
Apple	2	956	90	0	0	0	13	20	0	0	0	0	0	0	0	0	1	0	0	1	0	0	0	0	3	0	3	0	0	0	0	0	0	0	1089	0.88
Apricot	4	102	1122	0	8	0	36	20	0	0	0	0	0	0	0	0	0	1	0	0	0	0	0	0	10	0	8	0	0	0	0	0	0	0	1311	0.86
Bare Soil	0	0	0	5455	0	0	0	0	0	0	0	0	0	0	0	0	0	0	0	0	0	0	0	0	0	0	0	0	0	0	0	0	0	0	5455	1.00
Barley	1	0	5	0	3868	0	0	0	0	0	0	0	0	0	0	0	0	0	0	25	0	0	0	0	0	0	0	0	0	13	0	0	0	163	4075	0.95
Bean (Dry)	16	0	0	0	0	600	0	7	0	1	0	0	1	0	0	0	3	1	0	0	89	0	0	0	0	7	55	0	0	0	0	0	2	0	782	0.77
Cherry	0	18	36	0	2	0	222	1	18	2	0	5	1	0	0	0	0	0	0	0	0	0	0	0	1	0	1	0	0	0	0	0	0	0	307	0.72
Chickpea	0	0	2	0	107	0	0	4848	0	0	0	0	0	0	2	0	0	0	0	0	0	0	0	0	0	0	0	0	0	0	0	0	0	0	4959	0.98
Forest	0	4	0	0	0	0	0	0	2520	0	0	1	0	0	0	0	0	0	0	0	0	0	0	0	0	0	0	0	0	0	0	0	0	0	2525	1.00
Grape	0	6	16	0	0	0	0	0	0	126	0	0	0	0	0	0	0	8	0	0	0	0	0	0	0	0	6	0	0	0	0	0	0	0	162	0.78
Green Tea Leaves	0	0	0	0	0	0	0	0	0	0	57	3	0	0	0	0	0	0	0	0	0	0	0	0	0	0	0	0	0	0	0	0	0	0	60	0.95
Hazelnut	0	0	0	0	0	0	0	0	1	0	0	656	0	0	0	0	0	0	0	0	0	0	0	0	0	0	0	0	0	0	0	0	0	0	657	1.00
Maize	0	0	0	0	0	0	0	0	0	0	0	0	5559	0	0	0	112	0	0	0	0	0	0	0	0	268	10	0	2	0	0	0	0	0	5951	0.93
Melon	0	1	0	0	2	14	0	0	0	0	0	0	0	184	0	0	5	0	22	0	0	0	0	0	0	0	6	0	183	0	33	0	0	4	454	0.41
Oat	0	0	1	0	30	0	0	115	0	0	0	0	0	0	326	0	0	0	0	0	0	0	0	0	0	0	0	0	0	0	0	0	0	2	474	0.69
Olive	0	3	2	0	0	0	1	0	2	0	0	0	0	0	0	72	0	0	0	0	0	0	0	0	2	0	0	0	0	0	0	0	0	0	82	0.88
Onion (Dry)	0	0	0	0	0	1	0	2	0	0	0	0	21	0	0	0	521	0	51	0	0	0	0	0	2	7	0	0	3	0	0	0	0	0	608	0.86
Peach	0	69	8	0	0	0	0	0	0	0	0	0	1	0	0	0	0	84	0	0	0	0	0	0	0	0	0	0	0	0	0	0	0	0	162	0.52
Pepper	0	0	0	59	0	44	0	0	0	0	0	0	0	0	0	0	0	0	34	0	0	0	0	0	0	0	0	0	27	0	0	0	0	0	164	0.21
Poppy	0	0	0	0	28	0	0	0	0	0	0	0	0	0	0	0	0	0	0	1489	0	1	0	0	0	0	0	0	0	0	0	0	0	5	1523	0.98
Potato	0	0	1	1	0	5	0	2	0	0	0	0	4	0	0	0	0	0	0	0	1557	0	0	0	0	1	77	0	0	0	0	0	0	0	1648	0.94
Rapeseed	0	1	0	0	21	0	0	7	0	0	0	0	0	0	0	0	0	0	0	36	0	745	0	0	0	0	0	0	0	0	0	16	0	6	832	0.90
Red Lentil	0	0	64	0	42	0	0	24	0	6	0	0	0	0	0	0	0	0	0	0	0	0	42	0	0	0	0	0	0	0	0	0	0	0	178	0.24
Rice Paddy	0	0	0	0	0	0	1	0	0	0	0	0	0	0	0	0	0	0	0	0	0	0	0	673	0	0	0	0	0	0	0	0	0	0	674	1.00
Steppe	0	0	4	2	6	0	0	25	0	0	0	0	0	0	8	0	0	0	0	8	0	0	0	0	973	0	0	0	0	0	0	0	0	1	1027	0.95
SugerBeet	0	0	0	0	0	17	0	0	0	0	0	0	1	1	0	0	0	0	0	0	36	0	0	0	0	423	77	0	10	0	0	0	0	0	565	0.75
Sunflower	0	5	0	0	0	1	2	191	0	0	0	0	18	0	0	0	0	0	0	0	8	0	0	0	2	0	2555	0	5	0	0	0	0	0	2787	0.92
Tobacco	0	0	1	3	11	0	0	2	0	4	0	0	0	0	0	0	6	0	0	0	0	0	0	0	1	0	19	17	0	0	2	0	0	0	66	0.26
Tomato	0	0	0	0	0	0	0	0	0	0	0	0	0	0	0	0	1	0	2	0	2	0	0	0	0	0	2	0	170	0	0	0	0	0	177	0.96
Triticale	0	0	0	0	78	0	0	9	0	0	0	0	0	0	2	0	0	0	0	4	4	0	0	0	11	0	0	0	0	81	0	0	0	99	288	0.28
Urban	0	0	0	0	0	0	0	0	0	0	0	0	0	0	0	0	0	0	0	0	0	0	0	0	0	0	0	0	0	0	1108	0	0	0	1108	1.00
Vetch	0	0	0	0	61	0	0	2	0	0	0	0	0	0	3	0	0	0	0	36	0	0	0	0	5	0	0	0	0	0	0	109	0	1	217	0.50
Water	0	0	0	0	0	0	0	0	0	0	0	0	0	0	0	0	0	0	0	0	0	0	0	2	0	0	0	0	0	0	0	0	362	0	364	0.99
Watermelon	0	0	0	0	0	52	0	0	0	4	0	0	0	0	0	0	0	0	8	0	1	0	0	0	0	14	1	0	0	0	0	0	0	105	185	0.57
Wheat	0	0	0	0	497	0	0	0	0	0	0	0	0	0	0	0	0	0	0	56	0	0	0	0	0	0	0	0	0	0	0	0	0	0	2504	3057	0.82
Column Sum	435	1170	1361	5520	4782	734	276	5286	2541	143	57	665	5606	185	341	72	649	94	117	1659	1705	746	42	675	1010	720	2820	17	400	94	1143	125	362	111	2781	**OA=0.91**	
UA	0.95	0.82	0.82	0.99	0.81	0.82	0.80	0.92	0.99	0.88	1.00	0.99	0.99	0.99	0.96	1.00	0.80	0.89	0.29	0.90	0.91	1.00	1.00	1.00	0.96	0.59	0.91	1.00	0.43	0.86	0.97	0.87	1.00	0.95	0.90	**Kappa=0.92**

4.1.3 High-Temperature Zone

High-Temperature Zone also includes regions with high agricultural activities like MTZ. Especially cotton, sunflower, and fruits like olive, lemon, mandarin, grape, and orange crops are cultivated in regions covered by HTZ. Table 4.3 shows that the HTZ classifier gives the highest accuracy among the classifiers used in the study, with 94% overall accuracy and Kappa of 0.94. Among 34 landcover classes, 16 classes (sunflower, wheat, rice paddy, hazelnut, bare soil, forest, rapeseed, maize, cotton, potato, green house, grape, steppe, urban, water, olive) reach PA's higher than 90%, and three crop classes (tomato, mandarin, alfalfa) reach accuracies between 80% and 90%. In addition, cotton, sunflower, wheat, rice paddy, forest, rapeseed, potato, greenhouse, urban, and water pixels are classified with more than 99% accuracy. Peach, apple, tobacco, and chickpea crop pixels are mostly misclassified by the classifier, potentially due to the small number of training pixels available for these crop classes. One of the most noticeable misclassifications is between red lentil and wheat, as 248 of 458 red lentil pixels are classified as wheat. This confusion can be a result of similar growing periods over the same region (Southeastern Anatolia). Another misclassification occurred between citrus fruits orange, lemon, and mandarin, potentially due to the tree structures of the crops. The High-Temperature Zone classifier is decided to be used for the mapping step as it gives very high accuracies and Kappa coefficient.

Table 4.3. Confusion Matrix, Producer's Accuracy, User's Accuracy, Overall Accuracy, Cohen's Kappa, and Pixel number of High-Temperature Zone

	Alfalfa	Apple	Apricot	Bare Soil	Barley	Cherry	Chickpea	Cotton	Forest	Grape	Green House	Hazelnut	Lemon	Maize	Mandarin	Melon	Olive	Orange	Peach	Pepper	Potato	Rapeseed	Red Lentil	Rice Paddy	Steppe	Sunflower	Tobacco	Tomato	Urban	Water	Watermelon	Wheat	Row Sum	PA
Alfalfa	271	0	0	0	0	0	0	18	0	20	0	0	2	1	0	0	6	0	0	0	0	0	0	0	0	4	0	0	0	0	0	0	322	0.84
Apple	0	6	0	0	0	0	0	0	0	7	0	0	12	0	8	0	0	15	0	0	0	0	0	0	0	0	0	0	0	0	0	0	48	0.13
Apricot	3	0	279	0	0	0	0	1	0	25	0	0	65	1	19	0	1	8	0	0	0	0	0	0	0	0	0	0	0	0	0	0	402	0.69
Bare Soil	0	0	0	252	0	0	0	0	0	0	0	0	0	0	0	0	3	0	0	0	0	0	0	0	0	8	0	0	0	0	0	0	263	0.96
Barley	0	0	0	0	266	0	0	0	0	0	0	0	0	0	0	0	0	0	0	0	0	0	0	0	0	0	0	0	0	0	0	116	382	0.70
Cherry	0	0	0	0	0	29	0	0	0	5	0	1	1	0	3	0	0	0	0	0	0	0	0	0	0	0	0	0	0	0	0	0	39	0.74
Chickpea	0	0	0	0	0	0	60	0	0	0	0	0	1	0	0	0	69	0	0	0	0	0	0	0	0	16	0	0	0	0	0	19	165	0.36
Cotton	6	0	0	0	2	0	0	6644	0	0	0	0	0	20	0	0	0	0	0	1	0	0	0	0	0	2	0	37	0	0	0	1	6713	0.99
Forest	0	0	0	0	0	0	0	0	1032	0	0	0	0	0	0	0	1	0	0	0	0	0	0	0	0	0	0	0	0	0	0	0	1033	1.00
Grape	0	0	22	0	0	0	0	22	0	1986	0	0	4	0	9	0	26	0	0	0	0	0	0	0	0	6	0	0	0	0	0	0	2075	0.96
Green House	0	0	0	0	0	0	0	0	0	0	545	0	0	0	0	0	0	0	0	0	0	0	0	0	0	0	0	0	1	0	0	0	546	1.00
Hazelnut	0	0	0	0	0	0	0	0	0	0	0	140	4	0	0	0	0	1	0	0	0	0	0	0	0	0	0	0	0	0	0	0	145	0.97
Lemon	0	0	4	0	25	1	0	0	0	26	0	0	744	0	56	0	153	37	0	0	0	0	0	0	0	18	0	0	0	0	0	2	1066	0.70
Maize	0	0	0	0	0	0	0	54	0	0	0	0	0	3141	0	0	0	0	0	0	0	0	0	0	2	0	1	0	2	0	0	0	3200	0.98
Mandarin	0	0	0	0	0	0	0	0	18	11	0	0	46	0	1050	0	14	24	0	0	0	0	0	0	0	34	0	0	1	0	0	0	1198	0.88
Melon	0	0	0	0	0	0	0	3	0	0	0	0	0	0	0	29	0	0	0	0	0	0	0	0	4	0	15	0	3	0	0	0	54	0.54
Olive	0	0	0	0	0	0	0	0	4	8	0	0	0	0	3	0	1074	9	0	0	0	0	0	0	0	1	0	0	0	0	0	0	1099	0.98
Orange	0	0	0	0	0	0	0	0	0	9	0	0	140	0	219	0	16	527	0	0	0	0	0	0	0	0	0	0	0	0	0	0	911	0.58
Peach	0	0	0	0	0	0	0	0	0	7	0	0	13	28	2	0	1	3	5	0	0	0	0	0	0	0	0	0	0	0	0	1	60	0.08
Pepper	0	0	0	0	0	0	0	83	0	0	0	0	0	0	0	0	0	0	0	116	0	0	0	0	0	6	0	3	0	0	0	0	208	0.56
Potato	0	0	0	0	0	0	0	0	0	0	0	0	0	0	0	0	0	0	0	0	26	0	0	0	0	0	0	0	0	0	0	0	26	1.00
Rapeseed	0	0	0	0	0	0	0	0	0	0	0	0	0	0	0	0	1	0	0	0	0	616	0	0	0	0	0	0	0	0	0	0	617	1.00
Red Lentil	0	0	0	0	0	0	0	0	0	0	0	0	0	0	0	0	0	0	0	0	0	0	458	0	0	0	0	0	0	0	0	248	706	0.65
Rice Paddy	0	0	0	0	0	0	0	0	0	0	0	0	0	1	0	0	0	0	0	0	0	0	0	3102	0	1	0	0	0	0	0	0	3104	1.00
Steppe	0	0	0	0	5	0	0	0	0	0	0	0	0	0	0	0	13	0	0	0	0	0	49	0	1797	0	0	0	0	0	0	85	1949	0.92
Sunflower	0	0	0	0	0	0	0	0	0	5	0	0	0	0	3	0	0	0	0	0	0	0	0	0	0	2665	0	6	0	0	0	0	2679	0.99
Tobacco	0	0	0	0	0	0	0	0	0	0	0	0	0	0	0	0	0	0	0	0	0	0	0	0	0	17	11	0	16	0	0	0	44	0.25
Tomato	0	0	0	0	0	0	0	21	0	3	0	0	3	0	0	0	1	0	0	1	0	0	0	0	0	42	0	602	0	0	0	0	673	0.89
Urban	0	0	0	0	0	0	0	0	0	0	0	0	0	0	0	0	13	0	0	0	0	0	0	0	0	0	0	0	1438	0	0	0	1451	0.99
Water	0	0	0	0	0	0	0	0	0	0	0	0	0	0	0	0	0	0	0	0	0	0	0	0	0	0	0	0	0	438	0	0	438	1.00
Watermelon	0	0	0	0	0	0	0	0	0	0	0	0	0	0	0	5	0	0	0	0	0	0	0	0	0	8	0	29	0	0	68	0	110	0.62
Wheat	0	0	0	0	0	0	0	0	0	0	0	0	1	1	0	0	1	0	0	0	0	0	2	0	0	0	0	0	0	0	0	8435	8440	1.00
Column Sum	280	6	305	252	298	30	60	6846	1054	2112	545	141	1036	3193	1372	34	1393	624	5	118	26	616	509	3108	1806	2835	11	682	1456	438	68	8907	**OA=0.94**
UA	0.97	1.00	0.91	1.00	0.89	0.97	1.00	0.97	0.98	0.94	1.00	0.99	0.72	0.98	0.77	0.85	0.77	0.84	1.00	0.98	1.00	1.00	0.90	1.00	1.00	0.94	1.00	0.88	0.99	1.00	1.00	0.95	**Kappa=0.94**	

4.1.4 Combined Temperature Zones

Confusion matrices of temperature zones are combined to evaluate the accuracy of the whole test set. With this combined confusion matrix, it is possible to see how accurately the whole test data is classified with temperature zoning. The resultant confusion matrix is given in Table 4.4. shows 92% OA with a Kappa of 0.93. More than 85% of the test pixels are classified correctly for 23 of 40 land cover classes (barley, sunflower, bare soil, wheat, green tea leaves, rice paddy, tomato, hazelnut, forest, poppy, rapeseed, mandarin, maize, chickpea, cotton, green house, dry onion, steppe, urban, grape, water, alfalfa, olive). In addition to that, it is shown in the confusion matrix that more than 95% of the test pixels are classified correctly for 13 classes (forest, green house, water, urban, bare soil, rice paddy, hazelnut, cotton, poppy, olive, chickpea, sunflower, green tea leaves). On the other hand, PA's lower than or equal to 60% are obtained for classes peach, tobacco, triticale, pepper, melon, red lentil, orange, watermelon, and potato. These classes also reached lower accuracies in separate temperature zones except for potato in HTZ, where all potato test pixels are classified correctly. As discussed for each temperature zone previously, these misclassifications potentially occur due to the inadequate number of training pixels (e.g., for peach and tobacco) or similar spectral and phenological features of different crops. Misclassification of triticale as wheat and barley is an example of confusion due to similar features of different crops as it is a hybrid of wheat and barley. Another misclassification that is observed in the separate temperature zones is between wheat and barley. Even though the confusion between these crops decreases the accuracies for one of the classes in separate temperature zones, the combined PA's of the crops exceeds 90%. These accuracy measures represent the correct classification of only the predetermined test pixels and not the whole map. Nevertheless, the accuracy obtained from the combination of test sets of temperature zones is satisfactory when it is compared with the results of other large-scale studies (e.g., Yılmaz et al., 2020; Yang et al., 2019; d'Andrimont et al., 2021) and can give an opinion about the accuracy of the classification map.

Table 4.4. Confusion Matrix, Producer's Accuracy, User's Accuracy, Overall Accuracy, Cohen's Kappa, and Pixel number of Combined Temperature Zones

	Alfalfa	Apple	Apricot	Bare Soil	Barley	Bean (Dry)	Cherry	Chickpea	Cotton	Forest	Grape	Green House	Green Tea Leaves	Hazelnut	Lemon	Maize	Mandarin	Melon	Oat	Olive	Onion (Dry)	Orange	Peach	Pepper	Poppy	Potato	Rapeseed	Red Lentil	Rice Paddy	Steppe	SugerBeet	Sunflower	Tobacco	Tomato	Triticale	Urban	Vetch	Water	Watermelon	Wheat	Row Sum	PA
Alfalfa	914	5	9	0	25	0	1	11	26	0	20	0	0	0	2	1	0	0	4	6	0	0	0	0	4	2	0	0	0	0	0	4	0	0	0	0	0	0	0	0	1034	0.88
Apple	2	962	90	0	0	0	13	20	0	0	7	0	0	0	12	0	8	0	0	0	1	15	0	0	1	0	0	0	0	3	0	3	0	0	0	0	0	0	0	0	1137	0.85
Apricot	7	102	1401	0	8	0	36	20	1	0	25	0	0	0	65	1	19	0	0	1	0	8	0	0	0	1	0	0	0	10	0	8	0	0	0	0	0	0	0	0	1713	0.82
Bare Soil	0	0	0	7649	3	0	0	0	0	0	0	0	0	0	0	0	0	0	0	3	0	0	0	0	0	1	0	0	0	42	0	0	0	0	0	0	0	0	0	0	7698	0.99
Barley	17	0	5	0	5663	0	0	0	0	0	0	0	0	0	0	0	0	0	25	0	0	0	0	0	25	0	0	0	0	3	0	0	0	0	13	0	26	0	0	316	6093	0.93
Bean (Dry)	16	0	0	0	0	657	0	7	89	0	1	0	0	0	0	1	0	0	0	0	3	0	0	0	0	12	0	0	0	0	10	55	0	0	0	0	0	0	2	0	853	0.77
Cherry	0	18	36	0	2	0	299	1	0	22	7	0	0	6	1	1	3	0	0	0	0	0	0	0	0	0	0	0	0	1	0	1	0	0	0	0	0	0	0	0	398	0.75
Chickpea	0	0	2	0	107	0	0	5006	0	0	0	0	0	0	1	0	0	0	2	69	0	0	0	0	0	0	0	0	0	1	0	16	0	0	0	0	0	0	0	19	5223	0.96
Cotton	6	0	1	1	2	5	0	2	8201	0	0	0	0	0	0	24	0	0	0	0	0	0	0	0	1	0	0	0	0	0	1	79	0	37	0	0	0	0	0	1	8361	0.98
Forest	0	4	0	0	0	0	1	0	0	5012	0	0	0	1	0	0	0	0	1	1	0	0	0	0	0	0	0	0	0	0	0	0	0	0	0	0	0	0	0	0	5020	1.00
Grape	0	6	38	0	0	0	0	0	22	0	2112	0	0	0	4	0	9	0	0	26	0	0	0	0	0	8	0	0	0	0	0	12	0	0	0	0	0	0	0	0	2237	0.94
Green House	0	0	0	0	0	0	0	0	0	0	0	545	0	0	0	0	0	0	0	0	0	0	0	0	0	0	0	0	0	0	0	0	0	0	0	1	0	0	0	0	546	1.00
Green Tea Leaves	0	0	0	0	0	0	0	0	0	0	0	0	57	3	0	0	0	0	0	0	0	0	0	0	0	0	0	0	0	0	0	0	0	0	0	0	0	0	0	0	60	0.95
Hazelnut	0	0	0	0	0	0	0	0	0	1	0	0	0	796	4	0	0	0	0	0	0	1	0	0	0	0	0	0	0	0	0	0	0	0	0	0	0	0	0	0	802	0.99
Lemon	0	0	4	0	25	0	1	0	0	0	26	0	0	0	744	0	56	0	0	153	0	37	0	0	0	0	0	0	0	0	0	18	0	0	0	0	0	0	0	2	1066	0.70
Maize	0	0	0	0	0	0	0	0	54	0	0	0	0	0	0	8723	0	0	0	0	112	0	0	0	0	0	0	0	0	78	0	271	11	0	4	0	0	0	0	0	9253	0.94
Mandarin	0	0	0	0	0	0	0	0	0	18	11	0	0	0	46	0	1050	0	0	14	0	24	0	0	0	0	0	0	0	0	0	34	0	0	0	1	0	0	0	0	1198	0.88
Melon	0	1	0	0	2	14	0	0	3	0	0	0	0	0	0	0	0	213	0	0	5	0	0	22	0	0	0	0	4	0	0	21	0	186	0	33	0	0	4	0	508	0.42
Oat	26	0	1	1	95	0	0	115	0	0	0	0	0	0	0	0	0	0	798	0	0	0	0	0	0	0	0	0	0	13	0	0	0	0	0	0	72	0	0	2	1123	0.71
Olive	0	3	2	0	0	0	1	0	0	6	8	0	0	0	0	0	3	0	0	1146	0	9	0	0	0	0	0	0	0	3	0	0	0	0	0	0	0	0	0	0	1181	0.97
Onion (Dry)	0	0	0	0	0	1	0	2	0	0	0	0	0	0	0	21	0	0	0	0	521	0	0	51	0	0	0	0	0	2	7	0	0	3	0	0	0	0	0	0	608	0.86
Orange	0	0	0	0	0	0	0	0	0	0	9	0	0	0	140	0	219	0	0	16	0	527	0	0	0	0	0	0	0	0	0	0	0	0	0	0	0	0	0	0	911	0.58
Peach	0	0	0	0	0	0	0	0	0	0	7	0	0	0	13	28	2	0	0	1	0	3	5	0	0	0	0	0	0	0	0	0	0	0	0	0	0	0	0	1	60	0.08
Pepper	0	0	0	59	0	44	0	0	83	0	0	0	0	0	0	0	0	0	0	0	0	0	0	150	0	0	0	0	0	0	0	6	0	30	0	0	0	0	0	0	372	0.40
Poppy	0	0	0	0	28	0	0	0	0	0	0	0	0	0	0	0	0	0	0	0	0	0	0	0	1489	0	1	0	0	0	0	0	0	0	0	0	0	0	0	5	1523	0.98
Potato	22	69	8	1	1	0	0	0	0	1	0	0	0	0	0	1	0	0	21	0	0	0	0	0	0	238	0	0	0	6	0	0	0	0	0	0	32	0	0	0	400	0.60
Rapeseed	0	1	0	0	21	0	0	7	0	0	0	0	0	0	0	0	0	0	0	1	0	0	0	0	36	0	1361	0	0	0	0	0	0	0	0	0	16	0	0	6	1449	0.94
Red Lentil	0	0	64	0	42	0	0	24	0	0	6	0	0	0	0	0	0	0	0	0	0	0	0	0	0	0	0	500	0	0	0	0	0	0	0	0	0	0	0	248	884	0.57
Rice Paddy	7	0	0	0	0	0	1	0	0	0	0	0	0	0	0	1	0	0	0	0	0	0	0	0	0	0	0	0	3939	0	0	1	0	0	0	0	0	0	0	0	3949	1.00
Steppe	57	0	4	2	51	0	0	25	0	0	0	0	0	0	0	0	0	0	8	13	0	0	0	0	8	0	0	49	0	3395	0	0	0	0	0	0	0	0	0	86	3698	0.92
SugerBeet	0	0	0	0	0	17	0	0	36	0	0	0	0	0	0	1	0	1	0	0	0	0	0	0	0	17	0	0	0	0	549	77	0	10	0	0	0	0	0	0	708	0.78
Sunflower	0	5	0	0	0	1	2	191	8	0	5	0	0	0	0	18	3	0	0	0	0	0	0	0	0	0	0	0	0	2	0	5220	0	11	0	0	0	0	0	0	5466	0.95
Tobacco	0	0	1	3	11	0	0	2	0	0	4	0	0	0	0	0	0	0	0	0	6	0	0	0	0	0	0	0	0	1	0	36	28	0	0	18	0	0	0	0	110	0.25
Tomato	0	0	0	0	0	0	0	0	23	0	3	0	0	0	3	0	0	0	0	1	1	0	0	3	0	0	0	0	0	0	0	44	0	772	0	0	0	0	0	0	850	0.91
Triticale	0	0	0	0	78	0	0	9	4	0	0	0	0	0	0	0	0	0	0	2	0	0	0	0	4	0	0	0	0	11	0	0	0	0	81	0	0	0	0	99	288	0.28
Urban	0	0	0	3	0	0	0	0	0	0	0	0	0	0	0	0	0	0	0	13	0	0	0	0	0	0	0	0	0	0	0	0	0	0	0	2546	0	0	0	0	2562	0.99
Vetch	5	0	0	0	89	0	0	2	0	0	0	0	0	0	0	0	0	0	61	0	0	0	0	0	36	1	0	0	0	8	0	0	0	0	0	0	611	0	0	1	814	0.75
Water	0	0	0	0	0	0	0	0	0	0	0	0	0	0	0	0	0	0	0	0	0	0	0	0	0	0	0	0	0	2	0	0	0	0	0	0	0	840	0	0	842	1.00
Watermelon	0	0	0	0	0	52	0	0	1	0	4	0	0	0	0	0	0	5	0	0	0	0	0	8	0	0	0	0	0	0	14	9	0	29	0	0	0	0	173	0	295	0.59
Wheat	12	0	0	4	591	0	0	0	0	0	0	0	0	0	1	1	0	0	4	1	0	0	0	0	56	11	0	2	0	13	14	0	0	0	0	10	0	0	0	11032	11752	0.94
Column Sum	1091	1176	1666	7723	6844	791	355	5444	8551	5060	2255	545	57	806	1036	8822	1372	219	926	1465	649	624	5	235	1659	291	1362	551	4023	3514	866	5655	28	1082	94	2599	767	840	179	11818	**OA=0.92**	
UA	0.84	0.82	0.84	0.99	0.83	0.83	0.84	0.92	0.96	0.99	0.94	1.00	1.00	0.99	0.72	0.99	0.77	0.97	0.86	0.78	0.80	0.84	1.00	0.64	0.90	0.82	1.00	0.91	0.98	0.97	0.63	0.92	1.00	0.71	0.86	0.98	0.80	1.00	0.97	0.93	**Kappa=0.93**	

4.1.5 Comparison with the Classifier without the Temperature Zones

The dataset before the division of temperature zones is also used for classification. The training subset of this dataset contains all training data used in each temperature zone. So, the total number of training pixels used in each temperature classifier is used for one classifier, which is also the case for test and training pixels. The confusion matrix for this classifier which gives 92% OA with Kappa of 0.91, is given in Table 4.5. In addition, Table 4.6 is given for the comparison between OA and Kappa coefficient obtained using the classifier without the temperature zoning and the confusion matrix of combined temperature zones, and Table 4.7 show the PA's for each class for this comparison. OA and Kappa coefficients increase less than %1 when the study area is divided into temperature zones (OA increases 0.81% and Kappa increases 0.87%). Even though, on average, the use of temperature zones yielded marginally appoved results, when individual classes are inspected, PA's of 25 classes increase with temperature zones while PA's of 13 classes decrease with temperature zoning. Since the accuracies obtained using temperature zones is higher and the computational power and time required for the temperature zoning procedure is not high, dividing the study area into temperature zone is recommended.

One unexpected result from the classification without the temperature zones is that even though wheat pixels have different spectral curves in different temperature zones, the classification accuracy does not improve with temperature zones. It is also observed that classes with the highest increase in accuracy with temperature zones (dry beans, cherry, tomato, olive, lemon, and green tea leaves) have more than 80% of their training pixels in one temperature zone. In contrast, classes with the highest decrease in accuracy with temperature zones (rapeseed, pepper) have training pixels that are more equally distributed to temperature zones. So, it is possible that classifying a crop in the temperature zone that the crop is mostly cultivated in, rather than classifying it with a classifier that includes areas that the crop is not commonly cultivated, can increase the accuracy of that crop. In addition to that, dividing the

ground truth data into more temperature zones decreases the training pixel number, which can potentially be a reason for decreased accuracy with temperature zoning for classes distributed to temperature zones.

Table 4.5. Confusion Matrix, Producer's Accuracy, User's Accuracy, Overall Accuracy, Cohen's Kappa, and Pixel number of Classification on Test set without Temperature Zones

	Alfalfa	Apple	Apricot	Bare Soil	Barley	Bean (Dry)	Cherry	Chickpea	Cotton	Forest	Grape	Green House	Green Tea Leaves	Hazelnut	Lemon	Maize	Mandarin	Melon	Oat	Olive	Onion (Dry)	Orange	Peach	Pepper	Poppy	Potato	Rapeseed	Red Lentil	Rice Paddy	Steppe	SugerBeet	Sunflower	Tobacco	Tomato	Triticale	Urban	Vetch	Water	Watermelon	Wheat	Row Sum	PA
Alfalfa	892	2	3	0	72	0	1	7	11	0	18	0	1	0	0	0	0	0	4	0	0	0	0	1	2	11	0	0	0	6	1	1	0	0	0	0	0	0	0	1	1034	0.86
Apple	5	939	106	0	0	0	15	16	0	0	27	0	0	0	9	3	1	0	0	1	0	2	0	0	0	0	0	0	0	5	0	7	0	1	0	0	0	0	0	0	1137	0.83
Apricot	25	49	1428	0	9	0	16	8	0	0	81	0	0	0	26	5	10	0	1	15	0	6	0	0	0	1	0	0	0	11	0	22	0	0	0	0	0	0	0	0	1713	0.83
Bare Soil	0	0	0	7474	0	0	0	6	0	0	0	0	0	0	0	0	0	0	0	0	0	0	0	0	0	0	0	0	0	40	0	1	0	0	0	177	0	0	0	0	7698	0.97
Barley	21	1	5	0	5537	0	0	3	0	0	0	0	0	0	0	1	0	0	53	3	0	1	0	0	13	0	0	0	0	0	0	14	0	0	6	0	33	0	0	402	6093	0.91
Bean (Dry)	16	0	0	0	0	547	0	9	78	0	5	0	0	0	0	13	0	0	0	0	0	0	0	0	0	70	0	0	0	3	0	7	103	0	2	0	0	0	0	0	853	0.64
Cherry	0	8	38	0	0	0	252	0	0	27	45	0	0	4	7	3	0	0	0	7	0	1	0	0	0	0	0	0	0	2	0	2	0	0	0	0	0	0	0	2	398	0.63
Chickpea	0	0	2	1	118	0	0	5069	0	0	0	0	0	0	0	0	0	0	1	0	0	0	0	0	0	0	0	0	0	2	0	14	0	0	0	0	0	0	0	16	5223	0.97
Cotton	9	0	1	0	1	6	0	0	6630	0	0	0	0	0	0	16	0	1	0	2	0	0	0	0	0	16	0	0	0	0	1	1	0	27	0	0	0	0	0	2	6713	0.99
Forest	0	6	0	0	0	5	0	0	0	5005	1	0	0	1	0	0	0	0	0	2	0	0	0	0	0	0	0	0	0	0	0	0	0	0	0	0	0	0	0	0	5020	1.00
Grape	0	3	51	0	0	0	0	1	22	0	2107	0	0	0	1	0	3	0	0	30	0	0	0	0	0	0	0	0	0	6	0	13	0	0	0	0	0	0	0	0	2237	0.94
Green House	0	0	0	1	0	0	0	0	0	0	0	532	0	0	0	0	0	0	0	0	0	0	0	0	0	0	0	0	0	0	0	0	0	0	0	13	0	0	0	0	546	0.97
Green Tea Leaves	0	0	0	0	0	0	0	0	0	1	0	0	52	7	0	0	0	0	0	0	0	0	0	0	0	0	0	0	0	0	0	0	0	0	0	0	0	0	0	0	60	0.87
Hazelnut	0	0	0	0	0	0	0	0	0	7	0	0	0	793	2	0	0	0	0	0	0	0	0	0	0	0	0	0	0	0	0	0	0	0	0	0	0	0	0	0	802	0.99
Lemon	4	16	94	0	27	0	5	13	0	38	9	0	0	2	651	0	50	0	0	64	0	38	0	0	0	0	0	0	0	33	0	21	0	0	0	0	0	0	0	1	1066	0.61
Maize	0	0	0	0	15	0	0	0	55	1	0	0	0	0	0	8725	0	0	0	0	105	0	0	0	0	1	0	0	51	0	280	17	0	1	0	0	0	0	0	2	9253	0.94
Mandarin	0	4	34	0	0	0	0	4	0	27	4	0	0	0	43	0	1025	0	0	10	0	25	0	0	0	0	0	0	0	0	0	21	0	0	0	1	0	0	0	0	1198	0.86
Melon	0	0	0	0	3	8	0	0	0	0	6	0	0	0	0	0	0	213	0	0	0	0	0	13	0	0	0	0	0	4	0	7	27	0	187	0	40	0	0	0	508	0.42
Oat	16	0	10	0	75	0	1	151	0	0	4	0	0	0	0	0	0	0	723	0	0	0	0	0	2	0	0	0	0	18	0	13	0	0	0	0	103	0	0	7	1123	0.64
Olive	0	0	37	0	6	0	3	4	0	7	8	0	0	0	0	0	3	0	0	1042	0	12	0	0	0	0	0	0	0	59	0	0	0	0	0	0	0	0	0	0	1181	0.88
Onion (Dry)	0	0	0	1	0	1	0	16	1	0	1	0	0	0	0	21	0	0	0	0	475	0	0	31	0	0	0	0	0	0	43	10	0	8	0	0	0	0	0	0	608	0.78
Orange	1	3	23	0	0	0	0	0	0	6	9	0	0	0	121	0	191	0	0	13	0	541	1	0	0	0	0	0	0	0	0	0	0	0	0	0	0	0	0	2	911	0.59
Peach	0	22	11	0	1	0	3	0	0	0	58	0	0	0	12	31	0	0	0	0	0	5	79	0	0	0	0	0	0	0	0	0	0	0	0	0	0	0	0	0	222	0.36
Pepper	0	0	0	33	0	42	0	0	54	0	0	0	0	0	0	0	0	0	0	0	0	0	0	167	0	1	0	0	0	0	1	6	0	44	0	24	0	0	0	0	372	0.45
Poppy	0	0	0	0	53	0	0	0	0	0	0	0	0	0	0	0	0	0	0	0	0	0	0	0	1463	0	1	0	0	0	0	0	0	0	0	0	0	0	0	6	1523	0.96
Potato	7	0	0	0	1	4	0	2	12	0	0	0	0	0	0	10	0	0	6	2	0	0	0	0	0	1712	0	0	0	4	3	121	0	0	0	0	2	0	0	0	1886	0.91
Rapeseed	3	0	0	0	14	0	0	0	0	0	0	0	0	0	0	0	0	0	0	0	0	0	0	0	3	0	1421	0	0	0	0	1	0	0	0	0	0	0	0	7	1449	0.98
Red Lentil	0	0	2	0	3	0	0	87	0	0	0	0	0	0	0	0	0	0	0	3	0	0	0	0	0	0	0	509	0	0	0	0	0	0	0	0	0	0	0	280	884	0.58
Rice Paddy	7	0	0	0	0	0	0	0	0	1	0	0	0	0	0	1	0	0	0	0	0	0	0	0	0	0	0	0	3939	0	0	1	0	0	0	0	0	0	0	0	3949	1.00
Steppe	1	0	0	4	145	0	0	30	0	0	0	0	0	0	0	0	0	0	7	3	0	0	0	0	10	0	0	16	0	3445	0	0	0	0	0	2	0	0	0	35	3698	0.93
SugerBeet	0	0	0	0	0	29	0	0	3	0	1	0	0	0	0	2	0	1	0	0	0	0	0	0	0	44	0	0	0	0	550	68	0	10	0	0	0	0	0	0	708	0.78
Sunflower	0	0	0	0	0	14	1	112	0	0	9	0	0	0	0	19	2	0	0	0	0	0	0	0	0	8	0	0	0	2	1	5290	0	8	0	0	0	0	0	0	5466	0.97
Tobacco	0	0	0	2	9	0	0	5	0	0	0	0	0	0	0	0	0	1	0	0	0	0	0	0	0	0	0	0	0	3	0	52	19	0	0	19	0	0	0	0	110	0.17
Tomato	4	0	0	0	0	0	0	0	10	0	4	0	0	0	0	0	0	0	0	1	0	0	0	3	0	37	0	0	0	0	2	103	0	685	0	0	0	0	0	1	850	0.81
Triticale	0	0	0	0	90	0	0	6	0	0	0	0	0	0	0	0	0	0	1	0	0	0	0	0	1	4	0	0	0	8	0	2	0	0	69	0	0	0	0	107	288	0.24
Urban	0	0	3	37	0	0	0	2	0	0	0	1	0	0	0	0	0	0	0	10	0	0	0	0	0	0	0	0	0	0	0	0	0	0	0	2509	0	0	0	0	2562	0.98
Vetch	5	0	0	0	115	0	0	0	0	0	0	0	0	0	0	0	0	0	43	0	0	0	0	0	22	0	0	0	0	4	0	7	0	0	0	0	616	0	0	2	814	0.76
Water	0	0	0	0	0	0	0	0	0	0	0	0	0	0	0	0	0	0	0	0	0	0	0	0	0	0	0	0	0	2	0	0	0	0	0	4	0	836	0	0	842	0.99
Watermelon	0	0	1	0	0	50	0	0	0	0	5	0	0	0	0	0	0	10	0	0	0	0	0	7	0	3	0	0	0	0	11	27	0	11	0	0	0	0	170	0	295	0.58
Wheat	3	3	2	0	560	0	2	5	25	0	1	0	0	0	1	9	2	0	6	0	0	10	0	0	56	0	0	1	0	10	0	10	0	0	2	0	0	0	0	11044	11752	0.94
Column Sum	1019	1056	1851	7553	6854	701	304	5556	6901	5120	2403	533	53	807	873	8859	1287	226	845	1208	580	641	80	222	1572	1908	1422	526	3999	3658	907	5975	19	984	77	2789	754	836	170	11917	**OA=0.92**	
UA	0.88	0.89	0.77	0.99	0.81	0.78	0.83	0.91	0.96	0.98	0.88	1.00	0.98	0.98	0.75	0.98	0.80	0.94	0.86	0.86	0.82	0.84	0.99	0.75	0.93	0.90	1.00	0.97	0.98	0.94	0.61	0.89	1.00	0.70	0.90	0.90	0.82	1.00	1.00	0.93	**Kappa=0.91**	

Table 4.6. Kappa Coefficient and Overall Accuracy for Combined Temperature Zones and Classification Without Temperature Zones with Improvement in Accuracy with Temperature Zoning

	Combined Temperature Zones (%)	Without Temperature Zones (%)	Improvement with Temperature Zoning (%)
Overall Accuracy	92.35	91.54	0.81
Cohen's Kappa	91.86	90.99	0.87

Table 4.7. Producer's Accuracy for Each Class for Combined Temperature Zones and Classification Without Temperature Zones with Improvement in PA with Temperature Zoning

Class Name	PA for Combined Temperature Zones (%)	PA for Without Temperature Zones (%)	Improvement in PA with Temperature Zoning (%)
Bean (Dry)	77.02	64.13	12.90
Cherry	75.13	63.32	11.81
Tomato	90.82	80.59	10.24
Olive	97.04	88.23	8.81
Lemon	69.79	61.07	8.72
Green Tea Leaves	95.00	86.67	8.33
Tobacco	25.45	17.27	8.18
Onion (Dry)	85.69	78.13	7.57
Oat	71.06	64.38	6.68
Peach	40.09	35.59	4.50
Triticale	28.13	23.96	4.17
Green House	99.82	97.44	2.38
Bare Soil	99.36	97.09	2.27
Alfalfa	88.39	86.27	2.13
Mandarin	87.65	85.56	2.09
Barley	92.94	90.87	2.07
Apple	84.61	82.59	2.02
Poppy	97.77	96.06	1.71
Urban	99.38	97.93	1.44
Watermelon	58.64	57.63	1.02
Water	99.76	99.29	0.48
Hazelnut	99.25	98.88	0.37
Grape	94.41	94.19	0.22
Cotton	98.97	98.76	0.21
Forest	99.84	99.70	0.14
Melon	41.93	41.93	0.00
Rice Paddy	99.75	99.75	0.00
Maize	94.27	94.29	-0.02
Potato	90.72	90.77	-0.05
Wheat	93.87	93.98	-0.10
Sugar Beet	77.54	77.68	-0.14

Table 4.7 (continued)

Class Name	PA for Combined Temperature Zones (%)	PA for Without Temperature Zones (%)	Improvement in PA with Temperature Zoning (%)
Vetch	75.06	75.68	-0.61
Red Lentil	56.56	57.58	-1.02
Chickpea	95.85	97.05	-1.21
Sunflower	95.50	96.78	-1.28
Steppe	91.81	93.16	-1.35
Orange	57.85	59.39	-1.54
Apricot	81.79	83.36	-1.58
Rapeseed	93.93	98.07	-4.14
Pepper	40.32	44.89	-4.57

4.2 Visual Inspection of the Classification Map

As mentioned in the Methodology chapter, a crop classification map is created using the random forest classifiers. The resultant map is given in Figure 4.1. In this part of the thesis, the classification map is inspected to identify visible problems. The first problem that draws attention is the misclassification of Salt Lake as urban and greenhouse, as shown in Figure 4.2. This confusion potentially occurs due to the similar spectral characteristics of bare soil and urban surfaces (Piyoosh & Ghosh, 2018; Zhang et al., 2015).

Another significant misclassification is the abundance of pixels classified as olive in the west. A representative part of the map is given in Figure 4.3. The reason for this misclassification is potentially the absence of shrub class or specifically maquis, which is the characteristic plant formation of the Mediterranean climate that has a widespread distribution along the coast and east-west oriented valleys in the Aegean Region (Günal, 2013). In addition to the number of olive pixels, a rectangular region that is visibly classified differently from its surrounding can be seen in the center of the image. That rectangular region does not contain as many olive pixels as the rest of the image. The same patchy structure is also seen in other parts of the map, and an example region located in the southeastern part of Türkiye is given in Figure 4.4. Both patches correspond to different temperature zones from their surroundings,

which may mean that the temperature zones should have been smoothed to have a more homogeneous classification.

A large region classified as oat can be seen in the upper left corner of Türkiye in Figure 4.1. The region is also shown in Figure 4.5 in more detail. There is no information found in the literature or other sources that imply an abundant production of oat in the region. So, it can be concluded that the classification is incorrect in the specified region. The reason behind this error should be further investigated.

Figure 4.1. Crop Classification Map

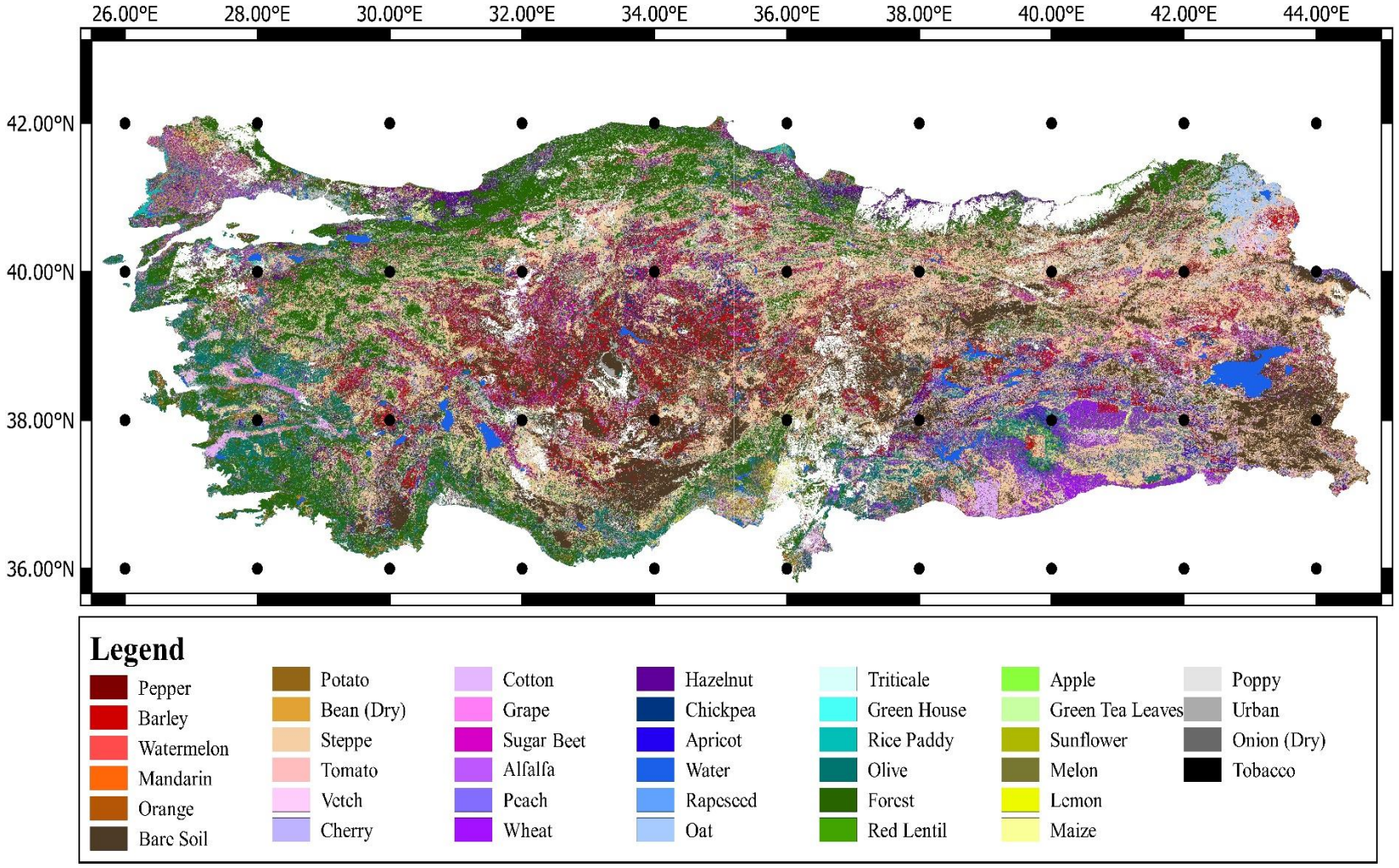

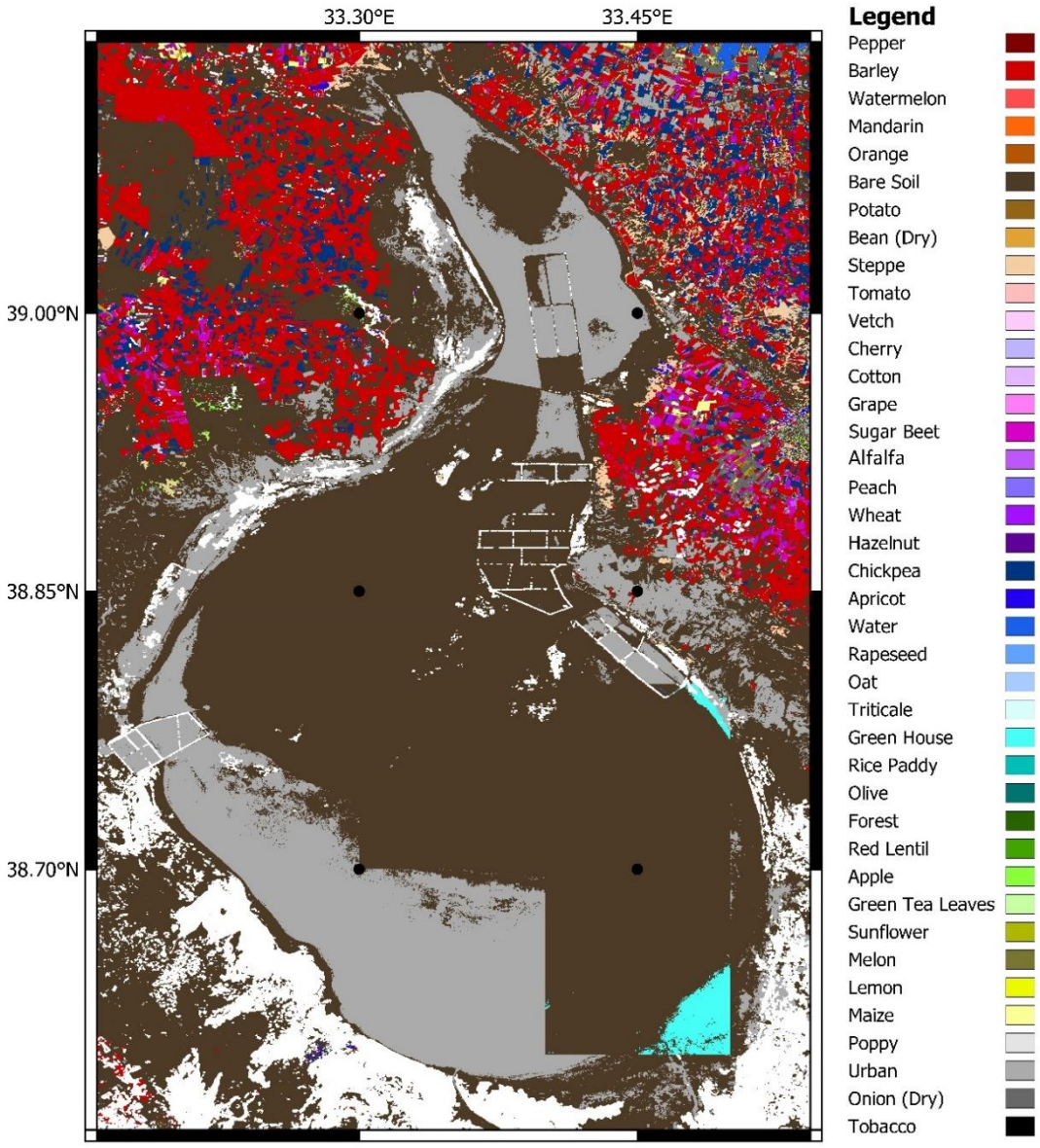

Figure 4.2. Misclassification of Salt Lake

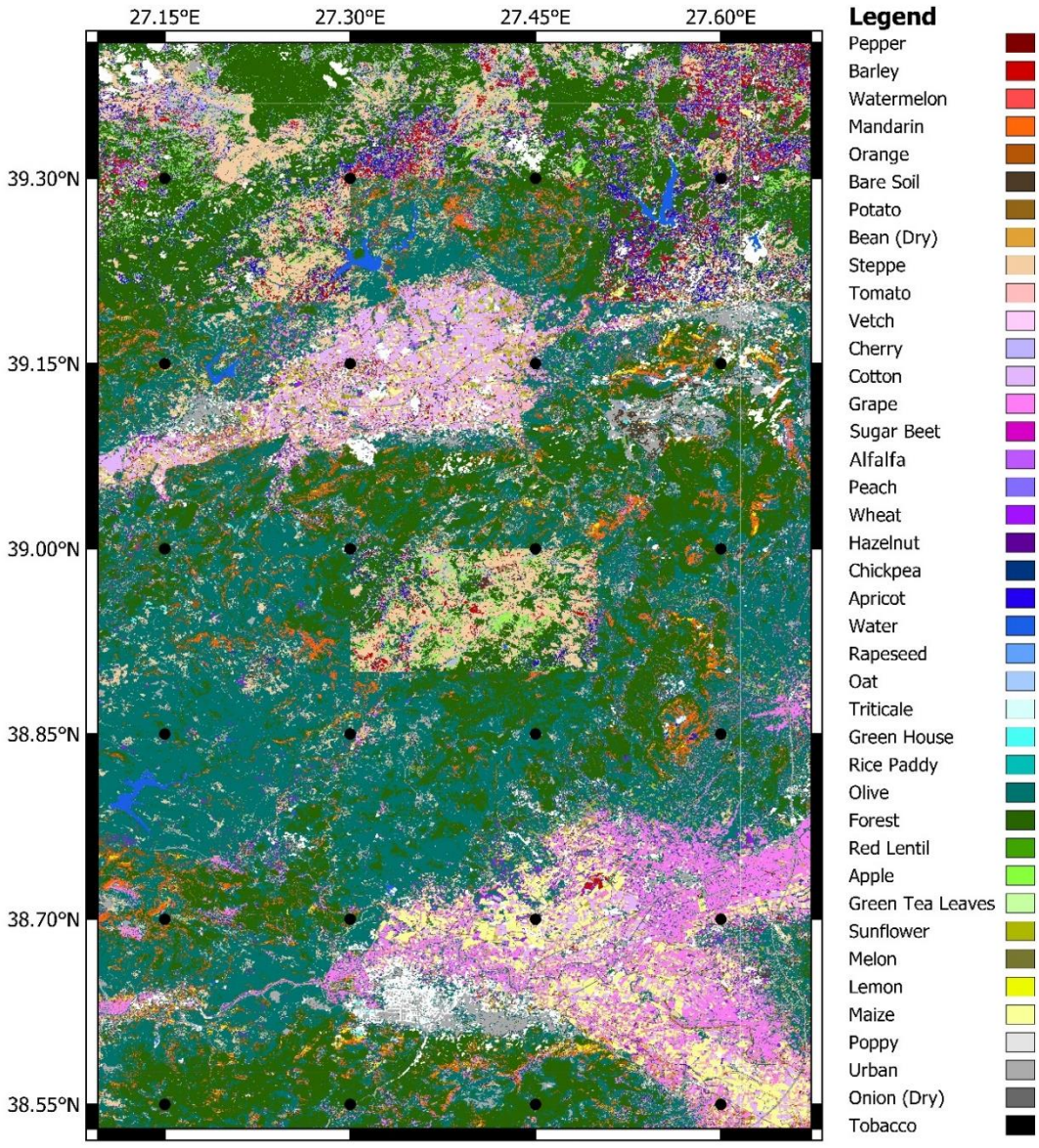

Figure 4.3. Misclassification as Olive in West Türkiye

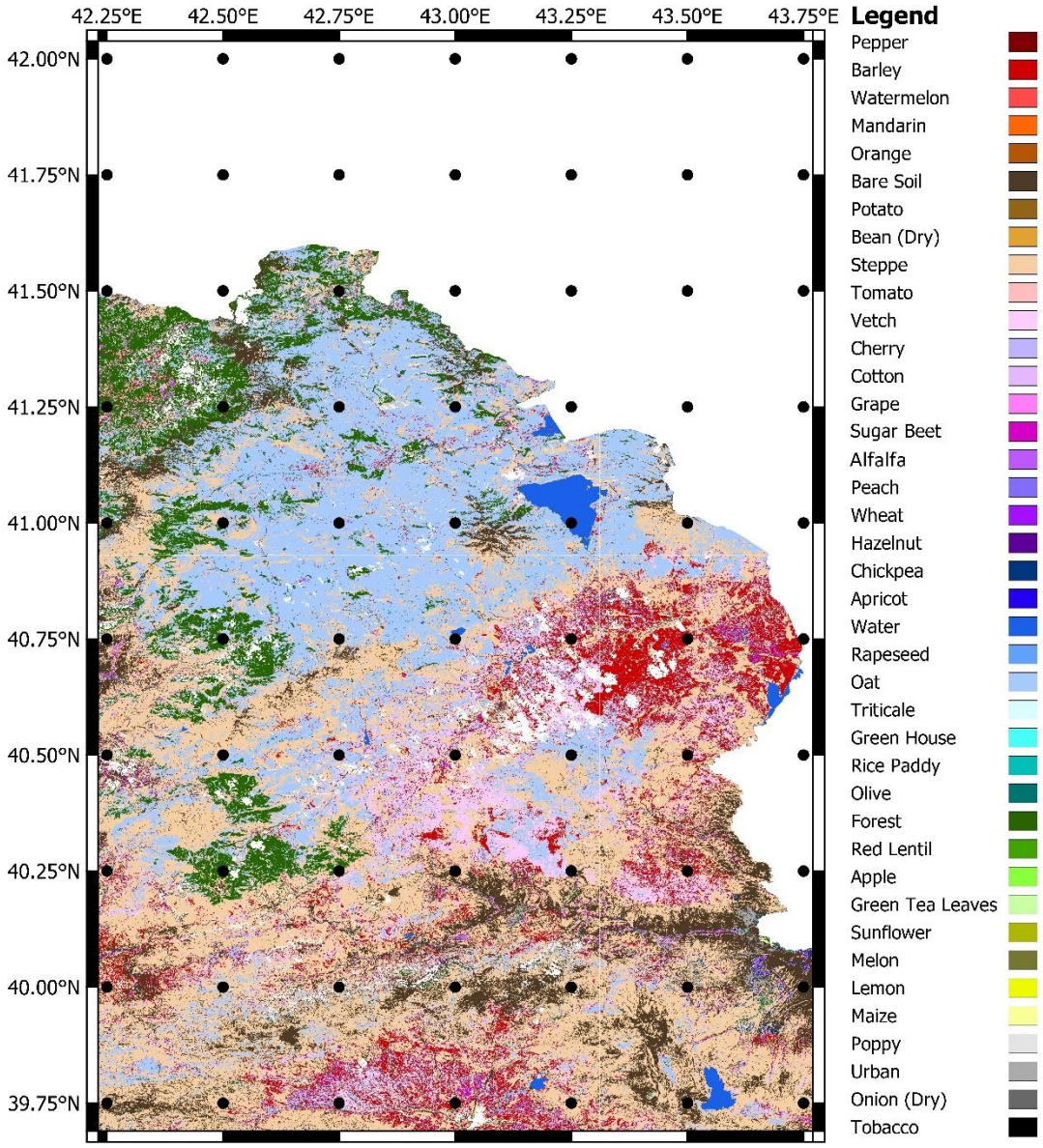

Figure 4.4. Misclassification as Oat in Northeast Türkiye

4.3 Percent Area Comparison with Province Production Data of Ministry of Agriculture and Forestry

Republic Of Türkiye Ministry of Agriculture and Forestry (TMA) publishes yearly production reports for certain crops that contain information about which provinces have the most production for the year. This information is usually in terms of percent

area, while in some reports, it is in tons of production. In this part of the Results and Discussion chapter, available production data for 2019 is compared with the classification map. First, the pixel number of each crop is obtained using Semi-Automatic Classification Plugin in QGis for each province. Then, crop percent areas are calculated and sorted by the highest percent area. Provinces with the highest production of a certain crop are compared with the data provided by the Ministry of Agriculture and Forestry, which contains data for only ten provinces with the highest production.

Area comparison for sugar beet crop is given in Figure 4.6 (Republic of Türkiye Ministry of Agriculture and Forestry, 2020a). Percent area for the crop is similar for both datasets except for Erzurum and Erzincan. These provinces have a high percent area in the classification map even though they do not appear in the TMA data. This means some other crop or crops are classified as sugar beet in these provinces. Erzurum and Erzincan are parts of the Low-Temperature Zone, and Table 4.1 shows that 14 out of 255 wheat pixels are classified as sugar beet in LTZ. So, sugar beet production may be high in these provinces because wheat pixels are misclassified as sugar beet.

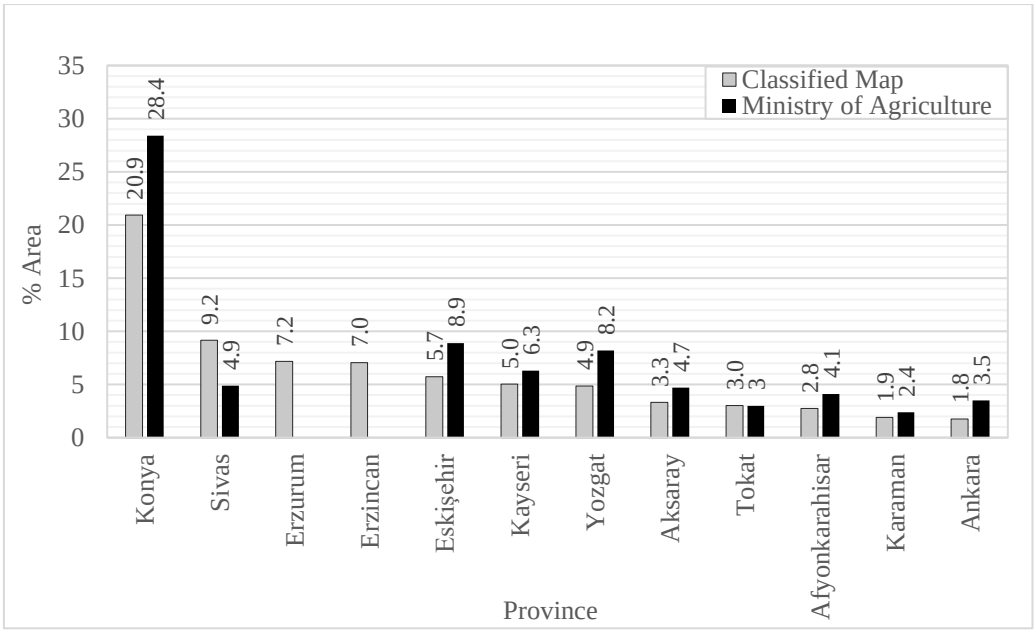

Figure 4.5. Percent Area Comparison with Province Production Data of Ministry of Agriculture and Forestry for Sugar Beet

The potato production area comparison is given in Figure 4.7 (Republic of Türkiye Ministry of Agriculture and Forestry, 2021a). Even though the first six provinces with the highest potato pixels in the classification map are coherent with the TMA data, the second half of the graph shows a discrepancy between the datasets. Eskişehir and Yozgat have a high number of pixels in the classification map, while they do not appear in the highest ten provinces of TMA potato production data. Most of the pixels of these provinces fall into MTZ. The confusion matrix of MTZ (Table 4.2) shows that potato reaches 89% UA, with eight grape pixels classified as potato. So, one explanation for the high number of potato pixels in Eskişehir and Yozgat can be the misclassification of grape pixels as potato. On the other hand, Bolu, Adana, and İzmir have a low number of pixels in the classification map, but they are in the highest ten provinces of TMA potato production data. These three provinces have pixels that fall into all three temperature zones. When confusion matrices for LTZ (Table 4.1) and MTZ (Table 4.2) are inspected, it can be seen that potato pixels are misclassified as cow vetches, alfalfa, oat, and apples. These misclassifications can be the reason for the discrepancy between the TMA data and the classification map for the potato class.

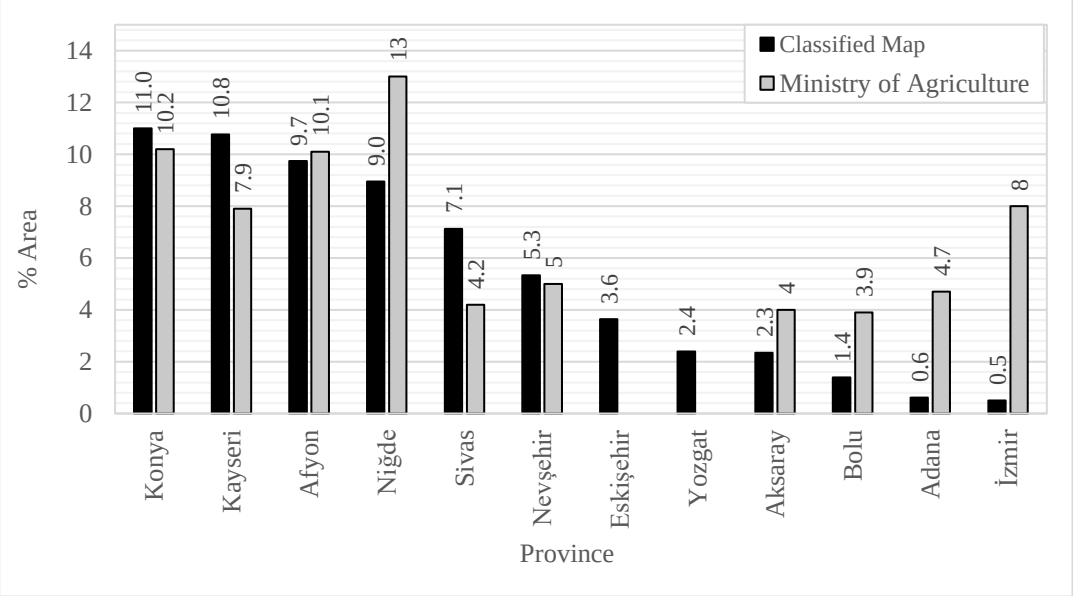

Figure 4.6. Percent Area Comparison with Province Production Data of Ministry of Agriculture and Forestry for Potato

Area comparison between classified map and TMA data for cotton is given in Figure 4.8. The distribution of the provinces with the highest areas is very similar for cotton, with a maximum of 3.7% difference, which occurs in Hatay. In the classification map, Hatay has large portions of missing data due to consistent cloud cover, which can be the reason for the lower percent area in the classification map.

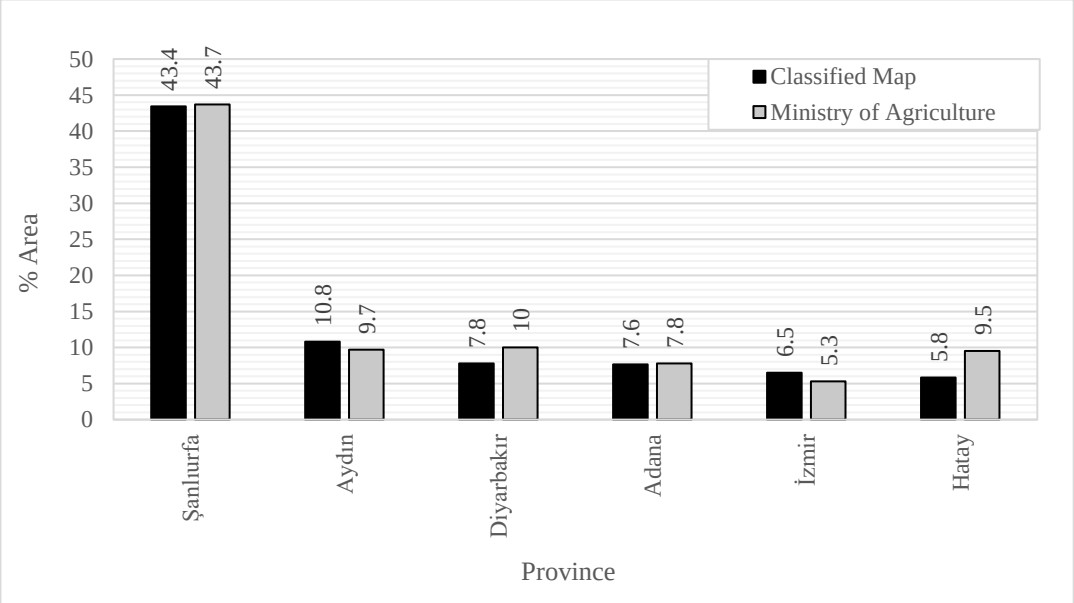

Figure 4.7. Percent Area Comparison with Province Production Data of Ministry of Agriculture and Forestry for Cotton

Area comparison between classified map and TMA data for cotton is given in Figure 4.9 (Republic of Türkiye Ministry of Agriculture and Forestry, 2020b). Similar to potato, chickpea classified area percentage and TMA data have similar values for the first half of the provinces with the highest area. Şanlıurfa has a high number of pixels in the classification map, while it does not appear in the highest ten provinces of TMA chickpea production data. More than 99% of the pixels in Şanlıurfa fall in HTZ. Chickpea has 100% UA and 36% PA in the HTZ test set, which means most of the misclassification of chickpea occurs due to chickpea pixels classified as another crop instead of the opposite case. So, having more percent area in the classification map than TMA for a province that falls into HTZ is not an expected result. Other classifiers also have high accuracies for the chickpea class (100% UA

and 99% PA for LTZ, 92% UA, and 98% PA for MTZ). No explanation is offered for the low percent areas in Adıyaman, Uşak, and Karaman.

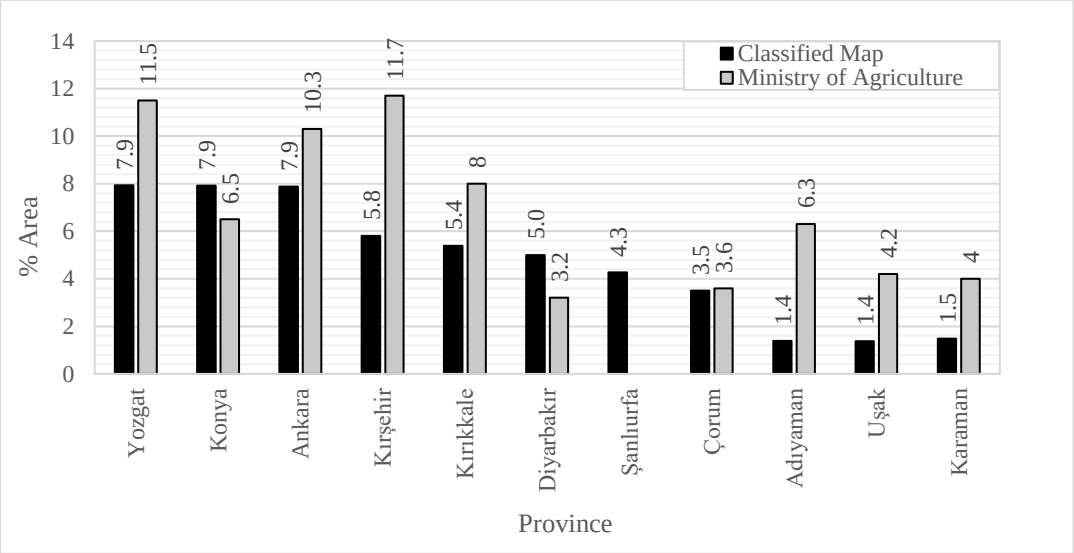

Figure 4.8. Percent Area Comparison with Province Production Data of Ministry of Agriculture and Forestry for Chickpea

The maize production percent area comparison is given in Figure 4.10 (Republic of Türkiye Ministry of Agriculture and Forestry, 2019). İzmir, Eskişehir, and Denizli provinces have a high percentage of maize area in the classification map even though they are not in the ten provinces with the highest maize production area. These provinces have pixels both in MTZ and HTZ. In the HTZ test set, 28 of 60 peach pixels are misclassified as maize, and it is the only significant misclassification decreasing the UA of maize in these temperature zones. Karaman, Adıyaman, and Osmaniye provinces, in which TMA data has a larger percentage area than the classification map, have pixels mostly in the HTZ. PA obtained for maize with the test of HTZ is 98%, so it is unclear which crop class or classes are taking up the areas that should be classified as maize.

Area comparison between classified map and TMA data for red lentil is given in Figure 4.11 (Agricultural Economic and Policy Development Institute, 2020). The percentage areas of the classified map and TMA data are mostly similar except for Şanlıurfa and Adıyaman. These two provinces have pixels mostly in HTZ, in which

248 of 706 red lentil test pixels are misclassified as wheat. This misclassification can potentially be the reason for the disproportionate percent areas.

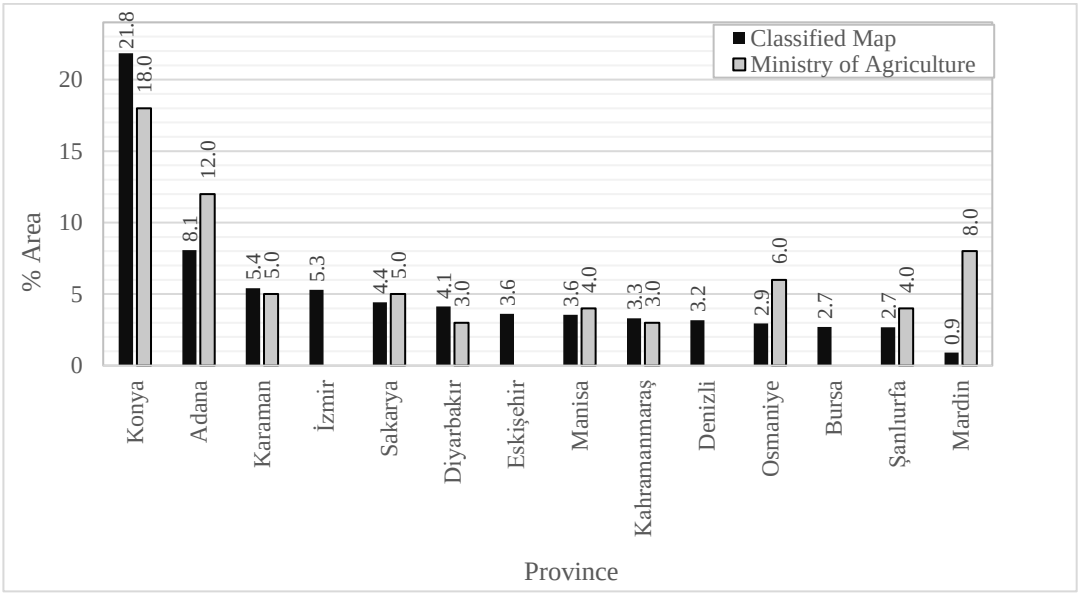

Figure 4.9. Percent Area Comparison with Province Production Data of Ministry of Agriculture and Forestry for Maize

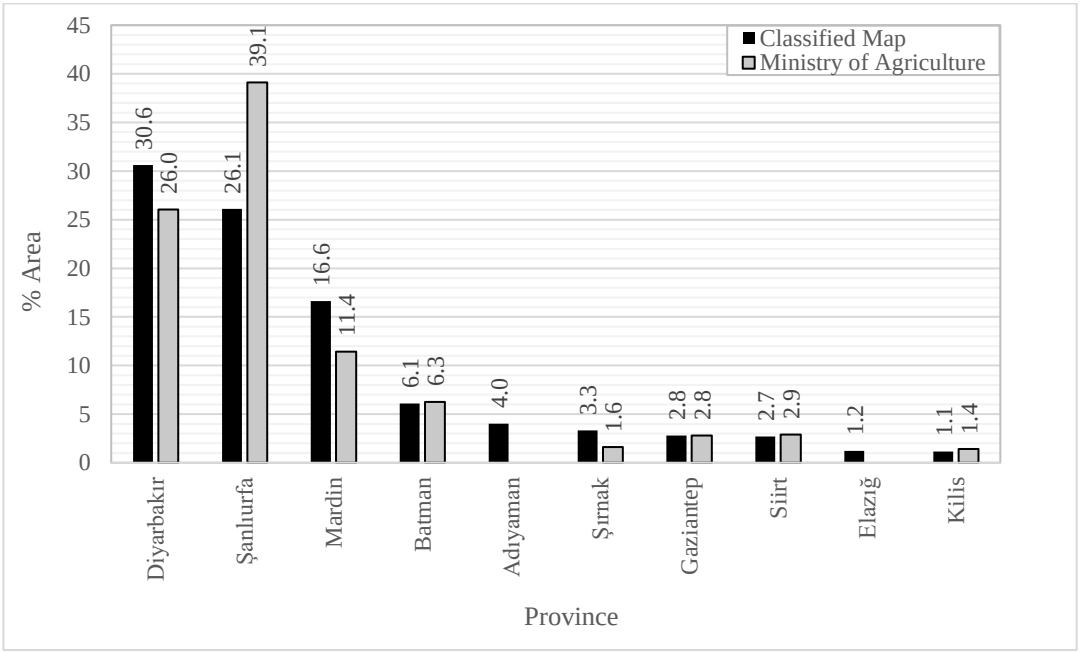

Figure 4.10. Percent Area Comparison with Province Production Data of Ministry of Agriculture and Forestry for Red Lentil

Barley production percent area comparison is given in Figure 4.12 (Republic of Türkiye Ministry of Agriculture and Forestry, 2020c). Percent area for the crop is similar for both datasets except for Yozgat, Erzurum, and Muş. These provinces have a high percent area in the classification map even though they do not appear in the TMA data. This means some other crops or crops are classified as barley in these provinces. Yozgat, Erzurum, and Muş have pixels mostly in LTZ, and some of the pixels in these provinces fall into MTZ. The confusion matrix of LTZ shows that 94 out of 255 wheat pixels are classified as barley. Also, the confusion matrix of MTZ shows that 497 of 3057 wheat pixels are classified as barley. So, barley production in these provinces may appear higher because of the misclassification between barley and wheat.

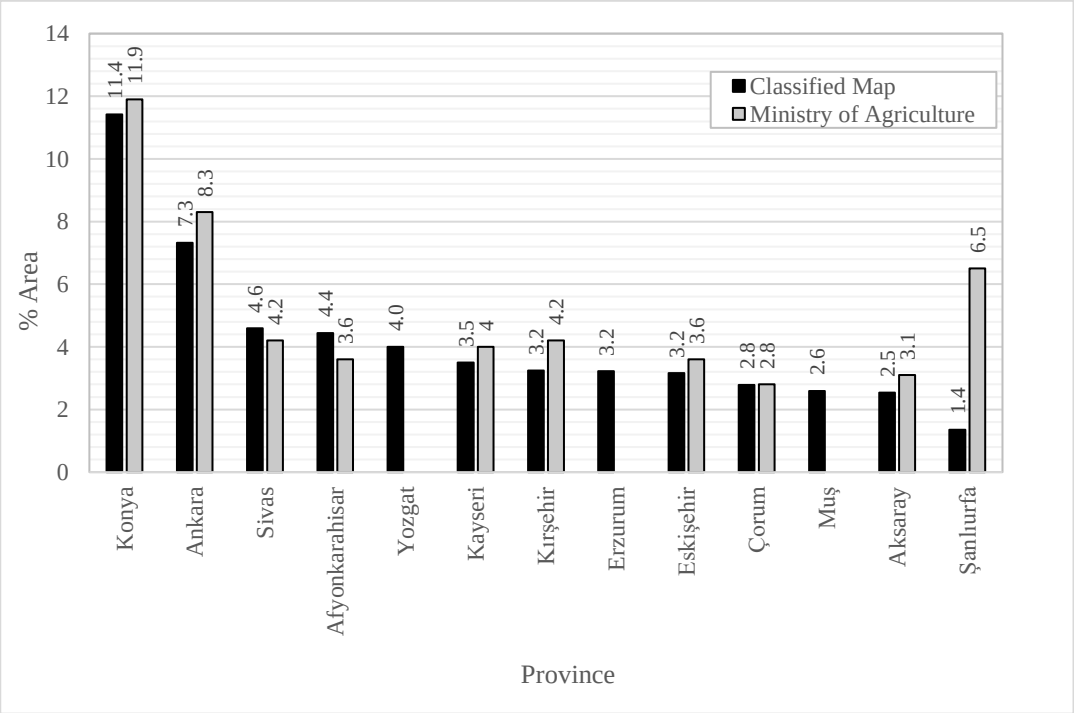

Figure 4.11. Percent Area Comparison with Province Production Data of Ministry of Agriculture and Forestry for Barley

Area comparison between classified map and TMA data for wheat is given in Figure 4.13 (Republic of Türkiye Ministry of Agriculture and Forestry, 2021b). Area percentages of the classified map do not reflect the area percentages provided by

TMA. Even though Diyarbakır, Şanlıurfa, Mardin, Tekirdağ, Konya, Ankara, Çorum, Yozgat, Sivas, and Eskişehir provinces are mutual for both datasets, Edirne, Kırklareli, Balıkesir, Çanakkale, Adıyaman, Batman, Şırnak and Gaziantep provinces have high area percentages for wheat and these provinces do not appear in the highest 10 provinces of TMA wheat production data. These provinces have pixels in all temperature zones. When confusion matrices of all classifiers are inspected, it can be seen that in LTZ barley, in MTZ barley and triticale, and in HTZ barley, red lentil and steppe are confused with wheat. This confusion may be the reason for the higher and lower percent areas of the classification map compared to the TMA data.

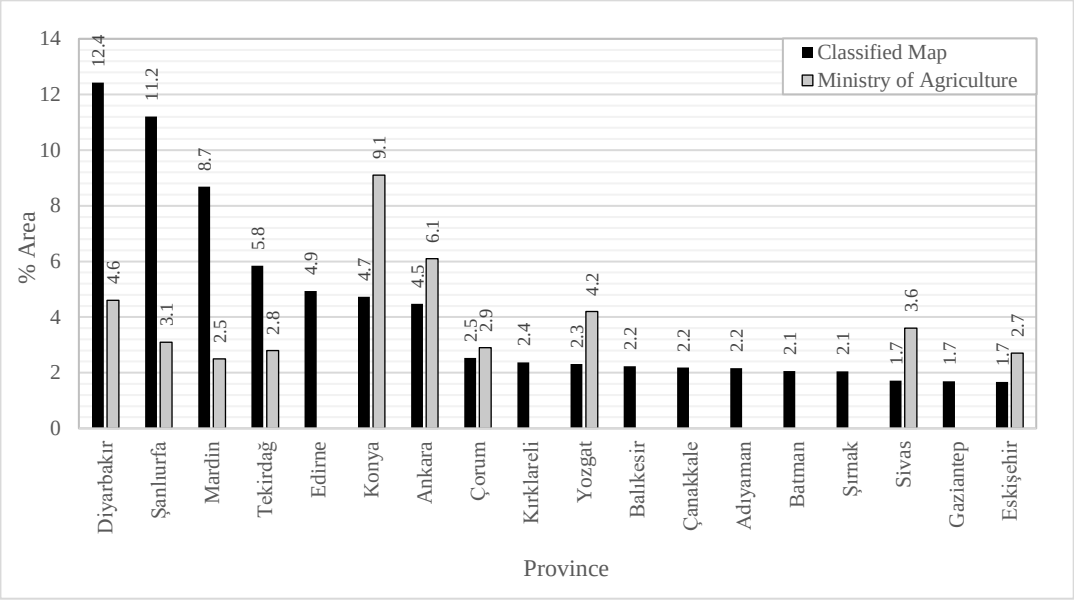

Figure 4.12. Percent Area Comparison with Province Production Data of Ministry of Agriculture and Forestry for Wheat

Rice paddy production percent area comparison is given in Figure 4.14 (Republic of Türkiye Ministry of Agriculture and Forestry, 2020d). Except for the 13.2% lower percent area of the classified map in Edirne and higher percent areas of the classified map in Adana and Şanlıurfa, two datasets have similar values for Rice paddy. These three provinces with dissimilar percent areas have pixels in HTZ and MTZ. When confusion matrices are inspected, it can be seen that rice paddy reaches 100% OA and UA with the test sets of both temperature zone classifiers. So, the difference in

the datasets may be due to cloud cover, spatial resolution, or other factors unrelated to the classifiers' performance.

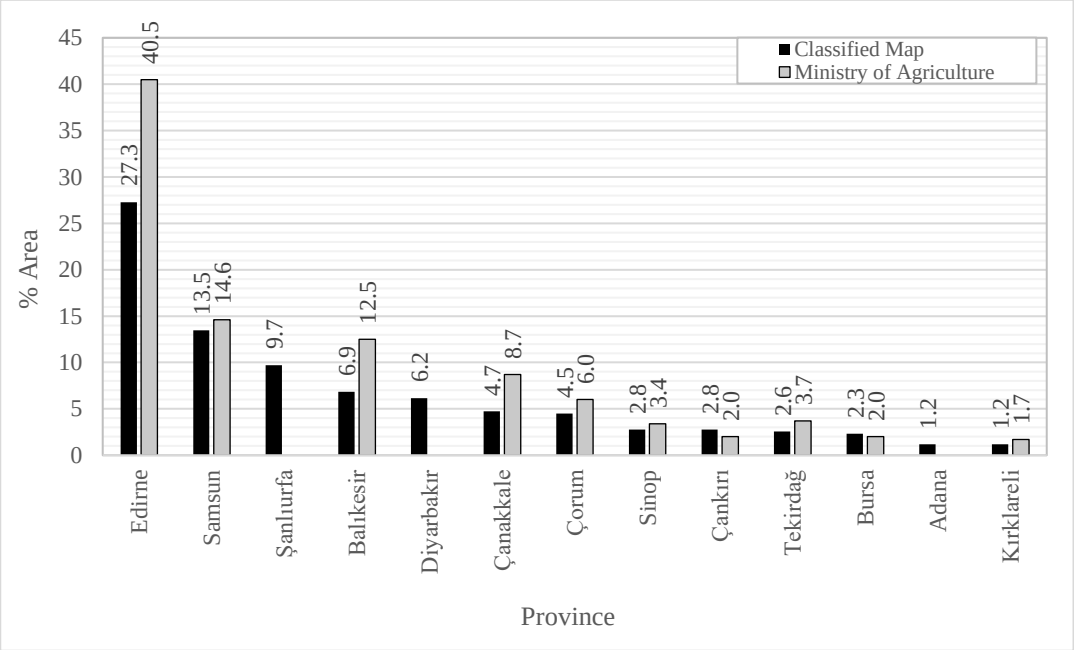

Figure 4.13. Percent Area Comparison with Province Production Data of Ministry of Agriculture and Forestry for Rice Paddy

CHAPTER 5

CONCLUSION

Agricultural crop cover information benefits water resources management and food security assessment. Creating crop maps using remotely sensed data and machine learning algorithms is an objective and time-efficient way of obtaining crop cover information. This way, it is possible to classify crop areas over a region with a limited amount of field observation data.

In this study, a crop cover map of Türkiye is created for 2019. All bands except Band 10 of Sentinel-2 Level-2A are reduced to 15-day median images from March 15, 2019, to October 15, 2019. Apart from the spectral bands of Sentinel-2, the Normalized Difference Vegetation Index, Normalized Difference Water Index proposed by Gao (1996), and Normalized Difference Water Index proposed by McFeeters (1996) are calculated to be used as classification features. When contributions of classification features are inspected through random forest importance, it is observed that indices used in the study contributed to the classification accuracy, and they are recommended for similar studies.

This study investigates the advantage of temperature zoning for large-scale crop mapping. When confusion matrices of the whole test set with and without temperature zoning are examined, even though overall accuracy differs marginally, it is observed that more classes reach better accuracies with temperature zoning. Considering that the product map is a large-scale map, minor increases in accuracy mean better performance over a large region. In addition, although the division of ground truth data is disadvantageous due to the decrease in the number of training samples for each class, the increase in accuracy with temperature zones shows the importance and success of temperature zoning. The process of temperature zoning is not computationally costly, so for the classification of large areas that have multiple

climate types, temperature zoning is recommended based on the results obtained from this study. In addition, because the crop map patches occur due to different temperature zones, smoothing of the temperature zones can be recommended for future work. The temperature thresholds (9°C & 14°C) selected arbitrarily for this study can be adjusted for better accuracy for future studies. Also, the study area can be divided into zones according to other factors affecting crop growth or crop distribution, like humidity (Heuvelink & Dorais, 2005) and elevation (Machado et al., 2002). For future work, temperature information can be used as classification input as it is in the study of Zhang et al. (2022), and results can be compared to a classification in which temperature is used for the division of the study area.

When classifiers are applied to the test set, the Low-Temperature Zone reached 89% overall accuracy with a 0.88 Kappa coefficient for 17 land cover classes. The Medium-Temperature Zone reached 91% overall accuracy with a 0.92 Kappa coefficient for 35 land cover classes, and High-Temperature Zone reached %94 overall accuracy with a 0.94 Kappa coefficient for 34 land cover classes, giving the best accuracy among the classifiers. Finally, test sets of the temperature zones are combined, and overall accuracy of 92% with a Kappa coefficient of 0.93 is achieved with this combined test set. When these accuracies are compared, the accuracy on the test set is observed to be higher than in other large-scale crop classification studies (e.g., Yılmaz et al., 2020; Yang et al., 2019; d'Andrimont et al., 2021; Woźniak et al., 2022) except for the study of Jiang et al. (2020), with 94% overall accuracy. Even the LTZ classifier, which gives the lowest accuracy, is satisfactory when the accuracies of other studies (Yılmaz et al., 2020; Yang et al., 2019; d'Andrimont et al., 2021) are considered. Another sign of the success of the crop map is the similarity of crop distribution with the crop area data provided by the Ministry of Agriculture and Forestry. It is also very important to consider that this study has 40 classes, which is more than any other large-scale crop mapping study, which means that there is more chance of crops with similar phenological and spectral similarities. So, it can be concluded that the methodology used in this study gives satisfactory results when the accuracy on the scale and content of the map is compared with similar studies.

Wheat and barley pixels are misclassified in LTZ and MTZ. According to tons of crop production data provided by the Turkish Statistical Institute (2019), among all products, wheat has the highest (16.9%), and barley has the fourth highest production percentage (6.44%). Although the misclassification of these two crops affects the overall accuracy of the classification map as large areas are covered by wheat and barley, the fact that these two crops have very similar water footprints (Batan, 2021; Bulut and Canbaz, 2022) shows that this misclassification would not affect water management practices as much as misclassification among crops with different water demands.

The classification map is visually inspected to detect significant problems. One of the most noticeable misclassifications occurred between urban and bare soil surfaces. To overcome this problem, NDBI proposed by Zha et al. (2003) to map urban and built-up areas, dry built-up index (DBI), and dry bare-soil index (DBSI) to map built-up and bare areas in a dry climate proposed by Rasul et al. (2018) can be utilized. In addition to that, training pixel number of urban class can be increased for better results.

Agricultural classification can also be performed over different years using the same algorithm for the years Sentinel-2 Level 2 data is available, and land cover change maps can be obtained over multiple years. For future work, the resultant crop maps can be compared to other crop maps such as CORINE (Bossard et al., 2000) for the years that both maps are available for the mutual land cover classes. To obtain future crop maps, it is only necessary to wait until the end of August of that year for the necessary inputs to be available. Nevertheless, obtaining agricultural crop maps for different years can be useful for agricultural production and irrigation management.

REFERENCES

Abdikan, S., Sekertekin, A., Ustuner, M., Sanli, F. B., & Nasirzadehdizaji, R. (2018). Backscatter analysis using multi-temporal Sentinel-1 SAR data for crop growth of maize in Konya Basin, Turkey. *Int. Arch. Photogramm. Remote Sens. Spat. Inf. Sci*, *42*, 9–13.

Agricultural Economic and Policy Development Institute (2020). Ürün Raporu: Nohut. Retrieved June 16, 2022, from https://arastirma.tarimorman.gov.tr/tepge/Belgeler/PDF%20%C3%9Cr%C3%BCn%20Raporlar%C4%B1/2020%20%C3%9Cr%C3%BCn%20Raporlar%C4%B1/Nohut%20%C3%9Cr%C3%BCn%20Raporu%202020-320%20TEPGE.pdf

Agricultural Economic and Policy Development Institute (2021). Ürün Raporu: Mercimek. Retrieved June 16, 2022, from https://arastirma.tarimorman.gov.tr/tepge/Belgeler/PDF%20%C3%9Cr%C3%BCn%20Raporlar%C4%B1/2021%20%C3%9Cr%C3%BCn%20Raporlar%C4%B1/Mercimek%20%C3%9Cr%C3%BCn%20Raporu%202021-341%20TEPGE.pdf

Ajadi, O. A., Barr, J., Liang, S.-Z., Ferreira, R., Kumpatla, S. P., Patel, R., & Swatantran, A. (2021). Large-scale crop type and crop area mapping across Brazil using synthetic aperture radar and optical imagery. *International Journal of Applied Earth Observation and Geoinformation*, *97*, 102294.

Akar, Ö., & Güngör, O. (2015). Integrating multiple texture methods and NDVI to the Random Forest classification algorithm to detect tea and hazelnut plantation areas in northeast Turkey. *International Journal of Remote Sensing*, *36*(2), 442–464.

Alganci, U., Sertel, E., Ozdogan, M., & Ormeci, C. (2013). Parcel-level identification of crop types using different classification algorithms and multi-resolution imagery in Southeastern Turkey. *Photogrammetric Engineering & Remote Sensing*, *79*(11), 1053–1065.

Apan, A. A. (1997). Land cover mapping for tropical forest rehabilitation planning using remotely-sensed data. *International Journal of Remote Sensing*, *18*(5), 1029–1049. https://doi.org/10.1080/014311697218557

Batan, M. (2021). Planning the use of water in Şanlıurfa province, which struggles with drought: Water footprint analysis. *Journal of the Faculty of Engineering and Architecture of Gazi University*, *36*(4), 2135-2149.

Bauer, M. E., Hixson, M. M., Davis, B. J., & Etheridge, J. B. (1978). Area estimation of crops by digital analysis of Landsat data. *Photogrammetric Engineering and Remote Sensing*, *44*(8), 1033-1043.

Bengtsson, L., Hagemann, S., & Hodges, K. I. (2004). Can climate trends be calculated from reanalysis data?. *Journal of Geophysical Research: Atmospheres*, *109*(D11).

Bernard, S., Heutte, L., & Adam, S. (2009). Influence of hyperparameters on random forest accuracy. *International Workshop on Multiple Classifier Systems*, 171–180.

Bossard, M., Feranec, J., & Otahel, J. (2000). *CORINE land cover technical guide: Addendum 2000* (Vol. 40). Copenhagen: European Environment Agency.

Braaten, J. (n.d.). *Sentinel-2 cloud masking with s2cloudless | Google Earth engine | google developers*. Google. Retrieved June 25, 2022, from https://developers.google.com/earth-engine/tutorials/community/sentinel-2-s2cloudless

Breiman, L. (2001). Random forests. *Machine Learning*, *45*(1), 5–32.

Bremer, D. J., Lee, H., Su, K., & Keeley, S. J. (2011). Relationships between Normalized Difference Vegetation Index and Visual Quality in Cool-Season Turfgrass: II. Factors Affecting NDVI and its Component Reflectances. *Crop Science*, *51*(5), 2219–2227. https://doi.org/10.2135/cropsci2010.12.0729

Bulut, A. P., & Canbaz, G. T. (2022) Sivas İlinde Buğday, Arpa, Şeker Pancarı ve Ayçiçeği Üretimi İçin Su Ayak İzinin Hesaplanması. *Bilecik Şeyh Edebali*

Üniversitesi Fen Bilimleri Dergisi, *9*(1), 249-255.

Cai, Y., Guan, K., Peng, J., Wang, S., Seifert, C., Wardlow, B., & Li, Z. (2018). A high-performance and in-season classification system of field-level crop types using time-series Landsat data and a machine learning approach. *Remote Sensing of Environment*, *210*, 35–47. https://doi.org/10.1016/j.rse.2018.02.045

Cakirli Akyüz, N., & Theuvsen, L. (2021). Organic agriculture in Turkey: status, achievements, and shortcomings. *Organic Agriculture*, *11*(4), 501–517. https://doi.org/10.1007/s13165-021-00362-2

Chen, Z., Wang, L., Wei, A., Gao, J., Lu, Y., & Zhou, J. (2019). Land-use change from arable lands to orchards reduced soil erosion and increased nutrient loss in a small catchment. *Science of the Total Environment*, *648*, 1097–1104. https://doi.org/10.1016/j.scitotenv.2018.08.141

Cohen, J. (1960). A coefficient of agreement for nominal scales. *Educational and Psychological Measurement*, *20*(1), 37–46.

Colwell, R. N., & Katibah, E. F. (1976). Optical Vs. electronic enhancement of remote sensing imagery. *Image Processing*, *0074*, 111–119. https://doi.org/10.1117/12.954707

Cover, T., & Hart, P. (1967). Nearest neighbor pattern classification. *IEEE transactions on information theory*, *13*(1), 21-27.

d'Andrimont, R., Verhegghen, A., Lemoine, G., Kempeneers, P., Meroni, M., & van der Velde, M. (2021). From parcel to continental scale – A first European crop type map based on Sentinel-1 and LUCAS Copernicus in-situ observations. *Remote Sensing of Environment*, *266*(October). https://doi.org/10.1016/j.rse.2021.112708

David, N., Giordano, S., & Mallet, C. (2021). Investigating operational country-level crop monitoring with Sentinel~ 1 and~ 2 imagery. *Remote Sensing Letters*,

12(10), 970–982.

Di Gregorio, A. (2005). *Land Cover Classification System (LCCS): Classification Concepts and User Manual* (Vol. 2).

Dimov, D., Löw, F., Ibrakhimov, M., Stulina, G., & Conrad, C. (2017). SAR and optical time series for crop classification. *2017 IEEE International Geoscience and Remote Sensing Symposium (IGARSS)*, 811–814. https://doi.org/10.1109/IGARSS.2017.8127076

Duda, R. O., & Hart, P. E. (1973). *Pattern classification and scene analysis* (Vol. 3, pp. 731-739). New York: Wiley.

Earth Resources Observation and Science (EROS) Center. (2018, July 16). *USGS EROS Archive - Sentinel-2*. Https://Www.Usgs.Gov/Centers/Eros/Science/Usgs-Eros-Archive-Sentinel-2?Qt-Science_center_objects=0#overview.

Erasmi, S., Twele, A., Ardiansyah, M., Malik, A., & Kappas, M. (2004). Mapping deforestation and land cover conversion at the rainforest margin in Central Sulawesi, Indonesia. *EARSeL EProceedings*, *3*(3), 388–397.

Fix, E., & Hodges Jr, J. L. (1952). *Discriminatory analysis-nonparametric discrimination: Small sample performance*. California Univ Berkeley.

Gao, B. (1996). NDWI—A normalized difference water index for remote sensing of vegetation liquid water from space. *Remote Sensing of Environment*, *58*(3), 257–266. https://doi.org/https://doi.org/10.1016/S0034-4257(96)00067-3

Genuer, R., Poggi, J.-M., & Tuleau-Malot, C. (2010). Variable selection using random forests. *Pattern Recognition Letters*, *31*(14), 2225–2236.

Gibson, J. K. (1997). ERA description. *ECMWF re-analysis project report series*, *1*.

Griffiths, P., Nendel, C., & Hostert, P. (2019). Intra-annual reflectance composites from Sentinel-2 and Landsat for national-scale crop and land cover mapping.

Remote Sensing of Environment, *220*, 135–151. https://doi.org/10.1016/j.rse.2018.10.031

Günal, N. (2013). Türkiye'de iklimin doğal bitki örtüsü üzerindeki etkileri. *Acta Turcica*, *1*, 1–22.

Han, H., Guo, X., & Yu, H. (2016). Variable selection using mean decrease accuracy and mean decrease gini based on random forest. *2016 7th Ieee International Conference on Software Engineering and Service Science (Icsess)*, 219–224.

Hao, P., Zhan, Y., Wang, L., Niu, Z., & Shakir, M. (2015). Feature selection of time series MODIS data for early crop classification using random forest: A case study in Kansas, USA. *Remote Sensing*, *7*(5), 5347–5369.

Harrington, P. (2012). *Machine learning in action*. Simon and Schuster.

Hassan, M. M. (2017). Monitoring land use/land cover change, urban growth dynamics and landscape pattern analysis in five fastest urbanized cities in Bangladesh. *Remote Sensing Applications: Society and Environment*, *7*, 69–83. https://doi.org/10.1016/j.rsase.2017.07.001

Hastie, T., Tibshirani, R., Friedman, J. H., & Friedman, J. H. (2009). *The elements of statistical learning: data mining, inference, and prediction* (Vol. 2). Springer.

Heuvelink, E., & Dorais, M. (2005). Crop growth and yield. *Crop Production Science in Horticulture*, *13*, 85.

James, G., Witten, D., Hastie, T., & Tibshirani, R. (2013). *An introduction to statistical learning* (Vol. 112, p. 18). New York: springer.

Ji, S., Zhang, C., Xu, A., Shi, Y., & Duan, Y. (2018). 3D convolutional neural networks for crop classification with multi-temporal remote sensing images. *Remote Sensing*, *10*(1). https://doi.org/10.3390/rs10010075

Jia, K., Liang, S., Wei, X., Yao, Y., Su, Y., Jiang, B., & Wang, X. (2014). Land cover classification of landsat data with phenological features extracted from time series MODIS NDVI data. *Remote Sensing*.

https://doi.org/10.3390/rs61111518

Jiang, Y., Lu, Z., Li, S., Lei, Y., Chu, Q., Yin, X., & Chen, F. (2020). Large-scale and high-resolution crop mapping in china using Sentinel-2 satellite imagery. *Agriculture*, *10*(10), 433.

Joshi, N., Baumann, M., Ehammer, A., Fensholt, R., Grogan, K., Hostert, P., Jepsen, M. R., Kuemmerle, T., Meyfroidt, P., Mitchard, E. T. A., Reiche, J., Ryan, C. M., & Waske, B. (2016). A review of the application of optical and radar remote sensing data fusion to land use mapping and monitoring. In *Remote Sensing* (Vol. 8, Issue 1). MDPI AG. https://doi.org/10.3390/rs8010070

Kussul, N., Lemoine, G., Gallego, F. J., Skakun, S. V, Lavreniuk, M., & Shelestov, A. Y. (2016). Parcel-based crop classification in Ukraine using Landsat-8 data and Sentinel-1A data. *IEEE Journal of Selected Topics in Applied Earth Observations and Remote Sensing*, *9*(6), 2500–2508.

Liaw, A., & Wiener, M. (2002). Classification and regression by randomForest. *R News*, *2*(3), 18–22.

Liu, H., Gong, P., Wang, J., Clinton, N., Bai, Y., & Liang, S. (2020). Annual dynamics of global land cover and its long-term changes from 1982 to 2015. *Earth System Science Data*, *12*(2), 1217–1243. https://doi.org/10.5194/essd-12-1217-2020

Long, J. A., Lawrence, R. L., Greenwood, M. C., Marshall, L., & Miller, P. R. (2013). Object-oriented crop classification using multitemporal ETM+ SLC-off imagery and random forest. *GIScience & Remote Sensing*, *50*(4), 418–436.

Machado, S., Bynum, E. D., Archer, T. L., Lascano, R. J., Wilson, L. T., Bordovsky, J., ... & Xu, W. (2002). Spatial and temporal variability of corn growth and grain yield: Implications for site-specific farming. *Crop Science*, *42*(5), 1564-1576.

Mandal, J., Ghosh, N., & Mukhopadhyay, A. (2019). Urban Growth Dynamics and Changing Land-Use Land-Cover of Megacity Kolkata and Its Environs.

Journal of the Indian Society of Remote Sensing, *47*(10), 1707–1725. https://doi.org/10.1007/s12524-019-01020-7

Maponya, M. G., Van Niekerk, A., & Mashimbye, Z. E. (2020). Pre-harvest classification of crop types using a Sentinel-2 time-series and machine learning. *Computers and Electronics in Agriculture*, *169*, 105164.

Mathur, A., & Foody, G. M. (2008). Crop classification by support vector machine with intelligently selected training data for an operational application. *International Journal of Remote Sensing*, *29*(8), 2227–2240. https://doi.org/10.1080/01431160701395203

McCulloch, W. S., & Pitts, W. (1943). A logical calculus of the ideas immanent in nervous activity. *The Bulletin of Mathematical Biophysics*, *5*(4), 115–133.

McFeeters, S. K. (1996). The use of the Normalized Difference Water Index (NDWI) in the delineation of open water features. *International Journal of Remote Sensing*, *17*(7), 1425–1432. https://doi.org/10.1080/01431169608948714

Ming, D., Zhou, T., Wang, M., & Tan, T. (2016). Land cover classification using random forest with genetic algorithm-based parameter optimization. *Journal of Applied Remote Sensing*, *10*(3), 035021. https://doi.org/10.1117/1.jrs.10.035021

Muñoz-Sabater, J., Dutra, E., Agustí-Panareda, A., Albergel, C., Arduini, G., Balsamo, G., Boussetta, S., Choulga, M., Harrigan, S., Hersbach, H., Martens, B., Miralles, D. G., Piles, M., Rodríguez-Fernández, N. J., Zsoter, E., Buontempo, C., & Thépaut, J. N. (2021). ERA5-Land: A state-of-the-art global reanalysis dataset for land applications. *Earth System Science Data*, *13*(9), 4349–4383. https://doi.org/10.5194/essd-13-4349-2021

Myneni, R. B., Hall, F. G., Sellers, P. J., & Marshak, A. L. (1995). The interpretation of spectral vegetation indexes. *IEEE Transactions on Geoscience and Remote Sensing*, *33*(2), 481–486.

Nasteski, V. (2017). An overview of the supervised machine learning methods. *HORIZONS.B, 4*, 51–62. https://doi.org/10.20544/HORIZONS.B.04.1.17.P05

Nitze, I., Schulthess, U., & Asche, H. (2012). Comparison of machine learning algorithms random forest, artificial neural network and support vector machine to maximum likelihood for supervised crop type classification. *Proceedings of the 4th GEOBIA, Rio de Janeiro, Brazil*, *79*, 3540.

Ok, A. O., Akar, O., & Gungor, O. (2012). Evaluation of random forest method for agricultural crop classification. *European Journal of Remote Sensing*, *45*(1), 421–432.

Ozdarici-Ok, A., & Akyurek, Z. (2014). Object-based classification of multi-temporal images for agricultural crop mapping in Karacabey Plain, Turkey. *The International Archives of Photogrammetry, Remote Sensing and Spatial Information Sciences*, *40*(7), 127.

Özür, N. & Ataol, M. (2018). Türkiye'de CORINE verilerinin kullanılmasına dair değerlendirme. *Çankırı Karatekin Üniversitesi Sosyal Bilimler Enstitüsü Dergisi*, *9*(2), 110-130.

Palacios-Orueta, A., Khanna, S., Litago, J., Whiting, M. L., & Ustin, S. L. (2006). Assessment of NDVI and NDWI spectral indices using MODIS time series analysis and development of a new spectral index based on MODIS shortwave infrared bands. *Proceedings of the 1st International Conference of Remote Sensing and Geoinformation Processing*, *1*, 207–209.

Pierce, L. E., Bergen, K. M., Dobson, M. C., & Ulaby, F. T. (n.d.). *Multitemporal Land-Cover Classification Using SIR-C/X-SAR Imagery*.

Piyoosh, A. K., & Ghosh, S. K. (2018). Development of a modified bare soil and urban index for Landsat 8 satellite data. *Geocarto International*, *33*(4), 423–442.

R Core Team. (2020). *R: A Language and Environment for Statistical Computing*.

https://www.r-project.org/

Rasul, A., Balzter, H., Ibrahim, G. R. F., Hameed, H. M., Wheeler, J., Adamu, B., ... & Najmaddin, P. M. (2018). Applying built-up and bare-soil indices from Landsat 8 to cities in dry climates. *Land*, *7*(3), 81.

Recanatesi, F., & Petroselli, A. (2020). Land Cover Change and Flood Risk in a Peri-Urban Environment of the Metropolitan Area of Rome (Italy). *Water Resources Management*, *34*(14), 4399–4413. https://doi.org/10.1007/s11269-020-02567-8

Republic of Türkiye Ministry of Agriculture and Forestry (2019). Ürün Masaları: Mısır Bülteni. Retrieved June 16, 2022, from https://www.tarimorman.gov.tr/BUGEM/Belgeler/M%C4%B0LL%C4%B0%20TARIM/MISIR%20KASIM%20B%C3%9CLTEN%C4%B0.pdf

Republic Of Türkiye Ministry of Agriculture and Forestry (2020a). Tarım Ürünleri piyasaları: Şeker Pancarı. Retrieved June 16, 2022, from https://arastirma.tarimorman.gov.tr/tepge/Belgeler/PDF%20Tar%C4%B1m%20%C3%9Cr%C3%BCnleri%20Piyasalar%C4%B1/2020-Temmuz%20Tar%C4%B1m%20%C3%9Cr%C3%BCnleri%20Raporu/%C5%9Eeker%20Pancar%C4%B1,%20Temmuz-2020,%20Tar%C4%B1m%20%C3%9Cr%C3%BCnleri%20Piyasa%20Raporu.pdf

Republic of Türkiye Ministry of Agriculture and Forestry (2020b). Tarım Ürünleri piyasaları: Pamuk. Retrieved June 16, 2022, from https://arastirma.tarimorman.gov.tr/tepge/Belgeler/PDF%20Tar%C4%B1m%20%C3%9Cr%C3%BCnleri%20Piyasalar%C4%B1/2021-Ocak%20Tar%C4%B1m%20%C3%9Cr%C3%BCnleri%20Raporu/Pamuk,%20Ocak-2021,%20Tar%C4%B1m%20U%CC%88ru%CC%88nleri%20Piyasa%20Raporu.pdf

Republic of Türkiye Ministry of Agriculture and Forestry (2020c). Tarım Ürünleri piyasaları: Arpa. Retrieved June 16, 2022, from https://arastirma.tarimorman.gov.tr/tepge/Belgeler/PDF%20Tar%C4%B1m%20%C3%9Cr%C3%BCnleri%20Piyasalar%C4%B1/2020-Temmuz%20Tar%C4%B1m%20%C3%9Cr%C3%BCnleri%20Raporu/Arpa,%20Temmuz-2020,%20Tar%C4%B1m%20%C3%9Cr%C3%BCnleri%20Piyasa%20Raporu.pdf

Republic of Türkiye Ministry of Agriculture and Forestry (2020d). Tarım Ürünleri piyasaları: Çeltik. Retrieved June 16, 2022, from https://arastirma.tarimorman.gov.tr/tepge/Belgeler/PDF%20Tar%C4%B1m%20%C3%9Cr%C3%BCnleri%20Piyasalar%C4%B1/2020-Temmuz%20Tar%C4%B1m%20%C3%9Cr%C3%BCnleri%20Raporu/%C3%87eltik,%20Temmuz-2020,%20Tar%C4%B1m%20%C3%9Cr%C3%BCnleri%20Piyasa%20Raporu.pdf

Republic of Türkiye Ministry of Agriculture and Forestry (2021a). Tarım Ürünleri piyasaları: Patates. Retrieved June 16, 2022, from https://arastirma.tarimorman.gov.tr/tepge/Belgeler/PDF%20Tar%C4%B1m%20%C3%9Cr%C3%BCnleri%20Piyasalar%C4%B1/2021-Ocak%20Tar%C4%B1m%20%C3%9Cr%C3%BCnleri%20Raporu/Patates,%20Ocak-2021,%20Tar%C4%B1m%20%C3%9Cr%C3%BCnleri%20Piyasa%20Raporu.pdf

Republic of Türkiye Ministry of Agriculture and Forestry (2021b). Tarım Ürünleri piyasaları: Buğday. Retrieved June 16, 2022, from https://arastirma.tarimorman.gov.tr/tepge/Belgeler/PDF%20Tar%C4%B1m%20%C3%9Cr%C3%BCnleri%20Piyasalar%C4%B1/2021-Ocak%20Tar%C4%B1m%20%C3%9Cr%C3%BCnleri%20Raporu/Bu%C4%9Fday,%20Ocak%202021,%20Tar%C4%B1m%20%C3%9Cr%C3%BCnleri%20Piyasa%20Raporu.pdf

Rodriguez-Galiano, V. F., Chica-Olmo, M., Abarca-Hernandez, F., Atkinson, P. M., & Jeganathan, C. (2012a). Random Forest classification of Mediterranean land cover using multi-seasonal imagery and multi-seasonal texture. *Remote Sensing of Environment*, *121*, 93–107.

Rodriguez-Galiano, V. F., Ghimire, B., Rogan, J., Chica-Olmo, M., & Rigol-Sanchez, J. P. (2012b). An assessment of the effectiveness of a random forest classifier for land-cover classification. *ISPRS Journal of Photogrammetry and Remote Sensing*, *67*(1), 93–104. https://doi.org/10.1016/j.isprsjprs.2011.11.002

Rußwurm, M., & Körner, M. (2017). Multi-temporal land cover classification with long short-term memory neural networks. *International Archives of the Photogrammetry, Remote Sensing & Spatial Information Sciences*, *42*.

Saini, R., & Ghosh, S. K. (2018). Crop classification on single date sentinel-2

imagery using random forest and suppor vector machine. *The International Archives of Photogrammetry, Remote Sensing and Spatial Information Sciences*, *42*, 683–688.

Scholkopf, B., Sung, K. K., Burges, C. J., Girosi, F., Niyogi, P., Poggio, T., & Vapnik, V. (1997). Comparing support vector machines with Gaussian kernels to radial basis function classifiers. *IEEE transactions on Signal Processing*, *45*(11), 2758-2765.

Schubert, S. D., Rood, R. B., & Pfaendtner, J. (1993). An assimilated dataset for earth science applications. *Bulletin of the American meteorological Society*, *74*(12), 2331-2342.

Sensoy, S., Demircan, M., Ulupinar, Y., & Balta, I. (2008). Climate of turkey. *Turkish State Meteorological Service, 401*.

Siebert, S., & Ewert, F. (2012). Spatio-temporal patterns of phenological development in Germany in relation to temperature and day length. *Agricultural and Forest Meteorology*, *152*(1), 44–57. https://doi.org/10.1016/j.agrformet.2011.08.007

Skriver, H., Mattia, F., Satalino, G., Balenzano, A., Pauwels, V. R., Verhoest, N. E., & Davidson, M. (2011). Crop classification using short-revisit multitemporal SAR data. *IEEE Journal of Selected Topics in Applied Earth Observations and Remote Sensing*, *4*(2), 423-431.

Sonobe, R., Yamaya, Y., Tani, H., Wang, X., Kobayashi, N., & Mochizuki, K. I. (2017). Assessing the suitability of data from Sentinel-1A and 2A for crop classification. *GIScience & Remote Sensing*, *54*(6), 918-938. https://doi.org/10.1080/15481603.2017.1351149

Sonobe, R., Yamaya, Y., Tani, H., Wang, X., Kobayashi, N., & Mochizuki, K. I. (2018). Crop classification from Sentinel-2-derived vegetation indices using ensemble learning. *Journal of Applied Remote Sensing*, *12*(2), 026019. https://doi.org/10.1117/1.jrs.12.026019

Southworth, J., Munroe, D., & Nagendra, H. (2004). Land cover change and landscape fragmentation - Comparing the utility of continuous and discrete analyses for a western Honduras region. *Agriculture, Ecosystems and Environment*, *101*(2–3), 185–205. https://doi.org/10.1016/j.agee.2003.09.011

Steduto, P., Faurès, J.-M., Hoogeveen, J., Winpenny, J., & Burke, J. (2012). Coping with water scarcity: an action framework for agriculture and food security. *FAO Water Reports*, *16*, 78.

Stehman, S. (1996). Estimating the kappa coefficient and its variance under stratified random sampling. *Photogrammetric Engineering and Remote Sensing*, *62*(4), 401–407.

Story, M., & Congalton, R. G. (1986). Accuracy assessment: a user's perspective. *Photogrammetric Engineering and Remote Sensing*, *52*(3), 397–399.

Sun, S. (2011). Meta-analysis of Cohen's kappa. *Health Services and Outcomes Research Methodology*, *11*(3–4), 145–163. https://doi.org/10.1007/s10742-011-0077-3

Tao, Y., Wang, H., Ou, W., & Guo, J. (2018). A land-cover-based approach to assessing ecosystem services supply and demand dynamics in the rapidly urbanizing Yangtze River Delta region. *Land Use Policy*, *72*, 250-258.

Turker, M, & Arikan, M. (2005). Sequential masking classification of multi-temporal Landsat7 ETM+ images for field-based crop mapping in Karacabey, Turkey. *International Journal of Remote Sensing*, *26*(17), 3813–3830. https://doi.org/10.1080/01431160500166391

Turker, M. & Ozdarici, A. (2011). Field-based crop classification using SPOT4, SPOT5, IKONOS and QuickBird imagery for agricultural areas: a comparison study. *International Journal of Remote Sensing*, *32*(24), 9735–9768.

Turkish Statistical Institute (2018). Bitkisel üretim istatistikleri, 2018. Retrieved June 16, 2022, from https://data.tuik.gov.tr/Bulten/Index?p=Bitkisel-Uretim-Istatistikleri-2018-27635

Turkish Statistical Institute (2019). Bitkisel üretim istatistikleri, 2019. Retrieved June 16, 2022, from https://data.tuik.gov.tr/Bulten/Index?p=Bitkisel-Uretim-Istatistikleri-2019-30685

Turkish Statistical Institute (2020). Bitkisel üretim verileri. Retrieved June 16, 2022, from https://www.tarimorman.gov.tr/sgb/Belgeler/SagMenuVeriler/BUGEM.pdf

Uddin, K., Matin, M. A., & Maharjan, S. (2018). Assessment of land cover change and its impact on changes in soil erosion risk in Nepal. *Sustainability (Switzerland)*, *10*(12). https://doi.org/10.3390/su10124715

UNDESA, P. (2017). *World population prospects: the 2017 revision*.

Ustuner, M., Sanli, F. B., Abdikan, S., Bilgin, G., & Goksel, C. (2019). A booster analysis of extreme gradient boosting for crop classification using PolSAR imagery. *2019 8th International Conference on Agro-Geoinformatics (Agro-Geoinformatics)*, 1–4.

van der Sande, C. J., de Jong, S. M., & de Roo, A. P. J. (2003). A segmentation and classification approach of IKONOS-2 imagery for land cover mapping to assist flood risk and flood damage assessment. *International Journal of Applied Earth Observation and Geoinformation*, *4*(3), 217–229. https://doi.org/10.1016/S0303-2434(03)00003-5

Vapnik, V., & Chervonenkis, A. Y. (1964). A class of algorithms for pattern recognition learning. *Avtomat. i Telemekh*, *25*(6), 937–945.

Vapnik, V., Guyon, I., & Hastie, T. (1995). Support vector machines. *Mach. Learn*, *20*(3), 273-297.

Viskovic, L., Kosovic, I. N., & Mastelic, T. (2019). Crop Classification using Multi-spectral and Multi-temporal Satellite Imagery with Machine Learning. In *2019 International Conference on Software, Telecommunications and Computer Networks (SoftCOM)*. https://www.satimagingcorp.com/satellite-sensors/other-satellite-sensors/aster/

Wallace, J. S. (2000). Increasing agricultural water use efficiency to meet future food production. *Agriculture, Ecosystems and Environment*. https://doi.org/10.1016/S0167-8809(00)00220-6

Weng, Q. (2013). *Introduction to Remote Sensing Systems, Data, and Applications* (pp. 3–20). https://doi.org/10.1201/b15159-3

Woźniak, E., Rybicki, M., Kofman, W., Aleksandrowicz, S., Wojtkowski, C., Lewiński, S., Bojanowski, J., Musiał, J., Milewski, T., Slesiński, P., & Łączyński, A. (2022). Multi-temporal phenological indices derived from time series Sentinel-1 images to country-wide crop classification. *International Journal of Applied Earth Observation and Geoinformation*, *107*. https://doi.org/10.1016/j.jag.2022.102683

Yang, N., Liu, D., Feng, Q., Xiong, Q., Zhang, L., Ren, T., Zhao, Y., Zhu, D., & Huang, J. (2019). Large-scale crop mapping based on machine learning and parallel computation with grids. *Remote Sensing*, *11*(12), 1–22. https://doi.org/10.3390/rs11121500

Yang, S., Gu, L., Li, X., Jiang, T., & Ren, R. (2020). Crop classification method based on optimal feature selection and hybrid CNN-RF networks for multi-temporal remote sensing imagery. *Remote Sensing*, *12*(19). https://doi.org/10.3390/RS12193119

Yang, Y., Zhan, Y., Tian, Q., Gu, X., Yu, T., & Wang, L. (2015). Crop classification based on GF-1/WFV NDVI time series. *Transactions of the Chinese Society of Agricultural Engineering*, *31*(24), 155–161.

Yılmaz, İ., İmamoğlu, M., Özbulak, G., Kahraman, F., & Aptoula, E. (2020). Large Scale Crop Classification from Multi-temporal and Multi-spectral Satellite Images. *2020 28th Signal Processing and Communications Applications Conference (SIU)*, 1–4.

Zakeri, H., Yamazaki, F., & Liu, W. (2017). Texture analysis and land cover classification of tehran using polarimetric synthetic aperture radar imagery.

Applied Sciences (Switzerland), *7*(5). https://doi.org/10.3390/app7050452

Zha, Y., Gao, J., & Ni, S. (2003). Use of normalized difference built-up index in automatically mapping urban areas from TM imagery. *International journal of remote sensing*, *24*(3), 583-594.

Zhang, C., Chen, Y., & Lu, D. (2015). Mapping the land-cover distribution in arid and semiarid urban landscapes with Landsat Thematic Mapper imagery. *International Journal of Remote Sensing*, *36*(17), 4483–4500.

Zhang, L., Gao, L., Huang, C., Wang, N., Wang, S., Peng, M., ... & Tong, Q. (2022). Crop classification based on the spectrotemporal signature derived from vegetation indices and accumulated temperature. *International Journal of Digital Earth*, 1-27.

Zhang, S., & Tao, F. (2013). Modeling the response of rice phenology to climate change and variability in different climatic zones: Comparisons of five models. *European Journal of Agronomy*, *45*, 165–176. https://doi.org/10.1016/j.eja.2012.10.005

Zhang, T., Su, J., Liu, C., Chen, W.-H., Liu, H., & Liu, G. (2017). Band selection in Sentinel-2 satellite for agriculture applications. *2017 23rd International Conference on Automation and Computing (ICAC)*, 1–6.

Zhang, X., Sun, Y., Shang, K., Zhang, L., & Wang, S. (2016). Crop Classification Based on Feature Band Set Construction and Object-Oriented Approach Using Hyperspectral Images. *IEEE Journal of Selected Topics in Applied Earth Observations and Remote Sensing*, *9*(9), 4117–4128. https://doi.org/10.1109/JSTARS.2016.2577339

Zheng, B., Myint, S. W., Thenkabail, P. S., & Aggarwal, R. M. (2015). A support vector machine to identify irrigated crop types using time-series Landsat NDVI data. *International Journal of Applied Earth Observation and Geoinformation*. https://doi.org/10.1016/j.jag.2014.07.002

Zhou, X., Zhu, X., Dong, Z., & Guo, W. (2016). Estimation of biomass in wheat using random forest regression algorithm and remote sensing data. *The Crop Journal*, *4*(3), 212–219.